A COST- DESIGN APPROACH FOR MULTIPLE DRIVE BELT CONVEYOR SYSTEMS

by

Mukalu Sandro Masaki

Submitted in partial fulfilment of the requirements for the degree
Master of Engineering (Electrical Engineering)

in the

Department of Electrical, Electronic and Computer Engineering
Faculty of Engineering, Built Environment and Information Technology

UNIVERSITY OF PRETORIA

May 2017

SUMMARY

A COST-EFFECTIVE DESIGN APPROACH FOR MULTIPLE DRIVE BELT CONVEYOR SYSTEMS

by

Mukalu Sandro Masaki

Supervisor(s):	Dr. Lijun Zhang
	Prof. Xiaohua Xia
Department:	Electrical, Electronic and Computer Engineering
University:	University of Pretoria
Degree:	Master of Engineering (Electrical Engineering)
Keywords:	Belt conveyor, life cycle cost, multiple drive, optimal design, component sizing, energy management

Multiple drive belt conveyors are being increasingly incorporated in mining plans worldwide because of their high economic performance and the ease of moving these installations around, especially in underground mines. A typical modern multi-drive conveyor system consists of one or more intermediate drive stations positioned along the upper stretch of the conveyor and a single drive station situated in the lower stretch. Despite the acknowledged cost saving potential of the multiple drive technology, no previous work was reported on the methodology to realize a cost-effective design of multi-drive belt conveyors.

This study investigates a design approach for multiple drive belt conveyors with the objective to achieve the lowest life cycle cost of multi-drive belt conveyors for a specified material transport task. For this purpose, an optimization model for the cost-effective design of multi-drive conveyor systems is formulated on the basis of the recommendations of the DIN 22101 and SANS 1313 standards. For a given number of intermediate drive stations, the proposed model optimizes a set of design parameters so that the minimum equivalent annual cost of a conveyor can be attained whilst handling the transport requirements and design conditions. The conveyor parameters optimized in this study are the rated

powers of motors, the rated torques of gear reducers, the diameters and wrap angles of drive pulleys, the belt width, the belt speed, the lengths of the belt sections not nestled between drive pulleys, the spacings between idler rolls and the shell diameters and shaft diameters of idler rolls. For benchmark analysis purposes, a similar optimization model is also developed for the single drive technology.

Described as mixed integer nonlinear programming (MINLP) problems, the two optimization models are solved using the MIDACO solver embedded in the MATLAB environment. The results of this study show the validity and effectiveness of the design model proposed for multi-drive belt conveyors. The results also indicate that the multiple drive technology is more beneficial for the conveying over long distances. The impact of the possible instability of inflation throughout the project lifetime is also investigated through three hypothetical scenarios, which involve a fixed inflation rate, a higher fluctuating inflation rate and a lower fluctuating inflation rate, respectively. The results of this sensitivity analysis show that the most cost-effective multi-drive belt conveyors obtained under a fixed inflation rate is robust enough against limited fluctuations of this parameter.

DEDICATION

To

The Most High, YHWH;

For the breath of life, the strength and his steadfast faithfulness (Isaiah 49:15-16);

My dear parents, Simon-Blaise Masaki Ngungu and Anne-Marie Tundu Makulongo;

For their love, sacrifices, encouragement and teaching on the value of hard work.

ACKNOWLEDGEMENT

This research work has been conducted with the National Hub for Energy Efficiency and Demand Side Management (EEDSM), hosted in the Department of Electrical, Electronic and Computer Engineering, University of Pretoria. The financial and material support provided by the University of Pretoria and the National Hub for EEDSM are gratefully acknowledged.

I am also grateful to the National Research Foundation of South Africa for the financial support through the DST Innovation Master's Scholarship program under grant unique number 105047.

I am grateful to my supervisor, Doctor Lijun Zhang, for initiating this study. His guidance, help and availability have been of an inestimable value throughout the conducting of this research work.

I would like to express my heartfelt gratitude and appreciation to my co-supervisor, Professor Xiaohua Xia, for his trust, support, encouragement and inspiration. Thank you so much, prof.

I am indebted to my entire family who unfailingly help me climb the steps towards my fulfilment. I am so proud of you.

PUBLICATIONS

JOURNAL PAPERS

[J1] M. S. Masaki, L. Zhang, and X. Xia, "A design approach for multiple drive belt conveyors minimizing life cycle costs," *Energy for sustainable development*, submitted, 2017.

CONFERENCE CONTRIBUTIONS

[C1] M. S. Masaki, L. Zhang, and X. Xia, "Cost optimization design approach for multiple drive belt conveyors," in *Proceedings of the 36th Chinese Control Conference (CCC2017)*, Da lian, China, 26-28 Jul. 2017.

[C2] M. S. Masaki, L. Zhang, and X. Xia, "A comparative study on the cost-effective belt conveyors for bulk material handling," in *9th International Conference on Applied Energy (ICAE2017)*, Cardiff, United Kingdom, 21-24 Aug. 2017.

[C3] M. S. Masaki, L. Zhang, and X. Xia, "Hierarchical power flow control of a grid-tied photovoltaic plant using a battery-supercapacitor energy storage system," in *Applied Energy Symposium and Forum, REM2017: Renewable Energy Integration with Mini/Microgrid*, Tianjin, China, 18-20 Oct. 2017.

LIST OF ABBREVIATIONS

α_i	Wrap angle of drive pulleys in the drive station i [°]
β	Equivalent angle of slope of the material [°]
γ_{belt}	Specific mass of the belt [kg/m^2]
δ_j	Inclination angle of the belt section j [°]
$\eta_{mot,i}$	Efficiency of motors in the drive station i
$\eta_{gear,i}$	Efficiency of gear reducers in the drive station i
λ	Troughing angle [°]
μ	Friction factor between the drive pulley and the conveyor belt
μ_1	Friction factor between belt and material conveyed
μ_2	Friction factor between the lateral chutes and the material transferred
μ_3	Friction factor between the belt cleaning device and the belt
ξ_o	Number of idler rolls per set on the carry side
ξ_u	Number of idler rolls per set on the return side
ρ	Material density [kg/m^3]
a	Constant factor for the calculation of clear width of lateral chutes
A_{Gr}	Effective contact area between belt cleaning device and belt [m^2]
A_{th}	Theoretical cross section of fill [m^2]
$A_{conveyor}$	Annual equivalent cost of the belt conveyor [USD/year]
A_{belt}	Annual equivalent cost of the belt [USD/year]
$A_{carryidler}$	Annual equivalent cost of all the carry idler rolls [USD/year]
A_{energy}	Annual equivalent energy cost [USD/year]
A_{eq}	Annual equivalent cost of an equipment [USD/year]
$A_{gear,i}$	Annual equivalent cost of each gear reducer in the drive station i [USD/year]
$A_{motor,i}$	Annual equivalent cost of each motor in the drive station i [USD/year]
$A_{returnidler}$	Annual equivalent cost of all the return idler rolls [USD/year]
B	Belt width [m]
$\mathfrak{B}$	Set of the recommended width of belt
b	Usable belt width [m]
B_f	Dynamic load factor related to bearing life
b_{Sch}	Clear width of lateral chutes [m]

$C_{eq,0}$	First cost of the item of an equipment purchased at the year zero [USD]
C_f	Belt flap factor
C_{Rank}	Rakine coefficient
C_{Schb}	Constant factor for additional resistance between material transferred and lateral chutes
c_{Tr}	Drive pulleys constant coefficient related to the type longitudinal tension members of the belt
$C_{w,i}$	Combined warp factor of the drive pulleys in the drive station i
$c_1, \ldots, c_{22}$	Initial cost coefficients
$\mathfrak{D}$	Set of the recommended diameters of idler roll
$\mathfrak{d}$	Set of the recommended shaft diameters of idler roll
$\mathfrak{D}_{tr}$	Set of the recommended diameters of drive pulley
d_{Gk}	Thickness of the longitudinal tension members of the belt [m]
D_j	Diameter of idler rolls in the belt section j [m]
d_j	Shaft diameter of idler rolls in the belt section j [m]
D_o	Diameter of idler rolls in the upper stretch [m]
d_o	Shaft diameter of idler rolls in the upper stretch [m]
D_u	Diameter of idler rolls in the lower stretch [m]
d_u	Shaft diameter of idler rolls in the lower stretch [m]
DIN	Deutsches Institut für Normung
e_o	Unit cost of energy at the year zero of the project [USD/kWh]
f_j	Hypothetical friction factor in the belt section j
$F_{Auf,j}$	Resistance due to the acceleration of the material in the loading zone of the belt section j [N]
F_{min}	Minimum belt tension in steady-state operating conditions [N]
$F_{G,j}$	Gradient resistance in the belt section j [N]
$F_{Gr,j}$	frictional resistance due to belt cleaning devices situated in the belt section j [N]
$F_{H,j}$	Primary resistance in the belt section j [N]
F_0	Belt tension at each side of the tail pulley [N]
$F_{N,j}$	Secondary resistance in the belt section j [N]
$F_{S,j}$	Special resistance in the belt section j [N]
$F_{s,o}$	Static load on the central carry idler roll in a three-idler troughing configuration [N]
$F_{s,u}$	Static load on a flat return idler in the lower stretch [N]

$F_{Schb,j}$	frictional resistance between belt and lateral chutes in the acceleration zone of the belt section j [N]
$F_{T1,i}$	Tight side tension of the first drive pulley in the drive station i [N]
$F_{T2,i}$	Slack side tension of the second drive pulley in the drive station i [N]
F_{TU}	Belt tension on both sides of the take-up device [N]
$F_{W,j}$	Total resistance to movement in the belt section j [N]
F_0	Belt tension at the conveyor tail [N]
g	Gravitational acceleration [m/s^2]
H	Lifting height [m]
h_{rel}	Maximum belt sag related to spacing between idler rolls
i	Integer index
i_d	Interest rate on debt
i_e	After-tax return required on equity funds with zero inflation rate
$i_{f,j}$	Inflation modified rate of return of the year j of the project
i_f^0	Time value of money with all cash flows converted from inflated value to constant year zero value
j	Integer index
K	Total length of the belt along the conveyor path [m]
k_b	Constant factor for calculation of the total length of the acceleration path
k_N	Nominal breaking strength of the belt related to belt width [N/m]
k_{eq}	Equivalent annual cost coefficient of an equipment
$k_{t,rel}$	Relative reference endurance strength of the belt
$k_0, \ldots, k_5$	Equivalent annual cost coefficients
L	Horizontal transport distance [m]
l_b	Total length of the acceleration path [m]
L_f	Dynamic load factor related to lump size of the material transferred
l_j	Length of the belt section j
$L_{o,j}$	Length of the belt section j in the upper stretch [m]
$l_{M,o}$	Length of the shell of a carry idler roll [m]
l_o	Spacing between idler rolls in the upper stretch [m]
$L_{u,j}$	Length of the belt section j in the lower stretch [m]
l_u	Spacing between idler rolls in the lower stretch [m]
M	Expected lifetime of each item of an equipment [year]

m'_G	Linear mass of the belt [kg/m]
$m'_{L,j}$	Linear mass of the transferred material in the belt section j [kg/m]
$m_{R,j}$	Mass of the rotating parts of each idler situated in the belt section j [kg]
$m'_{R,j}$	Linear mass of the rotating parts of idlers per running meter in the belt section j [kg/m]
$m_{R,o}$	Actual mass of the rotating parts of a carry idler roll [kg]
$\hat{m}_{R,o}$	Predicted mass of the rotating parts of a carry idler roll [kg]
$m_{R,u}$	Actual mass of the rotating parts of a return idler roll [kg]
$\hat{m}_{R,u}$	Predicted mass of the rotating parts of a return idler roll [kg]
m_1	Belt weight model coefficient [kg/m^2]
m_2	Belt weight model coefficient [s^2/m^2]
m_3	Steelcord diameter model coefficient [m]
m_4	Steelcord diameter model coefficient [m]
m_5	Steelcord diameter model coefficient [m]
MIDACO	Mixed Integer Distributed Ant Colony Optimization
MINLP	Mixed Integer NonLinear Programming
N	Number of intermediate drive stations
N_o	Number of belt sections in the upper stretch
N_u	Number of belt sections in the lower stretch
n_1	Dynamic speed load factor model coefficient
n_2	Dynamic speed load factor model coefficient [s/m]
o	Upper stretch
P_i	Rated power of motors in the drive station i [kW]
PED_{eq}	Present equivalent of depreciation of the items of an equipment [USD]
PEF_{eq}	Present equivalent of all the first cost of an equipment [USD]
PEV_{eq}	Present equivalent of all the salvage value of an equipment [USD]
p_{Gr}	Pressure between the belt cleaning device and the belt [N/m^2]
Q	Material flow rate [kg/s]
q_f	Remaining proportion of the initial value of an equipment at the end of the expected lifetime
q_i	Remaining proportion of the initial value of the item i of an equipment at the end of its actual lifetime
R	Number of items of an equipment to be purchased over the project lifetime
r_{avg}	Average general inflation rate over the project duration

r_d	Proportion of debt capital
$r_{e,j}$	Annual escalation rate of energy during the year j
$r_{eq,j}$	Annual cost escalation rate of an equipment during the year j
r_j	General inflation rate during the year j
SANS	South Africa National Standard
S_f	Dynamic load factor related to belt speed
S_0	Belt safety factor related to the splicing conditions
S_1	Belt safety factor related to the expected lifetime and the operation conditions
t	Income tax rate
t_a	Operating hours per annum [h]
T_i	Rated torque of gear reducers in the drive station i [kNm]
u	Lower stretch
v	Conveyor speed [m/s]
$v_{0,j}$	Initial speed of the material in the direction of belt travel in the belt section j [m/s]
w	Width of the contact area between belt and belt cleaning device [m]
X_i	Purchase year of the item i of an equipment
Y_i	Year of decommissioning of the item i of an equipment
y_1, y_2	Belt length model coefficients [m]
Z	Project lifetime [year]
$z_1, \ldots, z_4$	Idler roll mass model coefficients

TABLE OF CONTENTS

CHAPTER 1 INTRODUCTION **1**
1.1 CHAPTER OVERVIEW 1
1.2 PROBLEM STATEMENT 1
1.3 RESEARCH OBJECTIVES AND QUESTIONS 3
1.4 RESEARCH GOALS 4
1.5 HYPOTHESIS AND APPROACH 4
1.6 RESEARCH CONTRIBUTIONS 6

CHAPTER 2 LITERATURE STUDY **7**
2.1 CHAPTER OVERVIEW 7
2.2 POET FRAMEWORK 7
2.2.1 Technology efficiency 7
2.2.2 Equipment efficiency 8
2.2.3 Operation efficiency 8
2.2.4 Performance efficiency 9
2.3 BELT CONVEYOR EQUIPMENT EFFICIENCY 9
2.4 BELT CONVEYOR OPERATION EFFICIENCY 10
2.5 BELT CONVEYOR TECHNOLOGY EFFICIENCY 12
2.6 MULTIPLE DRIVE BELT CONVEYOR DEVELOPMENT 13
2.7 RESEARCH GAP 16

CHAPTER 3 PROBLEM FORMULATION **17**
3.1 CHAPTER OVERVIEW 17
3.2 DESCRIPTION OF THE MULTI-DRIVE BELT CONVEYORS 17
3.3 DESIGN OBJECTIVE 20
3.4 ECONOMIC CONSIDERATIONS 21

3.4.1 Operating costs of multiple drive belt conveyors . . . 21
3.4.2 Capital costs of multiple drive belt conveyors . . . 22
3.4.3 Equivalent annual cost of multiple drive belt conveyors . . . 24
3.5 RESISTANCES TO MOTION IN A MULTIPLE DRIVE BELT CONVEYOR . . . 24
3.5.1 Primary resistance . . . 24
3.5.2 Secondary resistance . . . 26
3.5.3 Slope resistance . . . 28
3.5.4 Special resistances . . . 28
3.6 FORMULATION OF THE TIGHT-SIDE TENSIONS, SLACK-SIDE TENSIONS AND TAIL TENSION OF MULTI-DRIVE BELT CONVEYORS . . . 29
3.7 DESIGN CONSTRAINTS . . . 32
3.7.1 Material transportation requirements . . . 32
3.7.2 Power balance in the belt conveyor . . . 32
3.7.3 Belt tension requirements . . . 33
3.7.4 Minimum drive pulley diameter requirements . . . 35
3.7.5 Idler rolls requirements . . . 36
3.7.6 Boundary limit requirements . . . 37
3.8 OPTIMAL DESIGN PROBLEMS . . . 38
3.8.1 Optimal design problem of multiple drive belt conveyors . . . 38
3.8.2 Optimal design problems of single drive belt conveyors . . . 40

CHAPTER 4 CASE STUDY . . . 44
4.1 CHAPTER OVERVIEW . . . 44
4.2 PROJECT DESCRIPTION . . . 44
4.2.1 Technical specifications . . . 44
4.2.2 General economic parameters . . . 46
4.3 BELT CONVEYOR COMPONENT PARAMETERS . . . 47
4.3.1 Belting . . . 47
4.3.2 Motors . . . 50
4.3.3 Gear reducers . . . 53
4.3.4 Carry idler rolls . . . 55
4.3.5 Return idler rolls . . . 56
4.4 INFLATION TREND SCENARIOS . . . 58

4.4.1 Scenario 1: Fixed inflation rate 5.6% . . . 58
4.4.2 Scenario 2: Fluctuating inflation rate at 5.2% on average . . . 58
4.4.3 Scenario 3: Fluctuating inflation rate at 5.8% on average . . . 59

CHAPTER 5 OPTIMAL DESIGN SIMULATION RESULTS AND ANALYSIS . . . 61
5.1 CHAPTER OVERVIEW . . . 61
5.2 BRIEF DESCRIPTION OF THE OPTIMIZER AND THE OPTIMIZATION PROCEDURE . . . 61
5.3 OPTIMAL CONVEYOR DESIGNS AND RELATED COSTS UNDER FIXED INFLATION RATE AT 5.6% . . . 63
5.3.1 Single drive conveyor layout . . . 63
5.3.2 Multi-drive conveyor layout . . . 66
5.4 OPTIMAL CONVEYOR DESIGNS AND RELATED COSTS UNDER FLUCTUATING INFLATION RATE AT 5.2% ON AVERAGE . . . 71
5.5 OPTIMAL CONVEYOR DESIGNS AND RELATED COSTS UNDER FLUCTUATING INFLATION RATE AT 5.8% ON AVERAGE . . . 76

CHAPTER 6 DISCUSSION . . . 81
6.1 CHAPTER OVERVIEW . . . 81
6.2 PROFILE OF THE MINIMUM CONVEYOR COSTS . . . 81
6.3 COST-EFFECTIVE BELT CONVEYOR FRONT . . . 81
6.4 INFLATION SENSITIVITY ANALYSIS . . . 84

CHAPTER 7 CONCLUSION . . . 88
7.1 SUMMARY . . . 88
7.2 FUTURE WORKS . . . 89

REFERENCES . . . 90

ADDENDUM A FORMULATION OF THE EQUIVALENT ANNUAL COST COEFFICIENTS . . . 95
A.1 CALCULATION OF THE EQUIVALENT ANNUAL ENERGY COST COEFFICIENT 95
A.2 CALCULATION OF THE EQUIVALENT ANNUAL COST OF EQUIPMENT . . . 97

ADDENDUM B DERIVATION OF IDLER ROLL MASS MODELS . . . 101
B.1 CARRY IDLER ROLLS . . . 101

B.2 RETURN IDLER ROLLS 104

ADDENDUM C DERIVATION OF BELT PARAMETER MODELS 108

ADDENDUM D DERIVATION OF IDLER ROLL PRICING MODELS 111

D.1 CARRY IDLER ROLLS 111

D.2 RETURN IDLER ROLLS 112

CHAPTER 1 INTRODUCTION

1.1 CHAPTER OVERVIEW

This introductory chapter presents the motivation of the study reported in this dissertation. It subsequently states the research objectives and questions and also set the research goals. The hypothesis made in this study and the approach to be followed in order to attain the research goals are also given. Finally, the major contributions of this study within the general topic of the cost-effective design of multi-drive belt conveyors are highlighted.

1.2 PROBLEM STATEMENT

Electricity-powered equipment is of prime importance in diverse industrial processes. While prices of energy and production machinery are rising steadily, the need to consistently produce goods at a reasonable cost requires a thorough assessment of future investment options from companies. When it comes to handling bulk materials across mining and mineral processing facilities, belt conveyors are amongst the most popular technology used due to their high efficiency of transportation [1, 2, 3]. Over the years, it has appeared that many conveyor systems worldwide were either oversized or not properly operated; resulting in excessive capital and operating costs [3, 4].

Providing an insight into the energy aspect, Eskom, the largest South African electric power utility, found that approximately 15% of its overall production in 2010 served to supply the mining sector. When analyzing this demand, about 23% of it was used for material handling purposes, in which the contribution of belt conveyors was significant[1].

[1]Eskom: "The Energy Efficiency series. Towards an energy efficient mining sector". Available at: http://www.eskom.co.za/sites/idm/Documents/121040ESKD_Mining_Brochure_paths.pdf

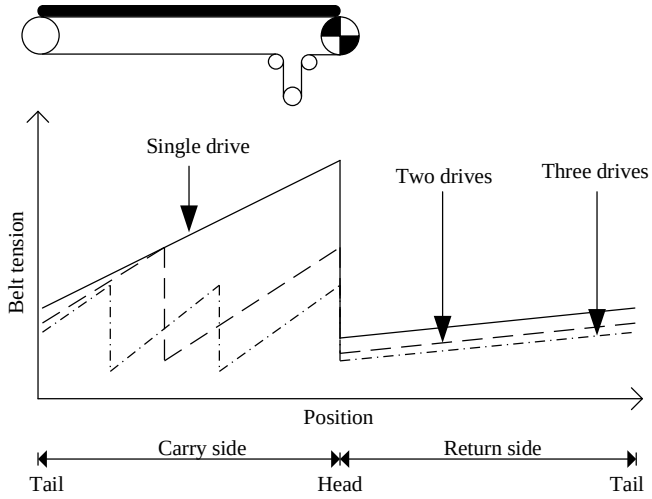

Figure 1.1. Belt tension profile vs. number of drives. Adapted with permission of Trans Tech Publications Ltd, from "The Evolution of Intermediate Driven Belt Conveyor Technology," M.A. Alspaugh, Vol. 23, No. 3, 2017.

To assist in increasing the overall economic performance of belt conveyors, one of the modern strategies consists of distributing the driving force along the transport path. In this case, the maximum belt tension of the system is gradually reduced and therefore lighter belts can be used, as displayed in Figure 1.1. This initiative will subsequently benefit the supporting structure, thereby enabling the use of a lighter design. Despite the significant saving potential and the increasing popularity of these transport facilities [5], only limited knowledge on this particular type of belt conveyors is available today. Currently, the question of the design of multiple drive conveyor systems is not consistently addressed in most standards.

In comparison with a common single drive belt conveyor, much more parameters are involved in the design process of a multiple drive conveyor system. Fundamentally, factors such as rated power of motors and rated torque of gear reducers will increase proportionally to the number of drive stations considered, while the distance between them and their total number will also act as additional design variables.

The study reported in this dissertation is involved with the minimization of the life cycle cost of multiple drive belt conveyors. To this end, an approach that aims to optimally set a number of design parameters is investigated.

1.3 RESEARCH OBJECTIVES AND QUESTIONS

Presently, a variety of standards are available for the dimensioning of belt conveyors, including ISO 5048, DIN 22101, CEMA, JIS B 8805, and FDA [6]. Built on the International standard ISO 5048, the 2011 version of the popular DIN 22101 standard provides some background on aspects relevant to the design of multiple drive conveyor systems [7]. Accordingly, the calculation methodology developed in this standard was adopted for this study.

Following most standards, the design approach described in DIN 22101 focuses on guaranteeing the mechanical performance of conveyors, with limited attention given to energy. For example, the individual influence of certain design parameters on the friction coefficient of the primary resistance to belt movement is specified in terms of ranges of values. As such, an attempt to simultaneously optimize all the variables involved in the design of a conveyor system becomes fastidious. Furthermore, the DIN 22101 standard is primarily devoted to the design of single drive belt conveyors. In this context, a number of design relations should either be adapted or added in order to accommodate multiple drive conveyor systems.

Therefore, the prime objective of this study is to investigate the possibility to minimize the life cycle cost of multiple drive belt conveyors through the optimum setting of a number of its parameters at one time. To this end, the set of parameters involved in this design process is first specified. Their effects on the relevant relationships described in the standard DIN 22101 are subsequently investigated. A suitable formulation of the life cycle cost of this type of conveyor system is also included among the objectives of this study. All these technical and economic functions that are mentioned will be combined together into an optimization model that will minimize the costs incurred over the conveyor life cycle.

The research questions are therefore as follows:

- Which are the additional degrees of freedom available in the design of a multiple drive belt conveyor?

- What impact does the distribution of the driving force along the conveying path have on the design method proposed in DIN 22101?

- How does the economic performance of the most cost-effective multiple drive design compare with the best design of a single drive conveyor system?

- How robust is the most cost-effective belt conveyor design for a specific transport operation against limited fluctuations of the inflation rate?

1.4 RESEARCH GOALS

The triple goals of this study can be stated as follows:

1. To formulate and test the validity and effectiveness of an optimization model intended to minimize the life cycle cost of a typical multiple drive belt conveyor system

2. To establish the economic superiority of the distributed drive layout compared to the single drive layout for certain transport requirements

3. To verify the robustness of the best belt conveyor design against limited fluctuations of the inflation rate

1.5 HYPOTHESIS AND APPROACH

It is hypothesized that the design parameters of a multiple drive belt conveyor can be specified by means of a unique optimization model which handles them all at once. Such a model is expected to serve as an effective means to further decrease the costs incurred throughout the conveyor's life cycle.

To achieve the specified outcomes of this study, the research work has been articulated around the approach described below.

1. Literature study - The literature relevant to the distributed drive technology, the design of conveyor systems, in general, and multiple drive conveyor systems, in particular, the characteristics of conveyor components, and the economic implications of conveyor systems have been reviewed.

2. Selection and modeling of the multiple drive belt conveyor - In practice, various layouts of multiple drive belt conveyors are available. An identification of the most preferred conception has therefore been conducted. Subsequently, the resistance forces to belt movement in such a conveyor system have been modeled.

3. Development of the optimization models - Next, the design conditions that apply to the chosen design variables have been derived from the literature. The different items of the operation and capital costs of these conveyor systems have also been investigated and modeled. Thereafter, the optimization problem intended to find the design of a multiple drive belt conveyor with the minimum life cycle cost has been formulated. For comparison analysis purposes, a second optimization model intended to the cost-effective design of single drive belt conveyors has been derived from the material presented previously.

4. Setup of the simulation environment - On the basis of the structure of the formulated optimization problems, an appropriate optimization solver has been identified, acquired and set up.

5. Simulation and analysis - A practical case study of a conveying operation has been considered and simulated using the above-mentioned optimization solver. A comprehensive analysis of the simulation results has also been carried out.

6. Discussion - A cross-analysis of the belt conveyor designs have been subsequently conducted in order to identify the most cost-effective design solution among the various alternatives obtained from the simulations. A sensitivity test of this belt conveyor against limited variations of the inflation rate throughout the project period has also been performed.

1.6 RESEARCH CONTRIBUTIONS

The various advantages involved in fitting intermediate drive stations along the pathway of belt conveyors have been known for several decades. While, in the past, the risks and challenges incurred restricted its emancipation, the distributed drive technology has since gained in reliability and in the ease of implementation through the technological advance [5]. Given a conveyor project, the large number of design options available with different economic trade-offs suggests that a proper decision-making tool is of paramount importance for both the designer of multiple drive conveyor systems and the conveyor owner.

As will be extensively discussed in the next chapter, there is to date limited research reported on the economic design of belt conveyors in general, among which, to the best of the author's knowledge, no one has addressed the particular case of multiple drive belt conveyors. Hence, the study reported in this dissertation is regarded as the first ever contribution in the area of the optimal design of belt conveyors based on the multiple drive technology.

In its formulation, the proposed design approach has the great benefit of using the equivalent annual costs of conveyors as the performance indicator in the optimization process instead of looking directly at their life cycle costs. This economic indicator constitutes a common ground for a straightforward comparison of different investment opportunities in competition, irrespective of the business field involved and the time-frame of the capital and operating expenditures incurred in each alternative.

CHAPTER 2 LITERATURE STUDY

2.1 CHAPTER OVERVIEW

This chapter presents the findings of the survey of the literature which focuses on improving the energy efficiency and economic performance of belt conveyor systems. Previous works conducted on the multiple drive technology are also studied in order to establish the research gap.

2.2 POET FRAMEWORK

In the literature on the improvement of energy efficiency of energy systems, the various initiatives proposed can be organized according to the POET framework [8, 9, 10], which involves the following four layers: performance efficiency (P), operation efficiency (O), equipment efficiency (E), and technology efficiency (T). A graphic description of this framework is shown in Figure 2.1.

2.2.1 Technology efficiency

Technology efficiency involves the measurement of efficiency in the conversion, processing, transmission, or usage of energy. Among the deterministic indicators used to evaluate technology efficiency, feasibility, life cycle cost and conversion rate can be mentioned. Part of equipment efficiency (E1), operation efficiency (O1) and performance efficiency (P1) are all directly affected by technology efficiency as shown in Figure 2.1.

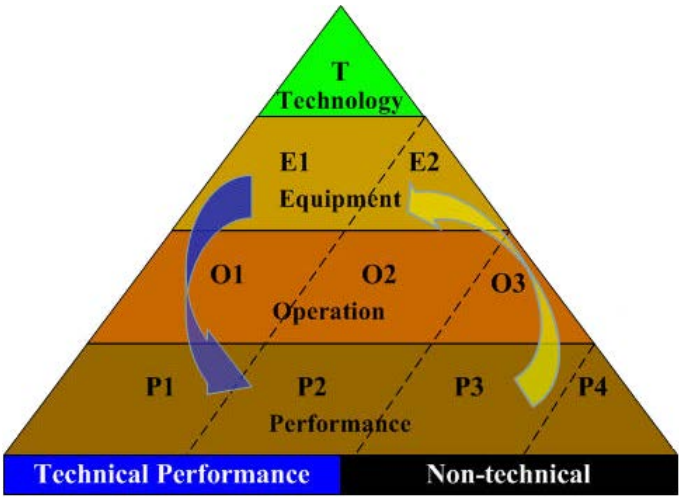

Figure 2.1. POET energy efficiency framework [8].

2.2.2 Equipment efficiency

Equipment efficiency is the measure of energy efficiency that focuses on the energy output of equipment part of an energy system, taking into account their respective design specifications. To this end, each targeted equipment is regarded as a subsystem isolated from the rest of the energy system components. To evaluate the equipment efficiency, indicators such as capacity, specifications, and maintenance are usually considered.

As shown in Figure 2.1, equipment efficiency consists of two parts, referred to as E1 and E2. E1 involves the gap between actual energy efficiency and design specification. On the other hand, E2 represents the effects of activities that attempt to keep the actual energy output as closely to the specification as possible. The dependency of E1 and E2 on technology efficiency is described in Figure 2.1.

2.2.3 Operation efficiency

The operation efficiency of an energy system consists of factors that focus on the proper coordination of its components. The scope of operation efficiency extends over the three areas outlined below:

- physical coordination: evaluated by means of sizing and matching factors

- time coordination: evaluated by means of time control factors

- human coordination: evaluated by means of skill of the operators

In Figure 2.1, operation efficiency is also broken down into three components: O1, O2 and O3. The first block O1 encompasses all the aspects conditioned by technology efficiency, and therefore also dependent upon equipment efficiency in E1. Sizing can be cited among the coordination aspects classified in this category. The second block O2 consists of aspects conditioned by equipment efficiency in E2. Coordinated selection of system components in view of maintenance specifications can be cited as part of operation efficiency aspects classified as O2. Finally, O3 appears to be autonomous from technology efficiency and equipment efficiency. It relates to human factors such as the operator's skill levels.

2.2.4 Performance efficiency

The performance efficiency of an energy system is the measurement of energy efficiency by means of external deterministic factors such as cost, power consumption, production and environmental footprint.

As displayed in Figure 2.1, performance efficiency consists of four different blocks: P1, P2, P3 and P4. P1 is the part conditioned by operation efficiency in O1, equipment efficiency in E1, and also technology efficiency. P2, which is conditioned by operation efficiency in O2 and equipment efficiency in E2, is often expressed by the power of the energy system. P3 is the part conditioned by operation efficiency in O3, and can relate to the soft kilowatt-hour generally determined by the operator's skill levels. P4 refers to the share of energy losses that vary irrespective of O, E and T. Energy losses due to theft can be classified in this block.

2.3 BELT CONVEYOR EQUIPMENT EFFICIENCY

Typically, the power necessary to move the belt alone will occupy the second rank and after that to move the payload of the conveyor. To assist in reducing the power demand from the belt component, the development of energy-optimized conveyor belts has been undertaken by conveyor belt manufacturers.

This involves the introduction of manufacturing concepts such as "Low Rolling Resistance (LRR)" belt covers and bareback belts, which are aimed at reducing the friction between the belt and the mechanical components in contact with it [11].

Other initiatives relevant to equipment efficiency of belt conveyor focus on the drive system through the application of energy-efficient motors and variable speed drives (VSD) [12]. The use of energy-efficient motors instead of standard efficiency equipment in retrofit or new projects leads to a direct reduction in electricity consumption, whose magnitude is primarily dictated by the motor size. With their ability to manipulate the supply frequency, VSDs allow for the controlling of the motor speed in order to keep the operating point of conveyor systems around the zones with the highest energy efficiency. An earlier field survey conducted in Europe has found that, depending on the type of industry considered, the retrofit of belt conveyors with VSDs could be cost-effective without exceeding three years of a payback period for between 0 and 33% of conveyor systems in operation [12].

Recently, certain research works have also focused on the possibility to monitor the condition of belt conveyor components by means of expert systems [13, 14]. Such maintenance tools can be useful in order to limit the risks of failure of equipment, and properly organize the content and scheduling of maintenance planning in order to improve efficiency of conveyor systems in terms of part of the POET.

2.4 BELT CONVEYOR OPERATION EFFICIENCY

Although a belt conveyor has a designed capacity expressed in tonne per hour, in practice, however, many conveyors are not required to operate at their full capacity. While the power absorbed under the no-load condition is also significant, the necessity of a proper control of conveyor systems becomes of paramount concern.

The first group of initiatives that aim to take advantage of the situation described above involves an adapted control strategy of the conveyor speed [4, 15]. Knowing the actual load condition, the objective is to control the motor speed and, consequently, the conveyor speed in such a way that the actual cross section of fill of the belt is kept as close as possible to the theoretical value. This situation is described in Figure 2.2, in which A_0 refers to the cross section before control and A_1 refers to an intermediate

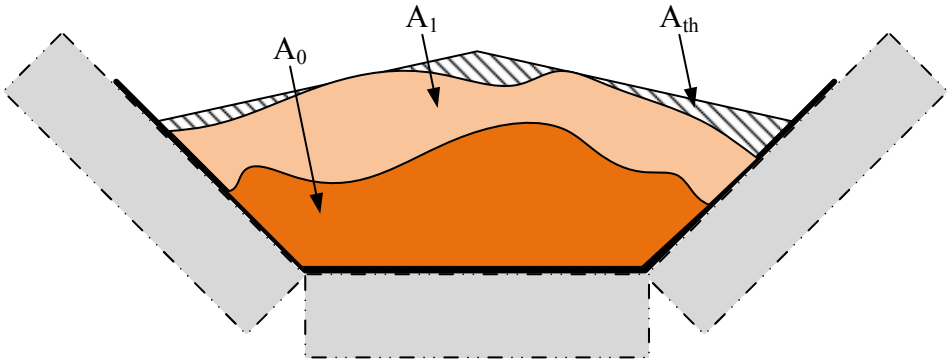

Figure 2.2. Optimal conveyor speed control: Cross section variation

cross-section during the control effort towards the achievement of the theoretical cross section A_{th}. In so doing, the belt and the motors are more efficiently used, while the required material throughput is still achieved. A variant of this method considers the control of the motor torque in the control strategy as well [16].

During the normal functioning of an industrial plant, the amount of material requested at the offloading point of a conveyor system can fluctuate over time or remain constant based on the characteristics of the production process downstream. Whenever a storage area is available in the vicinity of the offloading point, further cost savings can be expected when the control strategy also takes advantage of this resource. The economic benefits drawn from it can be substantial in case the belt conveyor is operated under an electricity tariff variable throughout the day. In light of the above, different scenarios of conveyor systems operated under time-of-use electricity tariff and controlled by optimal control strategies, with the conveyor speed and the material feeding rate as control variables, have been investigated in the past [3, 17, 18, 19, 20, 21]. Taking into account the possible risks of deviation due to factors such as the accuracy limitations of the models involved, alternative solutions built on the model predictive control theory was also proposed for systems supplied under time-of-use electricity tariff [22, 23] as well as under critical peak pricing [24].

Other studies on the optimal operation of conveyors in the literature include the optimal load shifting within a group of belt conveyors [25] and the optimal power flow management between motors [26].

2.5 BELT CONVEYOR TECHNOLOGY EFFICIENCY

On average, 60% of the power supplied to a belt conveyor is used to compensate the indentation resistance between the belt and the idler rolls [11]. To assist in reducing this friction resistance, the first strategy consists of improving the design of troughing idler systems. Here, the impact of various idler rolls has been investigated [27], and diverse configurations of troughing idler arrangements have been explored in the literature [28, 29]. The second strategy involves gaining a better understanding of the phenomena that underpins this frictional resistance. In this category, advanced modeling of the indentation resistance has been reported [30, 31, 32, 33]. The proposed models reduce the oversizing of equipment caused by the frequent overestimate of this resistance component.

Besides the interaction between the belt and the idler troughing system, some other factors relevant to the power consumption of belt conveyors include, but are not limited to, the efficiency of VSD, motor, and gear reducer, the degree of fill, belt width, and drive configuration. Their individual influence on the future power consumption of a conveyor system has been investigated in the past [34].

Generally, the scope of energy efficiency initiatives presented above focuses on the operating stage of belt conveyors. In this context, only part of the costs incurred in the life of a conveyor can be improved through the implementation of these initiatives. As with any industrial project, the total expenditure incurred over the life cycle of a belt conveyor consists, however, of two different components: the capital and operating costs. The possibility to improve the overall economic performance of belt conveyors have been investigated in the past [35, 36]. This involves the formulation of an optimization problem that intends to minimize the life cycle cost of the conveyor system, while the different operating and technical requirements are satisfied. The set of design parameters considered in these studies include the belt width, conveyor speed, rated motor power, rated gear reducer torque, idler roll diameters, and spacing, etc. While the proposed design strategies have proven to be effective, their scope is however limited to the single drive technology and conveyor systems made up of several single drive belt conveyors arranged one after the other. Despite the known potential of multiple drive belt conveyors in this particular matter, their cost-effective design has not been addressed in previous studies.

2.6 MULTIPLE DRIVE BELT CONVEYOR DEVELOPMENT

Facing the need for longer belt conveyors with higher transportation capacity in the late 1970s, the underground mining sector was first to conceive the idea of distributing drive power along the pathway of belt conveyors. With the continuous lenghetning of panels, aspects such as the weight of reinforced belting and the large size of high power drives became crucial when it came to handle and move around conveyors. Since then, conveyor manufacturers have started to develop the multiple drive technology, which is today largely adopted, especially, in underground coal mines [5].

In order to transmit power along the belt length, a certain number of alternatives have been tested over time. One of the pioneering approaches involved the use of simple car tyres, which is illustrated in Figure 2.3. In the absence of wrapping around pulleys, the power was transmitted by pressing tyres on both sides of the belting.

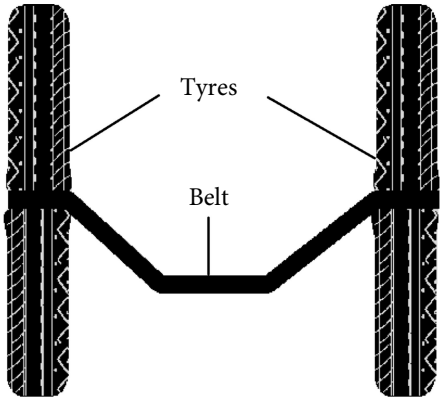

Figure 2.3. Belt conveyor using car tyres. Republished with permission of Trans Tech Publications Ltd, from "The Evolution of Intermediate Driven Belt Conveyor Technology," M.A. Alspaugh, Vol. 23, No. 3, 2017.

A second approach, which overtook the previous one and was more frequent in the past, is known as the belt-on-belt drive or linear drive. Illustrated in Figure 2.4, the concept consists of building small conveyors inside the main conveyor. While a normal flat pulley is used to transmit power to each small conveyor, the friction between the belt surfaces ensures the transmission of power from the smaller conveyors to the larger conveyor. Although conveyor manufacturers used to strongly recommend this design in the past, and many of them were installed in the mid to late 1980s, the application of belt-on-belt conveyors has been stopped since that time. Among the problems encountered were the

significant extra expenses necessary to implement the driving conveyors and the need for an interactive torque control mechanism [5].

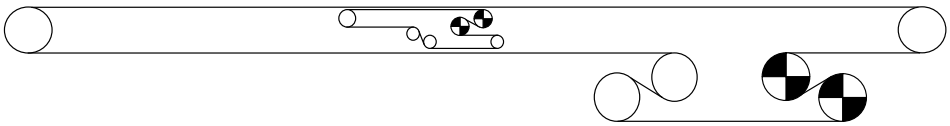

Figure 2.4. Belt-on-belt drive or linear drive concept. Adapted with permission of Trans Tech Publications Ltd, from "The Evolution of Intermediate Driven Belt Conveyor Technology," M.A. Alspaugh, Vol. 23, No. 3, 2017.

From the later 1980s, the conveyor manufacturers have progressively migrated to a third arrangement named tripper drive configuration shown in Figure 2.5. Although wrapping of the belt around flat pulleys was required, the decisive benefits associated with this concept include the ease of installation and removal, the soft interaction between belt and power drivers, and the low spillage and cleanup involved. Nowadays, no belt-on-belt conveyor is still in operation in the United States, and all new constructions are either similar to or variants of Figure 2.5 [5].

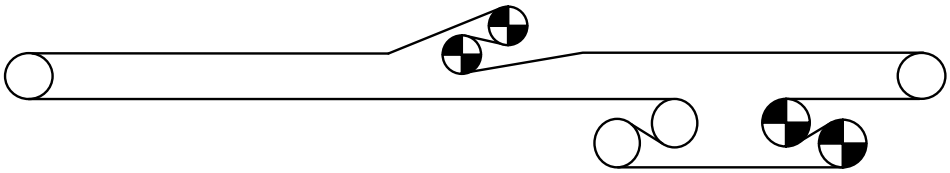

Figure 2.5. Belt conveyor using tripper drive. Adapted with permission of Trans Tech Publications Ltd, from "The Evolution of Intermediate Driven Belt Conveyor Technology," M.A. Alspaugh, Vol. 23, No. 3, 2017.

Except for these classical multi-drive belt conveyors, a number of special arrangements have been recently reported. The first illustrated in Figure 2.6 considers a drive strip vulcanized on the underside of the belt. To transmit power to the belt, two drive wheels with individual motors press on both sides of the strip. Initially, this arrangement was underpinned by the need for a trough-shaped belt with relatively low strength, in order to easily negotiate sharp radii of horizontal curves [37].

Closed belt conveyors illustrated in Figure 2.7 have also been proposed. The basic design principle consists to enclose the conveyed material inside the belt, which is then kept folded and closed. The drive wheels are placed at the top of the system, along the edges of the belt. Once the belt in Figure 2.7a, referred to as Enerka-Becker System (or EB-S), is folded and closed, the triangle profiles vulcanized

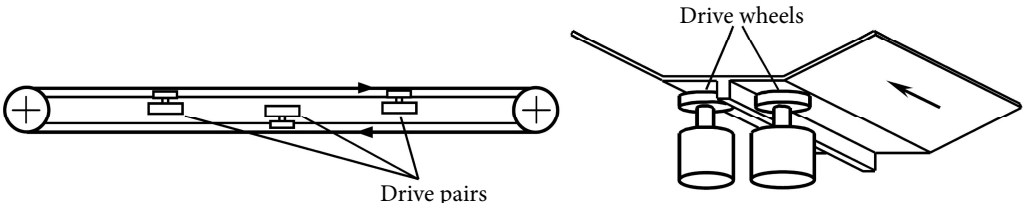

Figure 2.6. Belt conveyor using drive strip. Taken from [37], with permission.

onto its edges enable it, in theory, to relocate a drive wheel anywhere along the installation. In the case of Sicon pouch conveyor systems, shown in Figure 2.7b, such a displacement is prevented as it will appreciably affect the layout of the conveyor [37].

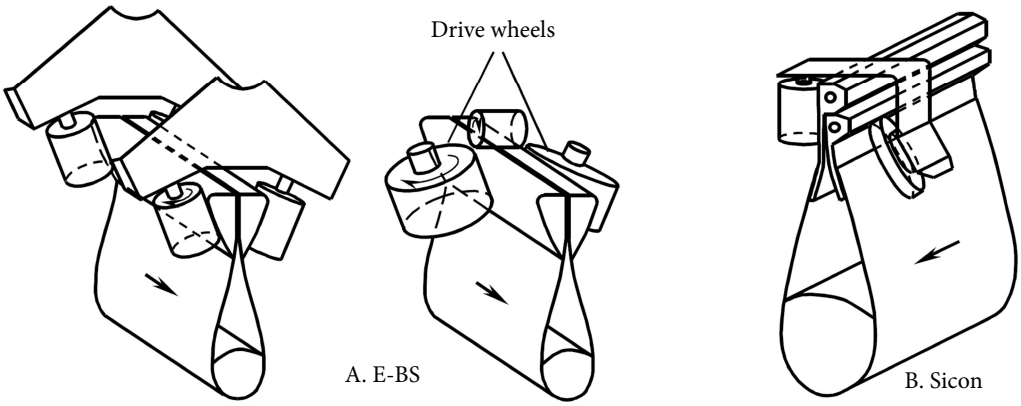

Figure 2.7. Closed belt conveyor systems. Taken from [37], with permission.

Some concerns that emerge with the application of a multiple drive layout in belt conveyor systems include:

- finding the most appropriate design solution for a specific task
- starting-up the conveyor system in such a way as to limit the stress on the belt
- managing the power drives in steady-state operation in order to reduce the operating cost incurred

While limited information on the start-up of these conveyor systems is available in the current guidelines, a recent study has established some similarities between the dynamic behaviors of a single driven belt conveyor and a multiple drive conveyor system when a speed controlled starting procedure is applied to both installations [38].

2.7 RESEARCH GAP

The review of the literature presented in the previous section has established the existence of a significant scientific literacy in the area of belt conveyor energy efficiency. Although many aspects have been investigated to improve the economic indicators of conveyor systems, the large majority of previous contributions have focused on their operating stage. In so doing, only part of the expenses incurred throughout the conveyor life cycle was considered by the proposed initiatives.

It has also been noticed that limited research efforts have been dedicated to improve the entire life cycle cost of belt conveyors at once. The particular case of multiple drive belt conveyors has not, however, been covered by these studies. Therefore, to the best of the author's knowledge, the question of the optimal design of multiple drive belt conveyors that minimizes their life cycle cost has not been investigated yet. In light of their economic potential, as discussed earlier in this dissertation, this problem is deemed worthwhile for investigation.

As the first contribution intended to fill the identified gap, the next chapters of the present document report the investigation of an optimal design approach for multiple drive belt conveyor systems. Since most of the modern belt conveyors of this type are based on the arrangement with trippers [5], this configuration has been adopted for the rest of this research work.

CHAPTER 3 PROBLEM FORMULATION

3.1 CHAPTER OVERVIEW

In this chapter, the development of an optimization model for the cost-effective design of multiple drive belt conveyors is undertaken. This mathematical model is expected to identify the optimal values for the design parameters of such a system in order to minimize its life cycle cost. To achieve this goal, a brief outline of the conveyor system concerned is first given, followed by a preliminary formulation of the optimization investigated. The expression of the equivalent annual cost of the conveyor system is then developed. Subsequently, the components of the resistance to the movement of the belt conveyor are identified, modeled and then associated to the position where they occur along the installation. Next, the various design and operation conditions that apply to the multi-drive belt conveyors are formulated. These relationships are derived from the design procedure indicated in the DIN 22101 and SANS 1313 standards. In the absence of standard recommendations on the start-up procedure of multiple drive belt conveyors, only the technical requirements regarding the steady-state operating conditions are considered in this study. The influence of the non-steady operating conditions is, however, partially taken into consideration through the belt safety factors [7]. Finally, the two optimization problems that minimize the life cycle cost of multi-drive belt conveyors and single drive belt conveyors, respectively, are presented. Part of the results of the investigations conducted in the chapter serve to answer the research questions 1 and 2.

3.2 DESCRIPTION OF THE MULTI-DRIVE BELT CONVEYORS

Fig. 3.1 shows a typical modern uphill multi-drive belt conveyor intended to transfer a bulk material of density ρ over a transport distance L with a lift height H. This system is made up of an upper stretch

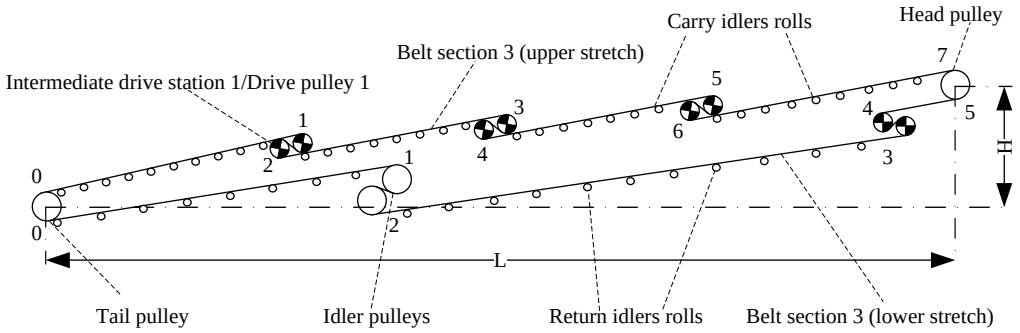

Figure 3.1. Multiple drive belt conveyor layout. Adapted with permission of Trans Tech Publications Ltd, from "The Evolution of Intermediate Driven Belt Conveyor Technology," M.A. Alspaugh, Vol. 23, No. 3, 2017.

and a lower stretch subsequently identified by the subscripts o and u, respectively. The upper stretch carries the bulk material fed from the loading stations distributed along the conveyor path, starting at the tail pulley, to the various offloading stations, also distributed along the conveyor path with the last one located at the head pulley. The lower stretch returns the empty belt from the head pulley to the tail pulley. Besides these idler pulleys, the conveyor system also includes in the upper stretch one or more pairs of drive pulleys mounted in tandem, and in the lower stretch, a unique pair of drive pulleys also mounted in tandem and one or more other pairs of idler pulleys. A motor-gear reducer system is mounted on the shaft of each drive pulley, which transfers by friction the power delivered by the motor to the belt. The other pulleys are freely driven by the belt. The arc of contact between the belt and a drive pulley is referred to as the wrap angle and is noted by α.

A drive station refers to the unit consisting of a pair of drive pulleys mounted in tandem along with their respective motor-gear reducer systems. A drive station located in the upper stretch of the conveyor is called intermediate drive station. Within a drive station, the drive pulley 1 and drive pulley 2 correspond to, respectively, the first and second pulleys following the belt travel direction. For example, the drive pulley 1 of the drive station 1 is indicated in Fig. 3.1 as the belt moves from right to left. In Fig. 3.1, the belt conveyor includes 3 intermediate drive stations, the general design will however consists of N ($N = 1, 2, \ldots$) intermediate drive stations. The drive stations will be later identified using a fixed index varying between 1 to $N+1$, with the intermediate drive station near the tail pulley identified by 1 and the drive station located in the lower stretch identified by $N+1$.

A belt section is defined as any part of the belt nestled between any two different pulleys. Within

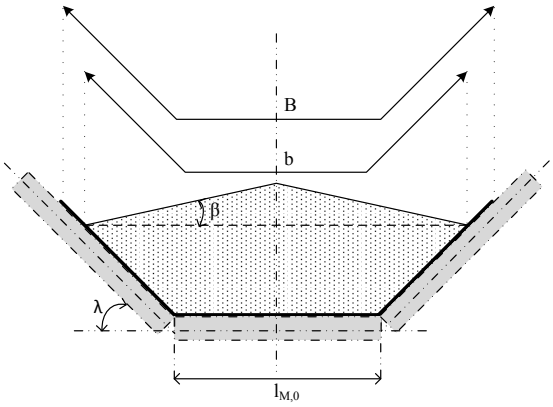

Figure 3.2. Theoretical cross section of fill

each stretch, the edges of each belt section not nestled between two pulleys mounted in tandem are designated by a unique index allocated in ascending order, beginning at the tail pulley noted by default as edge 0 in the two edges. Subsequently, such a belt section is identified using the greatest index between its two edges. For illustration purposes, the belt section 3 in the upper stretch is pointed out in Fig. 3.1, where the whole conveyor system comprises 7 and 5 belt sections in, respectively, the upper and lower stretches. In the more general multi-drive belt conveyor, the number N_o of belt sections not nestled between pulleys mounted in tandem in the upper stretch is determined by N, while the number N_u of belt sections not nestled between pulleys mounted in tandem in the lower stretch depend on the total number of pairs of idler pulleys situated in this stretch. Despite the fact that the number of idler pulleys can vary from one system to another, the present study only addresses multi-drive belt conveyors with a single pair. N_u is therefore fixed at 5. Thereafter, $L_{o,i}$ and $L_{u,j}$ will denote the lengths of the belt sections i and j in the upper and lower stretches, respectively, of the conveyor.

For the purpose of supporting long belt sections, carry and return idler rolls are mounted underneath these parts of the belt as indicated in Figure 3.1. The theoretical shape of the bulk material supported by the carry idler rolls as it transits along the belt conveyor is indicated in Figure 3.2. This concerns only the case of three-idler roll troughing configuration. In this figure, B denotes the belt width, b denotes the usable belt width, β denotes the equivalent angle of slope of the material, λ denotes the troughing angle, and $l_{M,o}$ denotes the length of the shell of a carry idler roll.

Noted by F_T, the belt tension at a given point of the belt is the resultant of the longitudinal forces measured on the transversal section at this specific point. The belt tension at the spot of the first contact between the belt and a drive pulley is called the tight-side tension and noted by F_{T1}. On the other side,

the belt tension at the spot of the last contact when the belt leaves a drive pulley is called the slack-side tension and noted F_{T2}. Analogously, $F_{T1,i}$ and $F_{T2,i}$ will denote, respectively, the tight-side tension and the slack-side tension of the drive station i. The nominal breaking strength of the belt related to belt width, noted by k_N, is the minimum rupture force of the belt per unit of belt width. Finally, long belt conveyors usually require to be fitted with a tensioning equipment, also referred to as take-up device (not shown in Figure 3.1), in order to prevent the slippage between the belt and the drive pulleys. The belt tension on each side of the take-up device is noted by F_{TU}. The rest of this study investigates the multi-drive belt conveyors fitted with a unique take-up device.

3.3 DESIGN OBJECTIVE

A conveying operation can be specified by L, H, Q, ρ and β. For such a material transfer task, a significant variety of multi-drive conveyor systems can be envisaged, which will generally have different cost implications over the project lifetime. The objective is therefore to find the design solution that results in the lowest life cycle cost. To ease the comparison between belt conveyor designs, the equivalent annual cost $A_{conveyor}$ of a belt conveyor is adopted as the performance indicator instead of directly inspecting the life cycle cost.

Given N, the optimization problem that allows the determination of the design solution with the lowest $A_{conveyor}$ is stated as

$$\begin{aligned} \min_{X} \quad & A_{conveyor} \\ \text{s.t.} \quad & G(X) = 0, \\ & H(X) \geq 0, \end{aligned}$$

where X denotes the set of design parameters and G and H denote, respectively, the sets of equality and inequality constraints relating to the belt dynamics and design conditions as is detailed later in this chapter. The direct comparison of the minimum $A_{conveyor}$ obtained for different values of N will subsequently lead to the most cost-effective multi-drive conveyor design in terms of N and X.

By keeping the two driving subsystems of each drive station i ($i = 1, \ldots, N+1$) identical in all respects, the design vector X considered in this study consists of the rated power of each motor in the drive station i, P_i, the rated torque of each gear reducer in the drive station i, T_i, the diameter of each drive

pulley in the drive station i, $D_{tr,i}$, the wrap angle of each drive pulley in the drive station i, α_i, $L_{o,j}$ of the belt sections j ($j = 1,3,\ldots,N_o$) not nestled between drive pulleys, the belt width, B, the belt speed, v, the spacing between idler rolls in the upper stretch, l_o, the spacing between idler rolls in the lower stretch, l_u, the diameter of idler rolls in the upper stretch, D_o, the diameter of idler rolls in the lower stretch, D_u, the shaft diameter of idler rolls in the upper stretch, d_o, the shaft diameter of idler rolls in the lower stretch, d_u, k_N and F_{TU}.

3.4 ECONOMIC CONSIDERATIONS

Various expenses are incurred during the life cycle of a belt conveyor. Fundamentally, all these costs can be classified into two different categories: the capital and operating costs. The former concerns all the expenditures incurred from the purchase to the commissioning of belt conveyor components, while the latter involves the expenditures necessary to operate these equipment throughout the project lifetime. The life cycle cost of the conveyor system is made up of all these costs. Its calculation considers factors such as the inflation rate, the tax rate, the proportions of debt capital and equity funds, their respective rate of return, etc. The life cycle cost of a conveyor can also be converted to an equivalent annual cost. The next sections formulate the equivalent annual costs of multi-drive belt conveyor systems.

3.4.1 Operating costs of multiple drive belt conveyors

Generally, the operating costs related to a conveyor system consists of the following three contributions:

- energy cost
- maintenance cost
- labour cost

The maintenance cost of a multi-drive belt conveyor can be expected to vary as a function of some of the design parameters listed in Section 3.3, including the number of drive stations and their respective

size, the conveyor speed and the belt width. On the other hand, the size of the plant, the planned production and the requirements of local labor laws are among the factors commonly used for setting the wage and number of workers [1]. To the best of our knowledge, there are, however, no previous studies that have investigated the actual relation between the design parameters listed in Section 3.3 and the operating costs for the maintenance and labor of belt conveyors. In this context, the energy cost is the only contribution considered in the rest of this study.

Denote k_0 the equivalent annual energy cost coefficient, e_{co} the energy cost in year zero of the project, t_a the operating hours of the system per annum and $\eta_{mot,i}$ the efficiency of motors situated in the drive station i, the equivalent annual energy cost in year zero A_{energy} of a multi-drive belt conveyor with N intermediate drive stations, each drive station made up of two driving systems motor-gear reducer-drive pulley, is given by:

$$A_{energy} = k_1 e_o t_a \sum_{i=1}^{N+1} 2P_i/\eta_{mot,i}. \tag{3.1}$$

The procedure for calculating k_0 is presented in Addendum A.1.

3.4.2 Capital costs of multiple drive belt conveyors

The following belt conveyor components are considered for the calculation of the capital costs of belt conveyors:

- belt
- electric motors
- gear reducers
- carry idler rolls
- return idler rolls

Despite their significance in the economy of belt conveyors, the difficulty faced in getting information from manufacturers of other components such as the supporting structure, pulleys and tensioning device compelled the author to temporarily ignore their impacts in this study. Moreover, given that the cost of the supporting structure is further dictated by the landforms, this capital cost item will vary from case to case.

Denote k_{eq} the equivalent annual cost coefficient of an equipment (belt, motor, etc.) and $C_{eq,0}$ the first costs of this equipment at the year zero of the project, the equivalent annual cost A_{eq} of the equipment is expressed by [35]:

$$A_{eq} = k_{eq} C_{eq,0}. \tag{3.2}$$

Addendum A.2 describes the procedure for calculating k_{eq}.

Taking into account the findings from previous investigations on the capital cost of belt conveyors [35, 36] as well as the manufacturers supplied information (see Chapter 4), the following function were established for the purchase costs of the belt conveyor components listed above as functions of the design parameters listed in Section 3.3:

$$C_{belt,0} = BK\left(c_1 + c_2 k_N^{c_3}\right), \tag{3.3}$$

$$C_{motor,i,0} = c_4 + c_5 P_i^{c_6}, \tag{3.4}$$

$$C_{gear,i,0} = c_7 + c_8 T_i^{c_9}, \tag{3.5}$$

$$C_{carryidler,0} = c_{10} + c_{11} d_o^{c_{12}} + c_{13} D_o^{c_{14}} + c_{15} B^{c_{16}}, \tag{3.6}$$

$$C_{returnidler,0} = c_{17} + c_{18} d_u^{c_{19}} + c_{20} D_u^{c_{21}} + c_{22} B^{c_{23}}. \tag{3.7}$$

In these equations, K denotes the total length of the belt along the conveyor path and c_1 to c_{23} are the initial cost coefficients, which are calculated using the price information supplied by the manufacturers. The total length of the belt is approximated by:

$$K = 2L/\cos\delta + y_1 N + y_2, \tag{3.8}$$

where y_1 and y_2 are constant coefficients related to, respectively, the part of the belt wrapped around the intermediate drive pulleys and a reserve factor.

Taking into account (3.2) and (3.3) to (3.7), the equivalent annual costs of the components of a multi-drive belt conveyor consisted of N intermediate drive stations are given by:

$$A_{belt} = k_1 BK\left(c_1 + c_2 k_N^{c_3}\right), \tag{3.9}$$

$$A_{motor} = k_2 \sum_{i=1}^{N+1} \left(c_4 + c_5 P_i^{c_6}\right), \tag{3.10}$$

$$A_{gear} = k_3 \sum_{i=1}^{N+1} \left(c_7 + c_8 T_i^{c_9}\right), \tag{3.11}$$

$$A_{carryidler} = \xi_o k_4 \sum_{j=1}^{N_o} \frac{L_{o,j}}{l_o} \left(c_{10} + c_{11} d_o^{c_{12}} + c_{13} D_o^{c_{14}} + c_{15} B^{c_{16}}\right), \tag{3.12}$$

$$A_{returnidler} = \xi_u k_5 \sum_{j=1}^{N_u} \frac{L_{u,j}}{l_u} \left(c_{17} + c_{18} d_u^{c_{19}} + c_{20} D_u^{c_{21}} + c_{22} B^{c_{23}}\right), \tag{3.13}$$

where k_1 to k_6 are the respective equivalent annual cost coefficients, ξ_o denotes the number of idler rolls per set on the carry side, and ξ_u denotes the number of idler rolls per set on the return side. In this study, ξ_o is equal to 3 (see Fig. 3.2) and ξ_u is equal to 1 (flat return idler).

3.4.3 Equivalent annual cost of multiple drive belt conveyors

Taking into account (3.1) and (3.9) to (3.13), the equivalent annual cost of a typical multiple drive belt conveyor with N intermediate drive stations is given by:

$$A_{conveyor} = A_{energy} + A_{belt} + 2\sum_{i=1}^{N+1} A_{motor,i} + 2\sum_{i=1}^{N+1} A_{gearreducer,i} + A_{carryidler} + A_{returnidler}. \tag{3.14}$$

3.5 RESISTANCES TO MOTION IN A MULTIPLE DRIVE BELT CONVEYOR

The resistance to belt movement in any belt section can be decomposed into the following four components: the primary resistance, the secondary resistance, the slope resistance and the special resistance. The models of these resistance forces in the next sections are derived from the DIN 22101 standard [7].

3.5.1 Primary resistance

The primary resistance $F_{H,j}(N)$ in a belt section j concerns the resistance forces distributed throughout the entire path of the belt conveyor. It consists of the resistance caused by the indentation of the belt

covers on the idler rolls, the rotational resistance of idler rolls, and the flexing resistance. Irrespective of the belt stretch, the total primary resistance $F_{H,j}$ can be approximated by:

$$F_{H,j} = L_j f_j \left[m'_{R,j} + \left(m'_G + m'_{L,j} \right) \cos \delta_j \right] g, \tag{3.15}$$

where L_j denotes the length of the section, f_j denotes the hypothetical friction coefficient, g denotes the gravitational acceleration, $m'_{R,j}$ denotes the total mass of the rotating part of idler rolls per running meter of belt, m'_G denotes the linear mass of the belt, $m'_{L,j}$ denotes the linear mass of the material conveyed, and δ_j denotes the inclination angle of the belt section j.The factor $m'_{L,j}$ vanishes for the sections situated in the lower stretch.

Varying usually between 0.010 and 0.040, the magnitude of f_j is influenced by factors such as internal friction of conveyed material, belt tension, idler roll diameters, conveyor speed, troughing angle, etc.

The total mass of the rotating part of idler rolls per running meter of the belt is given by:

$$m'_{R,j} = \xi_j m_{R,j} / l_j, \tag{3.16}$$

where $m_{R,j}$ denotes the total mass of the rotating parts of each idler roll situated in the belt section j, ξ_j denotes the number idler rolls per set in the section j, and l_j the average spacing between idler rolls in the same belt section. As derived in the Addendum B, the mass of the rotating parts of an idler roll is estimated by:

$$m_{R,j} = z_1 D_j^{z_2} B^{z_3} + z_4 d_j, \tag{3.17}$$

where z_1 to z_5 are the model coefficients, D_j denotes the shell diameter of idler rolls situated in the belt section j, and d_j denotes the shaft diameter of idler rolls situated in the same belt section.

The linear mass of the belt is obtained by:

$$m'_G = \gamma_{belt} B, \tag{3.18}$$

where γ_{belt} denotes the specific mass of the belt. As derived in Addendum C, the specific mass of steelcord belts can be estimated by:

$$\gamma_{belt} = m_1 + m_2 k_N, \tag{3.19}$$

where m_1 and m_2 denote the model coefficients.

The linear mass of the material conveyed is given by:

$$m'_{L,j} = \rho A_{th}, \tag{3.20}$$

where A_{th} denotes the theoretical cross section of fill. In the case of the three-idler roll troughing configuration shown in Figure 3.2, A_{th} is given by:

$$A_{th} = \left[l_{M,o} + (b - l_{M,o})\cos\lambda\right]^2 \frac{\tan\beta}{4} + \left(l_{M,o} + \frac{b - l_{M,o}}{2}\cos\lambda\right)\frac{b - l_{M,o}}{2}\sin\lambda\,. \tag{3.21}$$

3.5.2 Secondary resistance

The secondary resistance $F_{N,j}$ groups together the friction and inertia resistance forces that occur only in some spots of the belt conveyor.

The first resistance factor is caused by the inertia resistance of material conveyed and the friction resistance between the belt and conveyed material in the loading zone. Noted by $F_{Auf,j}$, this resistance component is given by:

$$F_{Auf,j} = \frac{Q}{\rho}\left(v - v_{0,j}\right), \tag{3.22}$$

where $v_{0,j}$ denotes the initial speed of material in the direction of belt movement.

The second resistance factor is induced by the friction between lateral chutes and the belt in the acceleration zone of a loading point, and is noted by $F_{Schb,j}$. The arrangement of the lateral chutes in the case of the three-idler troughing configuration is illustrated in Figure 3.3. On condition that $b_{Sch} > l_M$ and $0 \leq v_{o,j} \leq v$, $F_{Schb,j}$ is given by:

$$F_{Schb,j} = C_{Schb}C_{Rank}\left[\frac{2Q}{(v + v_{0,j})\rho^2} - \left(b_{Sch}^2 - l_M^2\right)\frac{\tan\lambda}{4}\right]^2 \frac{\rho g l_b \mu_2}{b_{Sch}^2}, \tag{3.23}$$

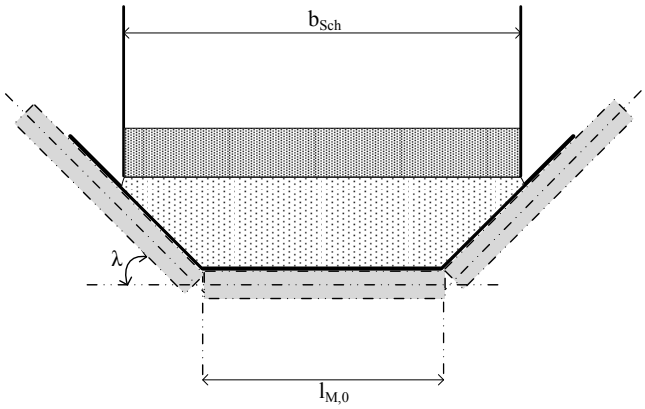

Figure 3.3. Lateral chutes arrangement

such as

$$l_b > l_{b,min} = \frac{v^2 - v_0^2}{2g\mu_1}, \tag{3.24}$$

$$c_{Rank} = \tan^2\left(45^\circ - \frac{\beta_{dyn}}{2}\right). \tag{3.25}$$

In (3.26), C_{Schb} is the coefficient that accounts for the additional resistance between material and lateral chutes due to the dynamic pressure of material flow on the belt, C_{Rank} is the Rankine factor, b_{Sch} denotes the clear width between lateral chutes, l_b denotes the length of the acceleration zone in the loading point, β_{dyn} denotes the dynamic angle of slope of the material conveyed, μ_1 denotes the friction coefficient between conveyed material and belt, and μ_2 denotes the friction coefficient between conveyed material and lateral chutes.

The last resistance factor is due to the contact between the belt cleaners and the belt, and is noted by $F_{Gr,j}$. The following relation is used to determine this factor:

$$F_{Gr,j} = \mu_4 p_{Gr} A_{Gr}, \tag{3.26}$$

with μ_4, p_{Gr}, and A_{Gr} denote, respectively, the friction coefficient between belt and belt cleaner, the pressure between belt and belt cleaner, and the effective contact area between belt and belt cleaner.

The overall model of the secondary resistance in a section j is therefore the combination of these three components:

$$F_{N,j} = F_{Auf,j} + F_{Schb,j} + F_{Gr,j}. \tag{3.27}$$

In order to reduce the lateral movement of the belt, chutes are usually positioned on both sides of the belt after each intermediate drive stations. Accordingly, in the case of a multi-drive belt conveyor with N intermediate drive stations, $F_{Auf,j}$ and $F_{Schb,j}$ will apply to the odd belt sections (1, 3, 5, 7, etc) in the upper stretch, while $F_{Gr,j}$ will be only considered in the belt sections where the belt cleaner are installed.

3.5.3 Slope resistance

The slope resistance $F_{G,j}$ in a belt section j is the force required to lift or lower the belt and the conveyed material to the difference height between the two edges of this belt section. The following relation is used to determine this resistance component:

$$F_{G,j} = L_j \sin\delta_j \left(m'_G + m'_{L,j}\right) g, \tag{3.28}$$

where δ_j denotes the inclination angle of the belt section. In applying the above equation, the inclination angle δ_i is such as $\delta_i > 0$ for uphill belt movement, and $\delta_i < 0$ for downhill belt movement.

3.5.4 Special resistances

The rest of resistances which arise only in belt conveyors designed for extraordinary purposes are classified as part of the special resistance component, noted by $F_{S,j}$. The common causes of special resistances include tilting of idler position, chutes outside loading points, devices for lateral material transfer along the conveyor path. Details on the calculation of these components are available in the reference [7].

The total resistance to belt movement $F_{W,j}$ in any section j can be therefore expressed by:

$$F_{W,j} = F_{H,j} + F_{N,j} + F_{G,j} + F_{S,j}. \tag{3.29}$$

Considering the individual contribution of the belt sections situated in the upper lower stretches, the overall resistance to belt movement $F_W(N)$ is given by:

$$F_W = F_{W,o} + F_{W,u} = \sum_{k=1}^{N_o} F_{W,o,k} + \sum_{k=1}^{N_u} F_{W,u,k}, \tag{3.30}$$

where $F_{W,o}$ and $F_{W,u}$ denote, respectively, the overall resistance in the upper and lower stretches of the system, and $F_{W,o,k}$ and $F_{W,u,k}$ denote the overall resistance in the belt section k in, respectively, the upper and lower stretches of the system.

3.6 FORMULATION OF THE TIGHT-SIDE TENSIONS, SLACK-SIDE TENSIONS AND TAIL TENSION OF MULTI-DRIVE BELT CONVEYORS

Considering the typical drive pulley displayed in Figure 3.4, the peripheral force applied by the drive pulley on the belt, noted by F_{Tr}, the tight-side and slack-side belt tensions of the pulley are related by:

$$F_{T1} = F_{Tr} + F_{T2}. \tag{3.31}$$

Also, the following relation is verified in the subsystem motor-gear reducer-pulley:

$$F_{Tr} v = \eta_{gear} P, \tag{3.32}$$

where P and η_{gear} denote the output power of the motor and the gear reducer efficiency, respectively.

In the upper stretch of a typical multi-drive belt conveyor, the belt tension $F_{T,o,i}$ at the edge i is given by:

$$F_{T,o,i} = \begin{cases} F_0 + F_{W,o,1}, & \text{for } i = 1, \\ F_0 + \sum_{j=1}^{i} F_{W,o,j} - 2\sum_{k=1}^{m} F_{Tr,k}, & \text{for } i = 2, \ldots, N_o, \end{cases} \tag{3.33}$$

with

$$m = \left\lceil \frac{i-1}{2} \right\rceil.$$

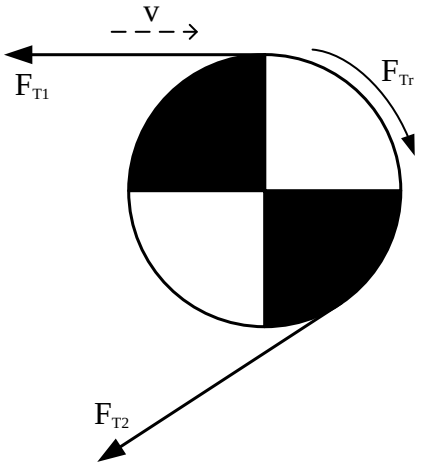

Figure 3.4. Belt tensions around a drive pulley

The ceiling function $\lceil \cdot \rceil$ rounds a real number upwards to the nearest integer. In (3.33), F_0 and $F_{Tr,k}$ denote, respectively, the belt tension at the tail pulley and the total peripheral force applied by the two drive pulleys situated in the drive station k.

On the other side, with a total number of belt sections N_u equal to 5, the belt tension $F_{T,u,i}$ at the edge i of the lower stretch is given by:

$$F_{T,u,i} = \begin{cases} F_0 + \sum_{j=1}^{N_o} F_{W,o,j} - 2\sum_{k=1}^{N+1} F_{Tr,k} + \sum_{j=i-1}^{N_u} F_{W,u,N_u}, & \text{for } i = 1,\ldots,N_u-2, \\ F_0 + \sum_{j=1}^{N_o} F_{W,o,j} - 2\sum_{k=1}^{N} F_{Tr,k}, & \text{for } i = N_u, \\ F_0 + \sum_{j=1}^{N_o} F_{W,o,j} - 2\sum_{k=1}^{N} F_{Tr,k} + F_{W,u,N_u}, & \text{for } i = N_u-1. \end{cases} \tag{3.34}$$

According to (3.32), $F_{Tr,k}$ in (3.33) and (3.34) is obtained by:

$$F_{Tr,k} = 2\frac{\eta_{gear,k} P_k}{v}. \tag{3.35}$$

Based on the relative locations of the drive stations, the tight-side tension $F_{T1,j}$ of the drive station j of a typical multi-drive belt conveyor is given by:

$$F_{T1,j} = \begin{cases} F_{T,o,2j-1}, & \text{for } j = 1,\ldots,N, \\ F_{T,u,N_u-1}, & \text{for } j = N+1, \end{cases} \tag{3.36}$$

Taking into account (3.33) to (3.35), (3.36) can be expressed by:

$$F_{T1,j} = \begin{cases} F_0 + F_{W,o,1}, & \text{for } j = 1, \\ F_0 + \sum_{i=1}^{2j-1} F_{W,o,1} - 2\sum_{i=1}^{j-1} \frac{\eta_i P_i}{v}, & \text{for } j = 2,\ldots,N, \\ F_0 + \sum_{i=1}^{N_o} F_{W,o,1} + F_{W,o,N_u} - 2\sum_{i=1}^{N} \frac{\eta_i P_i}{v}, & \text{for } j = N+1, \end{cases} \tag{3.37}$$

Similarly, the slack-side tension $F_{T2,j}$ of the drive station j of a typical multi-drive belt conveyor is given by:

$$F_{T2,j} = \begin{cases} F_{T,o,2j}, & \text{for } j = 1,\ldots,N, \\ F_{T,u,N_u-2}, & \text{for } j = N+1, \end{cases} \tag{3.38}$$

Taking into account (3.33) to (3.35), (3.38) can be expressed by:

$$F_{T2,j} = \begin{cases} F_0 + \sum_{i=1}^{2j} F_{W,o,i} - 2\sum_{k=1}^{j} \frac{\eta_{gear,k} P_k}{v}, & \text{for } j = 1,\ldots,N, \\ F_0 + \sum_{j=1}^{N_o} F_{W,o,j} + F_{W,u,N_u} - 2\sum_{k=1}^{N+1} \frac{\eta_{gear,k} P_k}{v}, & \text{for } j = N+1, \end{cases} \tag{3.39}$$

In the formulation of the belt tension F_0 at the tail pulley, it is assumed beforehand that the primary resistances in all the belt sections of the multi-drive belt conveyor have the same constant value of the hypothetical friction factor. Depending on the magnitude of the slope resistance in the belt sections 1 and 3 (or N_{u-2}) of the lower stretch, the belt tension of the system will reach the minimum value at either the tail or the slack-side of the drive station situated in the lower stretch. By systematically fitting the take-up device at the spot of the minimum belt tension, the belt tension F_0 at the tail of the conveyor can be therefore calculated as follows

$$F_0 = \begin{cases} F_{TD}, & \text{if } F_{W,o,1} \leq 0 \text{ and } F_{W,o,3} \leq 0, \\ F_{TD} + F_{W,o,1} + F_{W,o,3}, & \text{if } F_{W,o,1} \geq 0 \text{ and } F_{W,o,3} \geq 0, \end{cases} \tag{3.40}$$

where F_{TD} denotes the belt tension on both sides of the take-up device. The first case refers to the situation with the take-up device installed near the tail pulley, and the second case corresponds to a situation with the take-up device installed near the slack-side of the drive station situated in the lower stretch.

As a contribution to answer the research question 2, the above development indicates that the accommodation of the multi-drive conveyor technology by DIN 22010 requires a few provisions in the calculation of the tight-side and slack-side tensions of a drive station in order to account for the impact of the pulling force of the drive stations situated upstream.

3.7 DESIGN CONSTRAINTS

Unless stipulated otherwise, the belt dynamic and design conditions presented in this section are derived from the DIN 22101 [7].

3.7.1 Material transportation requirements

The following condition aims to ensure the achievement of the required material flow rate:

$$\rho A_{th} v = Q, \tag{3.41}$$

In the particular case of the three-idler troughing configuration shown in Figure 3.3, the usable belt width involved in the calculation of A_{th} in (3.21) is obtained by:

$$b = \begin{cases} 0.9B - 0.05 & \text{if } B \leq 2m, \\ B - 0.25 & \text{if } B > 2m. \end{cases} \tag{3.42}$$

To cover the requirements on the transport distance and the height of lift, the lengths of the carrying belt sections not nestled between drive pulleys, the drive pulley diameters and the horizontal conveying distance should satisfy:

$$\sum_{k=1,3,\ldots}^{N_o} L_{o,k} - \sum_{i=1}^{N} D_{tr,i} = L/\cos\delta. \tag{3.43}$$

3.7.2 Power balance in the belt conveyor

The output power of motors, the belt speed and the overall resistance to belt movement should satisfy:

$$2\sum_{i=1}^{N+1} P_i \eta_{gear,i} - vF_W = 0, \tag{3.44}$$

where $\eta_{gear,i}$ denotes the efficiency of the gear reducers situated in the drive station i.

In a drive station, the rated power of motors and the rated torque of gear reducers are subject to:

$$\frac{2T_i v}{D_{tr,i}} = \eta_{gear,i} P_i, \quad i = 1,\ldots,N+1. \tag{3.45}$$

3.7.3 Belt tension requirements

3.7.3.1 Transmission of pulley peripheral forces

Considering the isolated drive pulley in Figure 3.4, the following condition prevents the belt from slipping over the drive pulley:

$$\frac{F_{T1}}{F_{T2}} \leq e^{\mu\alpha}. \tag{3.46}$$

The successive substitution of (3.32) into (3.31), and (3.31) into (3.46) results in

$$F_{T2} \geq \frac{\eta_{gear} P}{(e^{\mu\alpha} - 1)\, v} \tag{3.47}$$

The wrap factor C_w of the drive pulley is expressed by:

$$C_w = \frac{1}{e^{\mu\alpha} - 1} \tag{3.48}$$

Within the drive station j of a multi-drive belt conveyor, the combined wrap factor $C_{w,j}$ of the pulleys mounted in tandem is given by [39]:

$$C_{w,j} = \frac{1}{e^{2\mu\alpha_j} - 1}, \tag{3.49}$$

where α_j denotes the wrap angle of belt around each pulley situated in the drive station j. Applied to this drive station of a typical multi-drive belt conveyor, the design condition (3.47) becomes:

$$F_{T2,j} \geq \frac{2C_{w,j} P_j \eta_{gear,j}}{v}, \quad j = 1,\ldots,N+1, \tag{3.50}$$

with $F_{T2,j}$ calculated using (3.39).

3.7.3.2 Belt sag limitation

Denote $F_{T,o,min}$ the minimum belt tension to be realized in the upper stretch in order to maintain a relative sag inferior or equal to a specified value h_{rel}, its value is given by:

$$F_{T,o,min} = \frac{g\left(m_L^{'} + m_G^{'}\right) l_o}{8h_{rel}}. \tag{3.51}$$

Apart from the first belt section, the slack-side tension of an intermediate drive station corresponds to the lowest belt tension of the belt section adjacent to it. In this context, the condition (3.51) applies as follows:

$$F_0 \geq \frac{g\left(m_L^{'} + m_G^{'}\right) l_o}{8h_{rel}}, \tag{3.52}$$

$$F_{T2,j} \geq \frac{g\left(m_L^{'} + m_G^{'}\right) l_o}{8h_{rel}}, \tag{3.53}$$

with $j = 1, \ldots, N$.

Similarly, the minimum belt tension $F_{T,u,min}$ to be realized in the lower stretch is given by:

$$F_{T,u,min} = \frac{g m_G^{'} l_u}{8h_{rel}} \tag{3.54}$$

Since the take-up device is always positioned at the spot of the minimum belt tension, the above condition applies as shown below:

$$F_{TD} \geq \frac{g m_G^{'} l_u}{8h_{rel}} \tag{3.55}$$

3.7.3.3 Minimum belt strength requirement

In the sizing of the belt, k_N and the maximum belt tension F_{max} should satisfy the following condition:

$$\frac{k_{t,rel} k_N}{S_0 S_1} \geq \frac{F_{max}}{B}, \tag{3.56}$$

where $k_{t,rel}$ denotes the relative reference endurance strength of the belt, S_0 denotes the belt safety factor related to the splicing conditions, and S_1 denotes the belt safety factors based on the expected

lifetime and the operational conditions. The influence of the nonstationary operating conditions on the maximum belt tension are not considered in this study. The dynamic effects of the transversal and longitudinal vibrations of the belt are also not taken into account. Accordingly, F_{max} will correspond to the greatest magnitude among the tight-side tensions of drive stations.

As displayed in Figure 1.1, the basic principle in designing multi-drive belt conveyor consists of equalizing the tight-side tensions of drive stations so that k_N can be reduced, which directly benefits the weight and the purchase cost of the belt [5, 37]. This additional design condition applies as follows:

$$F_{T1,i} = F_{T1,1}, \tag{3.57}$$

with $i = 2,\ldots,N+1$ and $F_{T1,i}$ determined using (3.37). The condition (3.56) is therefore reformulated as:

$$\frac{k_{t,rel}k_N}{S_0 S_1} \geq \frac{F_{T1,1}}{B}, \tag{3.58}$$

3.7.4 Minimum drive pulley diameter requirements

The useful lifetime of a conveyor belt is primarily determined by the evolution of the condition of two basic constituents: the belt itself and the splices. During the normal functioning of a conveyor system, the belt is subject to bending forces when it moves along a pulley. The smaller the pulley diameter is, the greater the belt deformation and, consequently, the mechanical stress on the belt structure. The following condition applies to the drive pulley diameters in order to ensure that the strength of the splices will endure for at least the expected service life of the belt:

$$D_{tr,j} \geq c_{Tr} d_{Gk}, \quad j = 1,\ldots,N+1. \tag{3.59}$$

Here, c_{Tr} is a constant parameter relevant to the nature of the tensile members (steelcord, polyester, etc.), and d_{Gk} denotes their thickness. In the case of steelcord belts, the k_N and d_{Gk} are related by (see Addendum C):

$$d_{Gk} = m_3 + m_4 k_N^{m_5}, \tag{3.60}$$

where m_3, m_4 and m_5 are model coefficients.

3.7.5 Idler rolls requirements

According to SANS 1313, the maximum load $F_{max,o}$ allowable on a central idler roll varies as a function of the type of idler roll arrangement, the belt length and the characteristics of the shaft of idler rolls [40]. The following condition on the central idler roll in a three-idler roll troughing configuration aims to prevent the risk of premature failure [41]:

$$S_f B_f L_f F_{s,o} \leq F_{max,o}. \tag{3.61}$$

where S_f, B_f , L_f denote the dynamic load factors due to, respectively, the belt speed, the bearing life, and the lump size, and $F_{s,o}$ denotes the static load on the idler roll, which is calculated by:

$$F_{s,o} = \left\{ \gamma_{belt} l_{M,o} + \frac{1}{2} \rho l_{M,o} \left[\frac{1}{2} l_{M,o} \tan\beta + (b - l_{M,o})(\sin\lambda + \cos\lambda \tan\beta) \right] \right\} g l_o. \tag{3.62}$$

Similarly, the load that applies on a flat return idler roll is limited by [41]:

$$S_f B_f C_f F_{s,u} \leq F_{max,u}, \tag{3.63}$$

where C_f denotes the belt flap factor, $F_{s,u}$ denotes the static load, and $F_{max,u}$ denotes the maximum load allowed. The static load is given by:

$$F_{s,u} = \gamma_{belt} l_{M,u} g l_u. \tag{3.64}$$

In accordance with the SANS 1313 standard, which recommends a maximum rotation velocity of 750 rpm for the idler rolls, the following two conditions apply to the carry idler rolls and return idler rolls, respectively:

$$\frac{60v}{\pi D_o} \leq 750, \tag{3.65}$$

$$\frac{60v}{\pi D_u} \leq 750. \tag{3.66}$$

3.7.5.1 Standardization requirements

Wherever the use of identical equipment and settings is mandatory for supply chain and operational effectiveness, the following requirements will add to the previous design conditions:

$$P_i = P_1, \tag{3.67}$$

$$T_i = T_1, \tag{3.68}$$

$$D_{tr,i} = D_{tr,1}, \tag{3.69}$$

$$\alpha_i = \alpha_1, \tag{3.70}$$

for $i = 2, \cdots, N+1$.

3.7.6 Boundary limit requirements

The design parameters should be set within the following ranges of values:

$$0 \leq P_i \leq P_{max}, \quad i = 1, \ldots, N+1, \tag{3.71}$$

$$0 \leq T_i \leq T_{max}, \quad i = 1, \ldots, N+1, \tag{3.72}$$

$$D_{tr,i} \in \mathfrak{D}_{tr}, \quad i = 1, \ldots, N+1, \tag{3.73}$$

$$\alpha_{min} \leq \alpha_i \leq \alpha_{max}, \quad i = 1, \ldots, N+1, \tag{3.74}$$

$$L_{min} \leq L_{o,j} \leq L_{max}, \quad j = 1, \ldots, N_o, \tag{3.75}$$

$$B \in \mathfrak{B}, \tag{3.76}$$

$$0 \leq v \leq v_{max}, \tag{3.77}$$

$$0 \leq k_N \leq k_{N,max}, \tag{3.78}$$

$$0 \leq F_{TU} \leq F_{TU,max}, \tag{3.79}$$

$$l_{o,min} \leq l_o \leq l_{o,max}, \tag{3.80}$$

$$l_{u,min} \leq l_u \leq l_{u,max}, \tag{3.81}$$

$$D_o \in \mathfrak{D}, \tag{3.82}$$

$$D_u \in \mathfrak{D}, \tag{3.83}$$

$$d_o \in \mathfrak{d}, \tag{3.84}$$

$$d_u \in \mathfrak{d}. \tag{3.85}$$

In the above, the quantities with the subscripts *min* and *max* denote, respectively, the lower and upper limits of the related design parameters, $\mathfrak{D}_{tr}$ denotes the set of the possible diameters of drive pulleys, $\mathfrak{B}$ denotes the set of possible belt widths, $\mathfrak{D}$ denotes the set of possible diameters of idler rolls and $\mathfrak{d}$ denotes the set of possible shaft diameters of idler rolls.

To complement the answer to the research question 2, the above development in section 3.7 shows that a few design requirements in DIN 22101 should be given at either drive station level or motor-gear reducer-drive pulley level so as to ensure an effective handling of the multiple drive conveyor technology.

3.8 OPTIMAL DESIGN PROBLEMS

This section provides the complete formulation of the optimization problem of the cost-effective design of multiple drive belt conveyors. The case of single drive belt conveyors is also discussed and the related optimal design problem is subsequently given. The single drive conveyor system will later serve as the reference configuration in the discussion conducted in Chapter 5.

3.8.1 Optimal design problem of multiple drive belt conveyors

Taking into account the design parameters listed in Section 3.3, the economic aspects presented in Section 3.4, and the technical requirements formulated in Section 3.7, the optimization problem of the cost-effective design of a multi-drive belt conveyors with N intermediate drive stations can be stated as: "minimization of (3.14) subject to (3.41), (3.43)–(3.45), (3.50), (3.52), (3.53), (3.55), (3.57)–(3.59), (3.61), (3.63), and(3.65)–(3.70), with the boundary limits (3.71)–(3.85)."

For readability reasons, the full optimization problem is reproduced below.

$$\min_{X} \quad A_{energy} + A_{belt} + 2\sum_{i=1}^{N+1} A_{motor,i} + 2\sum_{i=1}^{N+1} A_{gearreducer,i} + A_{carryidler} + A_{returnidler}$$

s.t. $\rho A_{th} v = Q,$

$$\sum_{k=1,3,\ldots}^{N_o} L_{o,k} - \sum_{i=1}^{N} D_{tr,i} = L/\cos\delta,$$

$$2\sum_{i=1}^{N+1} P_i \eta_{gear,i} - vF_W = 0,$$

$$\frac{2T_i v}{D_{tr,i}} = \eta_{gear,i} P_i, \quad i = 1,\ldots,N+1,$$

$$F_{T2,j} \geq \frac{2C_{w,j} P_j \eta_{gear,j}}{v}, \quad j = 1,\ldots,N+1,$$

$$F_0 \geq \frac{g\left(m_L^{'} + m_G^{'}\right) l_o}{8h_{rel}},$$

$$F_{T2,j} \geq \frac{g\left(m_L^{'} + m_G^{'}\right) l_o}{8h_{rel}}, \quad j = 1,\ldots,N,$$

$$F_{TD} \geq \frac{g m_G^{'} l_u}{8h_{rel}},$$

$$F_{T1,i} = F_{T1,1},$$

$$\frac{k_{t,rel} k_N}{S_0 S_1} \geq \frac{F_{T1,1}}{B},$$

$$D_{tr,j} \geq c_{Tr} d_{Gk}, \quad j = 1,\ldots,N+1,$$

$$S_f B_f L_f F_{s,o} \leq F_{max,o},$$

$$S_f B_f C_f F_{s,u} \leq F_{max,u},$$

$$P_i = P_1,$$

$$T_i = T_1,$$

$$D_{tr,i} = D_{tr,1},$$

$$\alpha_i = \alpha_1,$$

$$\frac{60v}{\pi D_o} \leq 750,$$

$$\frac{60v}{\pi D_u} \leq 750,$$

with the boundary limits

$$0 \leq P_i \leq P_{max}, \quad i = 1,\ldots,N+1,$$

$$0 \leq T_i \leq T_{max}, \quad i = 1,\ldots,N+1,$$

$$D_{tr,i} \in \mathfrak{D}_{tr}, \quad i = 1,\ldots,N+1,$$

$$\alpha_{min} \leq \alpha_i \leq \alpha_{max}, \quad i = 1,\ldots,N+1,$$

$$L_{min} \leq L_{o,j} \leq L_{max}, \quad j = 1,\ldots,N_o,$$

$$B \in \mathfrak{B},$$

$$0 \leq v \leq v_{max},$$

$$0 \leq k_N \leq k_{N,max},$$

$$0 \leq F_{TU} \leq F_{TU,max},$$

$$l_{o,min} \leq l_o \leq l_{o,max},$$

$$l_{u,min} \leq l_u \leq l_{u,max},$$

$$D_o \in \mathfrak{D},$$

$$D_u \in \mathfrak{D},$$

$$d_o \in \mathfrak{d},$$

$$d_u \in \mathfrak{d}.$$

3.8.2 Optimal design problems of single drive belt conveyors

To achieve a fair evaluation of the economic performance of multi-drive belt conveyors in comparison to the common belt conveyors, an optimization model is also formulated for the single drive conveyor technology. The layout considered in this study is shown in Figure 3.5. It consists of a unique drive system positioned at the head pulley.

While the conditions (3.41), (3.52), (3.55), (3.58), (3.59), (3.61), (3.63), (3.65) and (3.66) also apply to this layout, the rest of the design conditions relating to multi-drive belt conveyors need to be revised to account for the absence of intermediate drive stations.

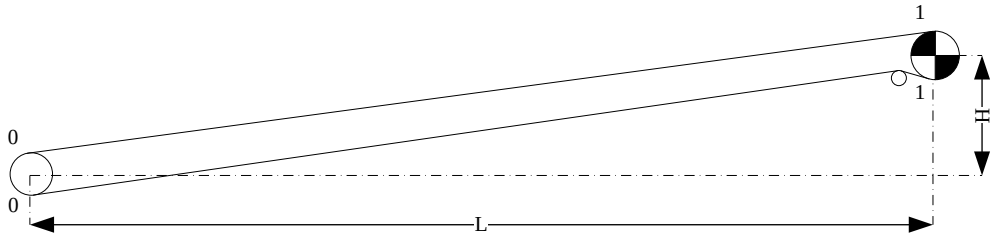

Figure 3.5. Belt conveyor with single pulley drive

In the case of single pulley drive belt conveyors, the relation between the driving power, belt speed and overall resistance given in (3.44) is simplified into:

$$\eta_{gear}P - vF_W = 0, \tag{3.86}$$

The rated torque T of the gear reducer of the conveyor and the output power P of the motor should satisfy:

$$\frac{2Tv}{D_{tr}} = \eta_{gear}P. \tag{3.87}$$

The requirement on the effective transmission of peripheral forces (3.50) becomes:

$$F_0 + F_{W,o} - \frac{\eta_{gear}P}{v} \geq \frac{C_w\eta}{v}. \tag{3.88}$$

The wrap factor C_w in the equation above is given by (3.48).

The design conditions (3.43), (3.53), (3.57) specific to the multi-drive conveyor technology does not apply to the single drive belt conveyor in Figure 3.5.

In regard to the equivalent annual cost of single drive conveyor systems, the cost function (3.14) relating to multi-drive belt conveyors becomes:

$$A_{conveyor} = A_{energy} + A_{belt} + A_{motor} + A_{gearreducer} + A_{carryidler} + A_{returnidler}. \tag{3.89}$$

Based on the above, the optimization problem of the cost-effective design of single drive belt conveyors can be stated as: "minimization of (3.89) subject to (3.41), (3.52), (3.55), (3.56), (3.59), (3.61), (3.63), (3.65), (3.66), (3.86), (3.87) and (3.88), with the same boundary limits as the multi-drive belt conveyors."

For readability reasons, the full optimization problem is reproduced below.

$$\min_{X} \quad A_{energy} + A_{belt} + A_{motor} + A_{gearreducer} + A_{carryidler} + A_{returnidler}$$

$$\text{s.t.} \quad \rho A_{th} v = Q,$$

$$\eta_{gear} P - v F_W = 0,$$

$$\frac{2Tv}{D_{tr}} = \eta_{gear} P,$$

$$F_0 + F_{W,o} - \frac{\eta_{gear} P}{v} \geq \frac{C_w \eta}{v},$$

$$F_0 \geq \frac{g\left(m_L^{'} + m_G^{'}\right) l_o}{8 h_{rel}},$$

$$F_{TD} \geq \frac{g m_G^{'} l_u}{8 h_{rel}},$$

$$\frac{k_{t,rel} k_N}{S_0 S_1} \geq \frac{F_{T1,1}}{B},$$

$$D_{tr} \geq c_{Tr} d_{Gk},$$

$$S_f B_f L_f F_{s,o} \leq F_{max,o},$$

$$S_f B_f C_f F_{s,u} \leq F_{max,u},$$

$$\frac{60v}{\pi D_o} \leq 750,$$

$$\frac{60v}{\pi D_u} \leq 750,$$

with the boundary limits

$$0 \leq P \leq P_{max},$$

$$0 \leq T \leq T_{max},$$

$$D_{tr} \in \mathfrak{D}_{tr},$$

$$\alpha_{min} \leq \alpha \leq \alpha_{max},$$

$$B \in \mathfrak{B},$$

$$0 \leq v \leq v_{max},$$

$$0 \leq k_N \leq k_{N,max},$$

$$0 \leq F_{TU} \leq F_{TU,max},$$

$$l_{o,min} \leq l_o \leq l_{o,max},$$

$$l_{u,min} \leq l_u \leq l_{u,max},$$

$$D_o \in \mathfrak{D},$$

$$D_u \in \mathfrak{D},$$

$$d_o \in \mathfrak{d},$$

$$d_u \in \mathfrak{d}.$$

In light of the research question 1, the above optimization problems given in sections 3.8.1 and 3.8.2 show that in comparison to the single drive technology, the multi-drive technology further allows the optimization of the number of drive stations, their spacing and their respective pulling capacity and mechanical parameters.

CHAPTER 4 CASE STUDY

4.1 CHAPTER OVERVIEW

This chapter presents the case study to test the validity and establish the effectiveness of the design approach developed in the previous chapter. The various technical and economic parameters of the contemplated project are given. Considering the possible variation of the inflation rate throughout the project and the related impact on the economic performance of conveyor designs, three scenarios with different inflation trends are also described. These scenarios will serve to conduct a sensitivity analysis of cost-effective belt conveyor designs against the possible fluctuations of inflation. The equivalent annual cost coefficients of energy and belt conveyor components relating to each scenario are also determined.

4.2 PROJECT DESCRIPTION

4.2.1 Technical specifications

The contemplated transportation task consists of transferring a bulk material of density equal to 1280 kg/m^3 over a distance of 2500 m. The incline of the system is of 1 in 100, while the required material flow rate is fixed at 3500 t/h. The synthesis of the transport specifications along with the characteristics of the conveyed material are given in Table 4.1.

Table 4.1. Conveying operation parameters

Parameter	Symbol	Value	Unit
Transport requirements			
Material flow rate	Q	3500	t/h
Transport distance	L	2500	m
Lift height	H	25	m
Maximum belt sag	h_{rel}	1	%
Material characteristics			
Bulk density	ρ	1280	kg/m^3
Equivalent angle of slope	β	20	°
Dynamic load lump adjustment factor	L_f	1	

The various parameters affecting the resistance to the belt movement are specified in Table 4.2. p_{Gr} and w are indicated, respectively, in N/mm^2 and mm for convenience.

Table 4.2. Parameters of the resistance to the belt movement

Parameter	Symbol	Value	Unit
Gravitational acceleration	g	9.81	m/s^2
Hypothetical friction resistance factor	f_j	0.03	
Lateral chute clear width coefficient	a	1.25	
Belt-lateral chute resistance coefficients	$C_{Schb}C_{Rank}$	1	
Acceleration path total length coefficient	k_b	1.1	
Conveyed material initial velocity	$v_{o,j}$	0	m/s^2
Belt-drive pulley friction coefficient	μ	0.3	
Belt-conveyed material friction coefficient	μ_1	0.6	
Conveyed material-lateral chute friction coefficient	μ_2	0.6	
Belt-belt cleaner friction coefficient	μ_3	0.65	
Belt cleaner-belt contact pressure	p_{Gr}	0.065	N/mm^2
Belt cleaner-belt width of contact area	w	0.031	mm

The lower and upper limits and the sets of possible sizes that apply to the design parameters are introduced in Table 4.3. Note that the boundary limits related to D_o, D_u, d_o and d_u are indicated in mm for convenience.

Table 4.3. Boundary limit values

Parameter	Unit	Min	Max	Set
P_i	kW	0	2000	-
T_i	kNm	0	950	-
$D_{tr,i}$	m	-	-	0.1-0.16-0.2-0.25-0.315-0.4-0.5-0.63-0.8-1-1.25-1.4-1.6-1.8-2-2.2
α_i	°	180	240	-
$L_{o,j}$	m	0	2500	-
B	m	-	-	0.6-0.75-0.9-1.05-1.2-1.35-1.5-1.8-2-2.2-2.4
v	m/s	0	10	-
k_N	kN/m	0	3000	-
F_{TU}	kN	0	500	-
l_o	m	1	2	-
l_u	m	1	4.5	-
D_o, D_u	m	-	-	63-76-89-102-108-127-133-152-159-194
d_o, d_u	m	-	-	25-30-35-40

4.2.2 General economic parameters

Table 4.4 displays the general economic information relating to the conveyor project. Except when otherwise indicated, the information presented in this table are based on the author's assumptions.

Table 4.4. Project economic parameters

Parameter	Symbol	Value	Unit
Income tax rate	t	28[1]	%
Reference inflation rate	r	5.6[2]	%

[1] Rate applied to companies as per South African Revenue Services (SARS). Available at: http://www.sars.gov.za/TaxRates/Income-Tax/Pages/Companies-Trusts-and-Small-Business-Corporations.aspx

[2] Average based on 2012-2015 Statistics South Africa. Available at: http://www.statssa.gov.za/publications/P0141/P0141April2016.pdf

Table 4.4. Project economic parameters (continued)

Parameter	Symbol	Value	Unit
Debt capital proportion	r_d	0	%
Required return on debt capital	i_d	0	%
Required return on equity funds with 0% of inflation rate	i_e	5	%
Electricity annual escalation rate	r_e	11.2[3]	%
Energy cost at time zero	e_{co}	0.071[4]	USD/kWh
Operating hours per annum	t_a	3600	h
Project lifetime	Z	20	years

4.3 BELT CONVEYOR COMPONENT PARAMETERS

As per the scope of the study defined in Chapter 3, the conveyor components involved in this optimal design investigation are the belt, electric motors, gear reducers, and carry and return idler rolls. The next subsections present the simulation parameters relating to these equipment.

4.3.1 Belting

Table 4.5 displays the price data of the steel cord belt as obtained from a belt manufacturer. The parameter p_{belt} denotes the price per unit of length and width of the belt.

Table 4.5. Conveyor belt price information

k_N [kN/m]	p_{belt} [USD/m^2]
500	34.17
630	34.17
800	34.17
1000	36.53
1250	37.81

[3] Average for mining sector over 2012-2015. Available at: http://www.eskom.co.za/CustomerCare/TariffsAndCharges/Pages/Tariff_History.aspx
[4] Megaflex tariff 2014/2015. Available at: http://www.eskom.co.za/CustomerCare/TariffsAndCharges/Pages/Tariffs_And_Charges.aspx

Table 4.5. Conveyor belt price information (continued)

k_N [kN/m]	p_{belt} [USD/m^2]
1400	44.49
1600	52.06
1800	53.41
2000	54.75
2250	56.44
2500	69.18
2800	71.58
3150	86.66
3500	89.93
4000	105.91
4500	111.14
5000	126.49

Based on the first cost function (3.3), Figure 4.1 shows the regression equations fitted to the data given in Table 4.5. Note that all the regression models presented in this work were developed using the Statistics and Machine Learning Toolbox of Matlab [5]

Among the statistical metrics commonly used to evaluate the quality of a regression fit is the coefficient of determination R^2, pronounced "R squared." It indicates the proportion of the variance in the dependent variable that is explained by the regression model. A minimum value of 0.75 for this metric is generally acceptable to guarantee sufficient accuracy of the future predictions [42].

Accordingly, with R^2 equal to 0.99, the regression equation plotted in Figure 4.1 is acceptable to estimate p_{belt} as a functions of k_N.

$$p_{belt} = 25.965 + 1.414 \cdot 10^{-3} k_N^{1.313}. \tag{4.1}$$

[5]MATLAB and Statistics and Machine Learning Toolbox Release 2015b, The MathWorks, Inc., Natick, Massachusetts, United States.

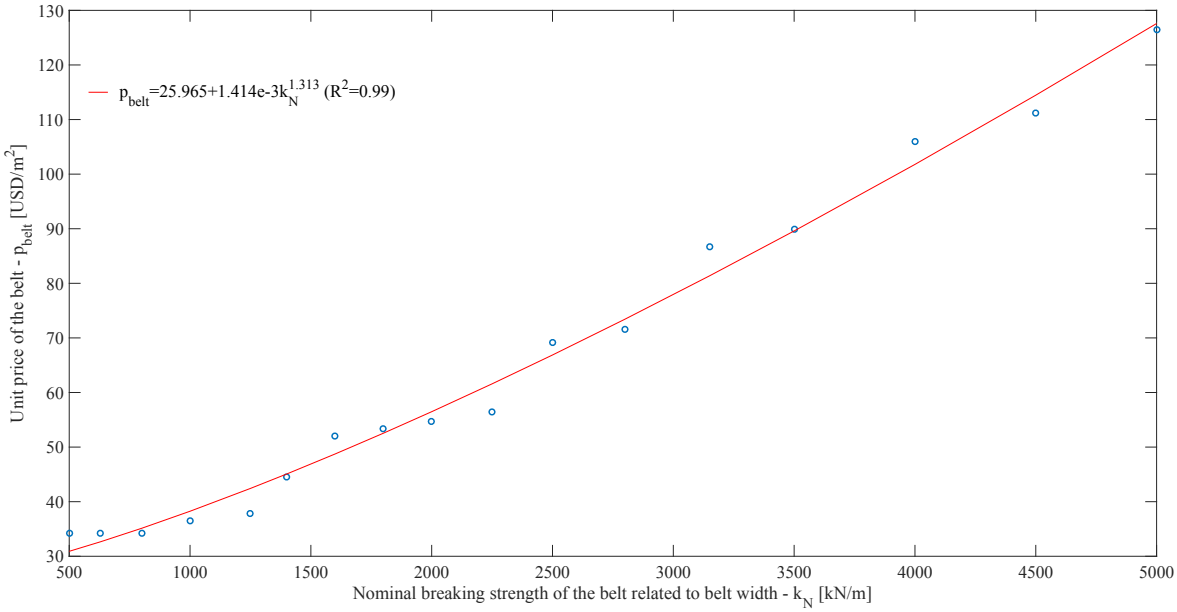

Figure 4.1. Belt price versus nominal breaking strength of the belt related to belt width

The rest of the simulation parameters of the belt are indicated in Table 4.6

Table 4.6. Conveyor belt parameters

Parameter	Symbol	Value	Unit
Troughing angle	λ	35	°
Belt safety factor related to splicing conditions	S_0	1.1 [8]	
Belt safety factor related to the expected service life and operating load	S_1	1.7[9]	
Relative reference endurance strength of the belt	$k_{t,rel}$	0.45 [10]	
Drive station-related belt length constant coefficient	y_1	3	m
Belt length reserve factor	y_2	20	m
Specific mass model coefficient	m_1	13.823[11]	kg/m^2
Specific mass model coefficient	m_2	$8.174 \cdot 10^{-3}$ [11]	kg/kNm
Tensile members' diameter model coefficient	m_3	$1.002 \cdot 10^{-3}$ [11]	mm
Tensile members' diameter model coefficient	m_4	$0.012 \cdot 10^{-3}$ [11]	
Tensile members' diameter model coefficient	m_5	0.771 [11]	

[8] Recommended value for normal belt quality and operational conditions [7]

[9] Recommended value for normal expected belt service life belt quality and operational conditions [7]

[10] Recommended value for steel cord belts [7]

[11] see Addendum C

Table 4.6. Conveyor belt parameters (continued)

Parameter	Symbol	Value	Unit
Expected lifetime	M_{belt}	16[12]	year
Annual escalation rate	r_{belt}	5.6[13]	%
Residual value	V_{belt}	0	%
Initial cost coefficient	c_1	25.965	USD
Initial cost coefficient	c_2	$1.414 \cdot 10^{-3}$	
Initial cost coefficient	c_3	1.313	

4.3.2 Motors

Table 4.7 displays the price data obtained from an electric motor manufacturer.

Table 4.7. Motor price information (induction motor-1500 rpm)

P [kW]	p_{motor} [USD]
0.18	143.24
0.25	165.10
0.37	170.07
0.55	184.62
0.75	211.52
1.1	233.38
1.5	293.10
2.2	342.55
3	395.86
4	450
5.5	547.38
7.5	670.55
9.2	932.76

[12]Recommendations of the US Bureau of Economic Analysis (BEA). Available at: https://bea.gov/scb/account_articles/national/wlth2594/tableC.htm

[13]Same the general inflation rate in Table 4.4

Table 4.7. Motor price information (induction motor-1500 rpm) (continued)

P [kW]	p_{motor} [USD]
11	1064.21
15	1381.66
18.5	1696.21
22	2049.38
30	2451.66
37	3378.69
45	3913.45
55	5037.17
75	6017.2
90	6928.62
110	8309.72
132	9681.17
160	10768.21
185	12765.03
200	13343.45
220	17425.59
250	19950.90
260	20322.41
280	22007.86
300	22696.83
315	23996.07
330	24934.34
355	25880.34
370	27946.28
400	29987.93

Figure 4.2 shows the regression equations fitted to the data given in Table 4.7 in relation to the first cost function (3.4).

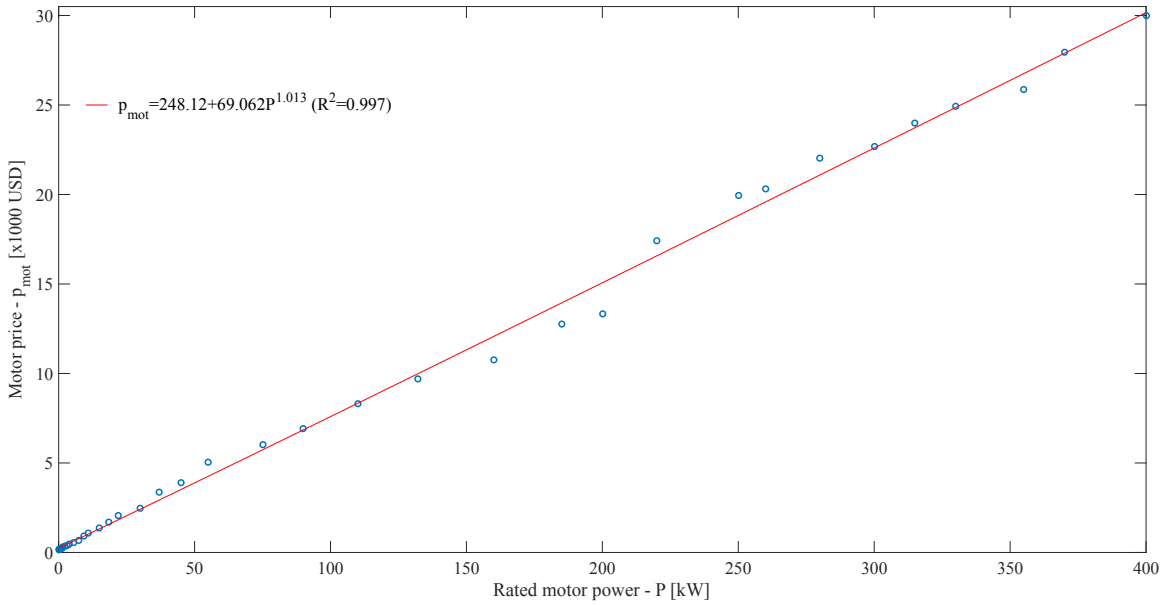

Figure 4.2. Motor price vs rated motor power

With a R^2 equal to 0.997, the regression model obtained for the motor is acceptable to describe the price of motors as a continuous function of their nominal power. This relation between the two variables is therefore given by

$$p_{motor} = 248.12 + 69.062P^{1.013}{}^{14}. \tag{4.2}$$

The simulation parameters of motors are summarized in Table 4.8.

Table 4.8. Simulation parameters of motors

Parameter	Symbol	Value	Unit
Efficiency	η_{mot}	95	%
Expected lifetime	M_{mot}	16[15]	year
Annual escalation rate	r_{mot}	5.6[16]	%
Residual value	V_{belt}	8	%
Initial cost coefficient	c_4	248.12	USD

[14] With P expressed in kW

[15] Recommendations of the US Bureau of Economic Analysis (BEA). Available at: https://bea.gov/scb/account_articles/national/wlth2594/tableC.htm

[16] Assumed equal to the general inflation rate in Table 4.4

Table 4.8. Simulation parameters of motors (continued)

Parameter	Symbol	Value	Unit
Initial cost coefficient	c_5	69.062	
Initial cost coefficient	c_6	1.013	

4.3.3 Gear reducers

Table 4.9 displays the price data supplied by a gear reducer manufacturer.

Table 4.9. Gear reducer price information

T [kNm]	p_{gear} [USD]
0.68	6572.06
0.93	7477.22
1.35	7922.95
1.84	8426.83
2.26	8977.45
2.69	10839.06
3.63	12017.81
4.53	13689.04
5.51	15551.79

Figure 4.3 shows the regression equations fitted to the data given in Table 4.9 in relation to the first cost function (3.5).

With a R^2 equal to 0.989, the regression model obtained for the gear reducer is acceptable to describe the price of gear reducers as a continuous function of their nominal torque. This relation between the two variables is therefore given by:

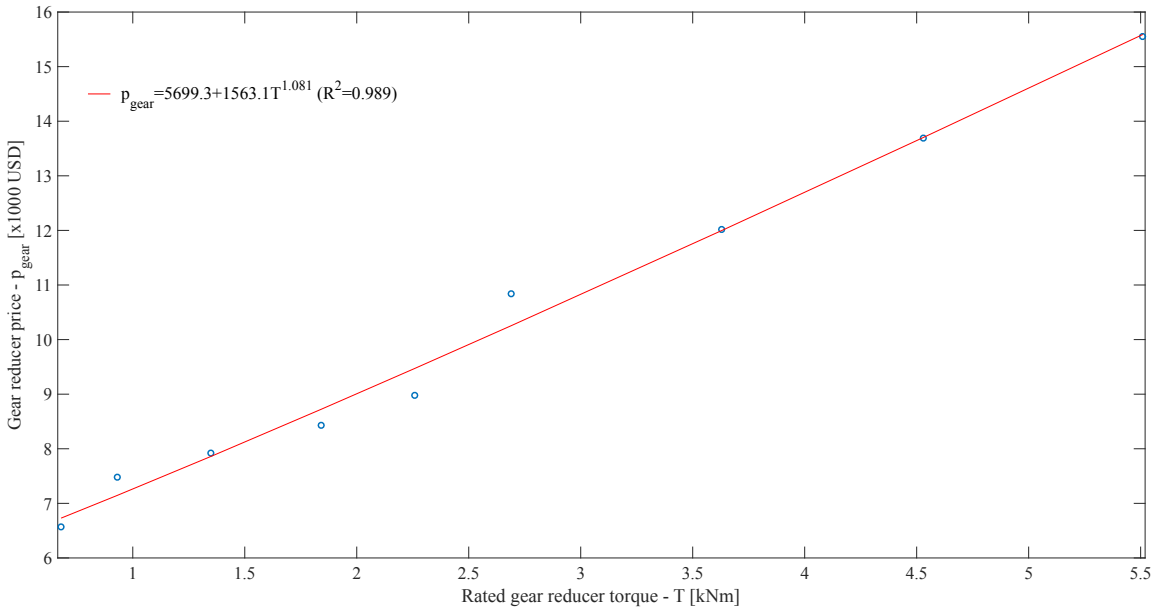

Figure 4.3. Gear reducer price vs rated torque

$$p_{gear} = 5699.3 + 1563.1T^{1.081}{}^{17}. \tag{4.3}$$

The simulation parameters related to the motors are summarized in Table 4.10.

Table 4.10. Simulation parameters of gear reducers

Parameter	Symbol	Value	Unit
Efficiency	η_{gear}	90	%
Expected lifetime	M_{mot}	16[18]	year
Annual escalation rate	r_{mot}	5.6[19]	%
Residual value	V_{belt}	10	%
Initial cost coefficient	c_7	5699.3	USD
Initial cost coefficient	c_8	1563.1	
Initial cost coefficient	c_9	1.081	

[17] With T expressed in kNm

[18] Recommendations of the US Bureau of Economic Analysis (BEA). Available at: https://bea.gov/scb/account_articles/national/wlth2594/tableC.htm

[19] Assumed equal to the general inflation rate in Table 4.4

4.3.4 Carry idler rolls

Table 4.11 displays the simulation parameters relating to the carry idler rolls.

Table 4.11. Simulation parameters of carry idler rolls

Parameter	Symbol	Value	Unit
Mass model coefficient	z_1	139.39 [20]	
Mass model coefficient	z_2	1.722[20]	
Mass model coefficient	z_3	1.025[20]	
Mass model coefficient	z_4	80.51[20]	kg/m
Expected lifetime	$M_{carryidler}$	11[21]	year
Annual escalation rate	$r_{carryidler}$	5.6[22]	%
Residual value	V_{belt}	0	%
Initial cost coefficient	c_{10}	-10.553 [23]	USD
Initial cost coefficient	c_{11}	389.63[24]	
Initial cost coefficient	c_{12}	0.951[24]	
Initial cost coefficient	c_{13}	189.37[24]	
Initial cost coefficient	c_{14}	1.755[24]	
Initial cost coefficient	c_{15}	2.407[24]	
Initial cost coefficient	c_{16}	1.747[24]	

The maximum loads allowable on the central idler roll in a three-idler roll troughing configuration as per the recommendations of the SANS 1313 standard are given in Table 4.12.

Table 4.12. Allowable load on the central idler roll in N [40]

	Shaft diameter (mm)			
Belt width (mm)	25	30	35	40
400	3698.37	4620.51	5454.36	6739.47

[20] see Addendum B.1
[21] 40 000 hours as per the SANS 1313 standard [40]
[22] Assumed equal to the general inflation rate in Table 4.4
[23] see Addendum D.1

Table 4.12. Allowable load on the central idler roll in N (continued)

	Shaft diameter (mm)			
Belt width (mm)	25	30	35	40
450	3698.37	4620.51	5454.36	6739.47
500	3698.37	4620.51	5454.36	6739.47
600	3698.37	4620.51	5454.36	6739.47
750	3698.37	4620.51	5454.36	6739.47
900	3629.7	4620.51	5454.36	6739.47
1050	3060.72	4620.51	5454.36	6739.47
1200	2580.03	4620.51	5454.36	6739.47
1350	2275.92	4316.4	5454.36	6739.47
1500	2001.24	3776.85	5454.36	6739.47
1650	1814.85	3423.69	5454.36	6739.47
1800	1657.89	3129.39	5424.93	6739.47
2000	1461.69	2756.61	4767.66	6739.47
2100	1412.64	2648.7	4591.08	6739.47
2200	1343.97	2521.17	4365.45	6739.47
2400	1226.25	2295.54	3973.05	6248.97

4.3.5 Return idler rolls

Table 4.13 displays the simulation parameters relating to the return idler rolls.

Table 4.13. Simulation parameters of return idler rolls

Parameter	Symbol	Value	Unit
Mass model coefficient	z_1	172 [24]	
Mass model coefficient	z_2	1.287[24]	
Mass model coefficient	z_3	1[24]	
Mass model coefficient	z_4	124.99[24]	kg/m

[24] see Addendum B.2

Table 4.13. Simulation parameters of carry idler rolls (continued)

Parameter	Symbol	Value	Unit
Expected lifetime	$M_{carryidler}$	11[25]	year
Annual escalation rate	$r_{carryidler}$	5.6[26]	%
Residual value	V_{belt}	0	%
Initial cost coefficient	c_{17}	-23.157 [27]	USD
Initial cost coefficient	c_{18}	757.88[27]	
Initial cost coefficient	c_{19}	1[27]	
Initial cost coefficient	c_{20}	153.42[27]	
Initial cost coefficient	c_{21}	1.051[27]	
Initial cost coefficient	c_{22}	2.808[27]	
Initial cost coefficient	c_{23}	1[27]	

The maximum loads allowable on a flat return idler roll as per the recommendations of the SANS 1313 standard are given in Table 4.14.

Table 4.14. Allowable load on the central idler roll in N [40]

	Shaft diameter (mm)			
Belt width (mm)	25	30	35	40
600	3698.37	4620.51	5454.36	6739.47
750	2972.43	4620.51	5454.36	6739.47
900	2423.07	4591.08	5454.36	6739.47
1050	2001.24	3776.85	5454.36	6739.47
1200	1736.37	3266.73	5454.36	6739.47
1350	1510.74	2835.09	4914.81	6739.47
1500	1343.97	2521.17	4365.45	6739.47
1650	1206.63	2256.3	3894.57	6131.25
1800	1098.72	2050.29	3541.41	5562.27

[25] 40 000 hours as per the SANS 1313 standard [40]
[26] Assumed equal to the general inflation rate in Table 4.4
[27] see Addendum D.2

Table 4.14. Allowable load on the central idler roll in N (continued)

	Shaft diameter (mm)			
Belt width (mm)	25	30	35	40
2000	971.19	1824.66	3149.01	4944.24
2100	912.33	1706.94	2943	4610.7
2200	882.9	1648.08	2835.09	4443.93
2400	794.61	1491.12	2570.22	4022.1

4.4 INFLATION TREND SCENARIOS

As suggested by the expressions of the equivalent annual cost coefficient derived in Addendum A, the trend of the inflation rate in the course of the project will mechanically reflect on the values of these coefficients and will, consequently, more or less modify the respective equivalent annual costs.

In order to subsequently evaluate the sensitivity of the future cost-effective conveyor designs against the inflation rate, three different scenarios of inflation rate evolution have been envisaged in this study: a fixed inflation rate scenario and two fluctuating inflation rate scenarios.

4.4.1 Scenario 1: Fixed inflation rate 5.6%

The first scenario assumes an inflation rate at 5.6% per year during the 20 years of the project lifetime. Table 4.15 displays the equivalent annual cost coefficients calculated for this case.

4.4.2 Scenario 2: Fluctuating inflation rate at 5.2% on average

The second scenario assumes that the inflation rate of each year is 5% inferior to the first scenario and perturbed by a stochastic factor varying between $\pm 1\%$. The trend of the inflation rate obtained in this case is indicated in Table 4.16

Table 4.17 displays the equivalent annual cost coefficients calculated for this scenario.

Table 4.15. Equivalent annual cost coefficients with fixed inflation rate at 5.6%

Parameter	Symbol	Value
Equivalent annual cost coefficient of energy	k_0	1.653
Equivalent annual cost coefficient of belt	k_1	0.138
Equivalent annual cost coefficient of motor	k_2	0.055
Equivalent annual cost coefficient of gear reducer	k_3	0.055
Equivalent annual cost coefficient of carry idler roll	k_2	0.148
Equivalent annual cost coefficient of return idler roll	k_2	0.148

Table 4.16. Annual inflation rate with fluctuating inflation rate at 5.2% on average

year	1	2	3	4	5	6	7	8	9	10
r[%]	4.9	5.7	5.4	5.4	4.9	5.7	5.4	5.1	5.3	5.2
year	11	12	13	14	15	16	17	18	19	20
r[%]	4.8	5.0	4.9	5.0	5.0	5.2	4.8	5.7	5.8	5.3

Table 4.17. Equivalent annual cost coefficients with fluctuating inflation rate at 5.2% on average

Parameter	Symbol	Value
Equivalent annual cost coefficient of energy	k_0	1.716
Equivalent annual cost coefficient of belt	k_1	0.138
Equivalent annual cost coefficient of motor	k_2	0.053
Equivalent annual cost coefficient of gear reducer	k_3	0.052
Equivalent annual cost coefficient of carry idler roll	k_2	0.145
Equivalent annual cost coefficient of return idler roll	k_2	0.145

4.4.3 Scenario 3: Fluctuating inflation rate at 5.8% on average

The third scenario assumes that the inflation rate of each year is 5% superior to the first scenario and perturbed by a stochastic factor varying between $\pm 1\%$. The trend of the inflation rate obtained in this case is indicated in Table 4.18

Table 4.18. Annual inflation rate with fluctuating inflation rate at 5.8% on average

year	1	2	3	4	5	6	7	8	9	10
r[%]	5.9	5.7	6.3	5.8	5.5	6.2	5.8	5.6	5.8	5.5
year	11	12	13	14	15	16	17	18	19	20
r[%]	5.5	6.4	6.4	6.0	5.4	5.6	5.7	6.3	5.4	5.4

Table 4.19 displays the equivalent annual cost coefficients calculated for this scenario.

Table 4.19. Equivalent annual cost coefficients with fluctuating inflation rate at 5.8% on average

Parameter	Symbol	Value
Equivalent annual cost coefficient of energy	k_0	1.613
Equivalent annual cost coefficient of belt	k_1	0.137
Equivalent annual cost coefficient of motor	k_2	0.057
Equivalent annual cost coefficient of gear reducer	k_3	0.057
Equivalent annual cost coefficient of carry idler roll	k_2	0.147
Equivalent annual cost coefficient of return idler roll	k_2	0.147

CHAPTER 5 OPTIMAL DESIGN SIMULATION RESULTS AND ANALYSIS

5.1 CHAPTER OVERVIEW

This chapter introduces the results of the simulations carried out for the single and multiple drive belt conveyors. As a first step, a brief description of the solver and the simulation procedure is provided. The simulation results are subsequently set out in relation to the inflation trend scenario considered. An immediate analysis of the results is also conducted.

5.2 BRIEF DESCRIPTION OF THE OPTIMIZER AND THE OPTIMIZATION PROCEDURE

In the formulation of the optimization problems of the cost-effective design of single and multi-drive belt conveyors in Section 3.7, the following design parameters have been described as of discrete type because of the limited sizes subject to the recommendations in the DIN 22101 and SANS 1313 standards: $D_{tr,i}$, B, D_o, D_u, d_o and d_u. On the other hand, while a continuous design parameter, e.g. P_i, can freely take on values within a continuous interval delimited by an upper and a lower limit, a discrete design parameter is compelled to vary discontinuously within a specific set of possible values. On the other hand, some of the design conditions listed in Section 3.8 consist of linear and nonlinear functions of the two types of design parameters identified above. Such optimization problems are commonly referred to as mixed integer nonlinear programming (MINLP). Known as relatively complex to solve, this class of optimization problems usually calls for dedicated optimizers.

The commercial optimization software "Mixed Integer Distributed Ant Colony Optimization", in short MIDACO, was acquired in the course of the research work in order to solve the different MINLPs formulated in Chapter 3. The MIDACO software is a general-purpose solver intended for single- and multi-objective numerical optimization problems. Relying on an extended Ant Colony Optimization algorithm, the MIDACO software is regarded as state-of-the-art for evolutionary computing on MINLP, constrained and large-scale optimization [43]. Owing to the black-box layout of MIDACO, no particular restriction applies to the mathematical properties and formulation of the objective and constraint functions prior to being handled by this solver.

On the handling of discrete design parameters by MIDACO, treated as of integer type by the generator of "ants" or "iterates," the values of these parameters contained in the various solutions submitted by this generator are initially mapped to the corresponding physical sizes within the sets of possible values prior to evaluating the objective and constraint functions.

Given a number of intermediate drive stations, the optimizer generates a specific MINLP problem and, afterward, attempts to find the set of values of the design parameters that minimizes the objective function, that is the equivalent annual cost of the conveyor, while satisfying all the design conditions and boundary limits. In order to visualize the optimization process, and also conduct further comparative analysis, the simulations were carried out individually for each possible size of the belt width.

This simulation procedure of multi-drive belt conveyors is summarized in the flowchart shown in Fig. 5.1. At the beginning, the general economic and technical data relating to the project and the belt conveyor components are loaded in the memory. Once the number of intermediate drive stations is provided by the user, a first MINLP based on this value and the minimum possible belt width is generated and immediately solved by the MIDACO solver. The best design obtained and the associated conveyor cost, energy cost and capital costs of the belt conveyor components are stored in a dedicated database. The above process will automatically repeat until the maximum belt width is reached. In case the user submits a new number of drive stations, the entire process restarts using the different belt width, otherwise the solver ends.

It is worthwhile mentioning that the computation time required by MIDACO to find the MIDACO-based optimal solution of a problem varied between 1h30 and 20 hours. This time was affected by

factors such as conveyor technology, number of intermediate drive stations and belt size. The solver was run on a PC Core(TM) i3, 3.40 GHz, with 4 GB of RAM, operating on Windows 7.

5.3 OPTIMAL CONVEYOR DESIGNS AND RELATED COSTS UNDER FIXED INFLATION RATE AT 5.6%

The simulation results obtained for the fixed inflation rate scenario are presented in this section.

5.3.1 Single drive conveyor layout

Table 5.1 displays the specifications of the MIDACO-based optimal single drive belt conveyors with the driving system installed at the head pulley. It can be noted that no belt width inferior to 900 mm is reported for the transport task considered. This is because their use will require higher conveyor speeds that result in the violation of the constraints on the maximum rotation velocity of idler rolls, having regard to the set of possible idler roll diameters.

Table 5.1. MIDACO-based optimal single drive belt conveyors (N=0) under 5.6% inflation rate

	Belt width (mm)								
Parameter	900	1050	1200	1350	1500	1800	2000	2200	2400
P_i, kW	1556.67	1408.66	1337.29	1297.62	1267.82	1238.13	1225.63	1214.99	1208.6
v, m/s	7.25	5.21	3.97	3.07	2.47	1.69	1.36	1.09	0.9
T_i, kNm	60.87	76.59	121.17	151.99	185.11	328.82	404.16	500.51	754.52
α_i, rad	4.19	4.19	4.19	4.19	4.19	4.19	4.19	4.19	4.19
l_o, m	2	2	2	2	1.85	1.96	2	1.72	1.33
l_u, m	4.5	4.5	4.5	4.34	4.5	4.4	4.5	4.5	4.5
F_{TU}, kN	61.78	80.15	101.78	129.5	159.8	230.2	284.89	355.39	430.85
k_N, kN/m	1177.51	1279.51	1401.48	1568.27	1724.77	2049.72	2271.46	2562.1	2836.3
B, mm	900	1050	1200	1350	1500	1800	2000	2200	2400
D_o, mm	194	133	102	89	63	63	63	63	63
D_u, mm	194	133	102	89	63	63	63	63	63
d_o, mm	25	25	30	30	30	35	40	40	40
d_u, mm	25	25	25	25	30	30	35	35	40
$D_{tr,i}$, mm	630	630	800	800	800	1000	1000	1000	1250
A_{energy}, ×1000 USD/year	690.04	624.43	592.79	575.21	561.99	548.83	543.29	538.58	535.74
A_{belt}, ×1000 USD/year	25.71	31.27	37.53	45.07	53.15	71.76	86.05	104.08	123.58
A_{motor}, ×1000 USD/year	6.57	5.94	5.63	5.46	5.34	5.21	5.16	5.11	5.09
A_{gear}, ×1000 USD/year	15.14	19.24	31.18	39.67	48.94	90.54	113	142.22	221.3
$A_{carryidler}$, ×1000 USD/year	9.1	5.23	5.48	5.62	6.21	7.89	9.44	11.96	16.9

Table 5.1. MIDACO-based optimal single drive belt conveyors (N=0) under 5.6% inflation rate (continued)

	Belt width (mm)								
Parameter	900	1050	1200	1350	1500	1800	2000	2200	2400
$A_{returnidler}$, ×1000 USD/year	2.47	1.41	1.12	1.1	1.22	1.32	1.61	1.66	1.97
$A_{conveyor}$, ×1000 USD/year	749.02	687.52	673.74	672.13	676.85	725.56	758.54	803.61	904.58

It is also shown that the greatest possible wrapping angle is consistently applied by the optimizer, which relieves the slack side tension of drive stations in the fulfillment of the belt slippage condition (3.50). This, therefore, benefits the maximum belt tension of the conveyor, which is relevant to the belt cost through k_N.

On the other hand, considering the spacing between idler rolls, the low weight of the emptied belt in the lower stretch stimulates the use of large idler spacing on this side of the conveyor. On the other hand, the optimal spacing of idler rolls in the carry side appears to be more sensitive to the belt width, and therefore on the amount of bulk material resting on each carry idler roll set.

The analysis of idler roll diameters in the carry and return sides in Table 5.1 reveals a strong preference for the smallest possible sizes with respect to the belt speed, which allows for achieving low cost and weight for these components. This trend could, however, be challenged in case more sophisticated frictional resistance models were adopted, since, in practice, large idler roll diameters usually result in lower primary resistances [7, 36]. On the specification of the shaft diameters of carry and return idler rolls, Table 5.1 shows that the use of the smallest diameters in relation to the optimum idler roll spacing will lead to low costs for these components.

The trend of the drive pulley diameter in Table 5.1 suggests that small diameters are more beneficial in order to reduce as far as possible the rated torque of gear reducers as suggested by (3.45). The transition towards larger a diameter only takes place to ensure the longevity of the belt through (3.59), which involves the thickness of the steel cords inside the belt.

Regarding the cost items of conveyors, Table 5.1 indicates that the energy cost consistently forms by far the largest proportion. Depending on the conveyor speed, the cost of energy will represent between

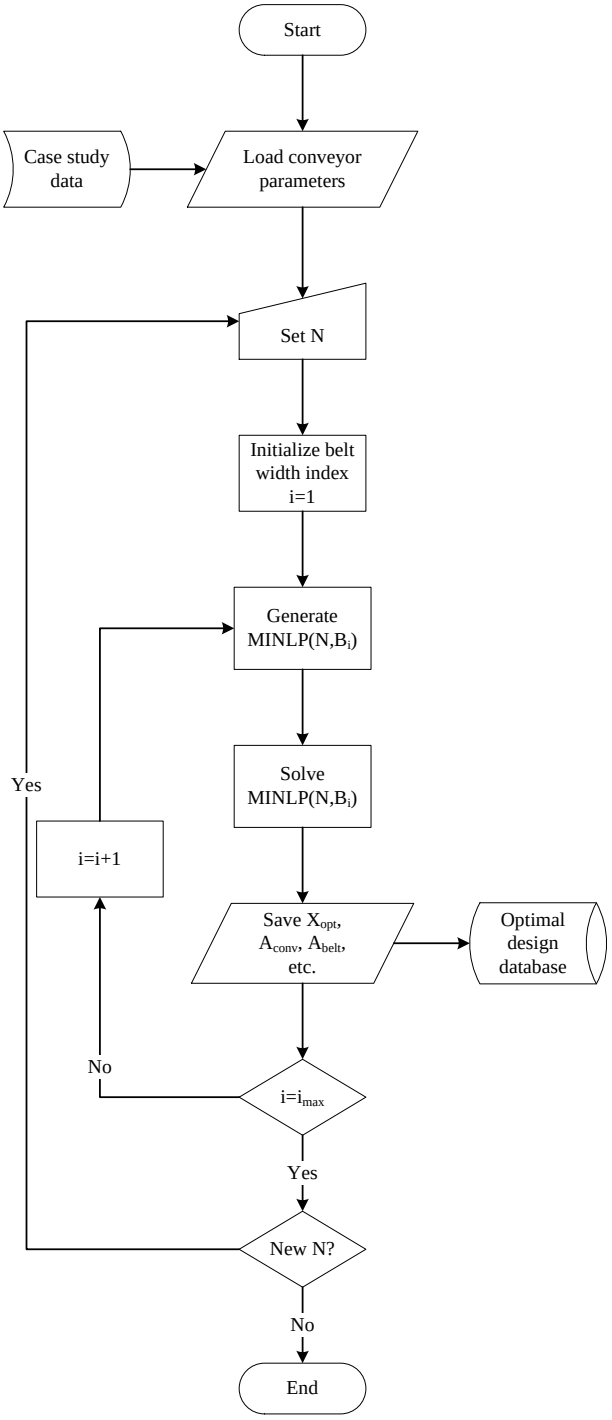

Figure 5.1. Simulation procedure flowchart

60% and 93% of the total cost of conveyors. This percentage declines with increases in the width of the belt, and therefore a reduction in the conveyor speed. Within the capital cost of conveyors, the belt and the gear reducers will generally represent the two largest items, followed by the motors. The narrow spacing of the carry idler rolls in comparison to the return idler rolls contributes to higher costs for the former.

5.3.2 Multi-drive conveyor layout

Table 5.2 displays the technical specifications and the resulting economic performances of the multi-drive belt conveyors optimized for one intermediate drive station. It is immediately apparent that the observations pointed out in the single drive design also apply to this case. Moreover, the shorter length of the belt section 1 compared to the belt section 3 in the upper stretch is explained by the empty belt on the return side and the loading point situated at the tail pulley. These two presences give rise to a concentration of resistance forces upstream the intermediate drive station. A large primary resistance in the last carry belt section (section 3) is therefore required to ensure the equality of the tight side tensions of drive stations.

Table 5.3 shows the technical specifications and the associated economic performances of the multi-drive belt conveyors optimized for two intermediate drive stations. All the various analysis conducted so far are also valid for this conveyor design. In addition to this, the resistance to belt movement caused by the belt cleaning device positioned downstream the head pulley leads to a shorter carry belt section 5 in the upper stretch compared to the belt section 3 of the same conveyor stretch.

Tables 5.4 to 5.6 display the technical specifications and the associated economic performances of the multi-drive belt conveyors optimized for three to five intermediate drive stations. The various analysis mentioned so far also apply to these multi-drive conveyor designs. The equality of length of the belt sections nestled between intermediate drive stations ensures a direct equalization of tight side tensions of drive stations because the equality of material they lift.

Table 5.2. MIDACO-based optimal multi-drive belt conveyors with one intermediate station (N=1) under 5.6% inflation rate (continued)

	Belt width (mm)								
Parameter	900	1050	1200	1350	1500	1800	2000	2200	2400

Table 5.2. MIDACO-based optimal multi-drive belt conveyors with one intermediate station (N=1) under 5.6% inflation rate

	Belt width (mm)								
Parameter	900	1050	1200	1350	1500	1800	2000	2200	2400
P_i, kW	410.21	359.23	334.02	321	311.3	302.16	298.1	294.86	292.29
v, m/s	7.25	5.21	3.97	3.07	2.47	1.69	1.36	1.09	0.9
T_i, kNm	10.18	15.5	18.92	23.5	28.41	40.12	61.93	76.52	91.97
$L_{o,1}$, m	1176.3	1192.56	1201.27	1206.74	1212.04	1217.93	1219.33	1221.95	1223.25
$L_{o,3}$, m	1324.22	1308.06	1299.35	1293.88	1288.58	1282.69	1281.42	1278.8	1277.5
α_i, rad	3.47	3.16	3.26	4.19	3.97	3.76	4.18	4.19	4.19
l_o, m	2	2	2	2	1.87	1.15	1.45	1.13	1.3
l_u, m	4.5	4.5	4.5	4.5	4.5	4.5	4.5	4.11	4.5
F_{TU}, kN	25.25	38.16	52.01	68.73	80.77	65.37	110.93	103.38	150
k_N, kN/m	586.82	641.82	704.14	790.24	853.37	891.99	1047.49	1113.01	1270.76
B, mm	900	1050	1200	1350	1500	1800	2000	2200	2400
D_o, mm	194	133	102	89	63	63	63	63	63
D_u, mm	194	133	102	89	63	63	63	63	63
d_o, mm	25	25	25	25	25	30	30	30	35
d_u, mm	25	25	25	25	25	30	30	30	35
$D_{tr,i}$, mm	400	500	500	500	500	500	630	630	630
A_{energy}, ×1000 USD/year	727.34	636.96	592.25	569.17	551.98	535.77	528.56	522.81	518.26
A_{belt}, ×1000 USD/year	20.03	23.92	28.07	32.77	37.41	45.64	54.16	61.22	71.27
A_{motor}, ×1000 USD/year	6.84	5.99	5.57	5.35	5.19	5.03	4.97	4.91	4.87
A_{gear}, ×1000 USD/year	5.45	7.87	9.46	11.63	13.99	19.75	30.83	38.43	46.61
$A_{carryidler}$, ×1000 USD/year	9.1	5.24	5.49	5.63	6.12	11.85	11.71	16.56	17.3
$A_{returnidler}$, ×1000 USD/year	2.46	1.41	1.12	1.06	0.95	1.29	1.34	1.53	1.71
$A_{conveyor}$, ×1000 USD/year	771.22	681.38	641.95	625.59	615.64	619.34	631.57	645.47	660.02

Table 5.3. MIDACO-based optimal multi-drive belt conveyors with two intermediate stations (N=2) under 5.6% inflation rate

	Belt width (mm)								
Parameter	900	1050	1200	1350	1500	1800	2000	2200	2400
P_i, kW	292.6	248.83	227	216.26	208.71	201.02	197.89	195.47	193.72
v, m/s	7.25	5.21	3.97	3.07	2.47	1.69	1.36	1.09	0.9
T_i, kNm	7.26	8.59	10.28	15.83	19.05	26.69	32.63	40.26	48.37
$L_{o,1}$, m	726.98	750.1	763.97	771.59	778.68	788.61	790.95	795.58	798.07

Table 5.3. MIDACO-based optimal multi-drive belt conveyor designs with two intermediate stations (N=2) under 5.6% inflation rate (continued)

	Belt width (mm)								
Parameter	900	1050	1200	1350	1500	1800	2000	2200	2400
$L_{o,3}$, m	906.15	892.33	883.55	878.24	873.42	866.5	864.37	861.04	859.05
$L_{o,5}$, m	867.79	858.49	853.4	851.29	849.02	846.01	845.8	844.5	844
α_i, rad	4.19	4.19	4.19	4.19	3.91	4.02	3.82	4.19	4.19
l_o, m	2	2	1.71	1.98	2	1.15	1.46	1.12	1.1
l_u, m	4.5	4.5	4.5	4.5	4.5	4.5	4.5	4.5	4.5
F_{TU}, kN	25.49	38.47	43.12	68.6	87.87	66.91	112.75	103.87	124.59
k_N, kN/m	453.1	492.21	505.47	601.02	665.53	647.48	776.64	804.61	885.81
B, mm	900	1050	1200	1350	1500	1800	2000	2200	2400
D_o, mm	194	133	102	89	63	63	63	63	63
D_u, mm	194	133	102	89	63	63	63	63	63
d_o, mm	25	25	25	25	30	30	30	30	35
d_u, mm	25	25	25	25	30	30	30	30	35
$D_{tr,i}$, mm	400	400	400	500	500	500	500	500	500
A_{energy}, ×1000 USD/year	778.21	661.79	603.74	575.18	555.1	534.65	526.33	519.89	515.23
A_{belt}, ×1000 USD/year	18.94	22.46	25.81	30.24	34.54	41.13	48.3	53.77	60.73
A_{motor}, ×1000 USD/year	7.31	6.22	5.67	5.4	5.22	5.02	4.95	4.89	4.84
A_{gear}, ×1000 USD/year	6.25	7.12	8.24	12.03	14.27	19.74	24.07	29.73	35.85
$A_{carryidler}$, ×1000 USD/year	9.1	5.24	5.32	5.67	6.66	11.82	11.68	16.78	20.49
$A_{returnidler}$, ×1000 USD/year	2.46	1.41	1.12	1.06	1.21	1.29	1.34	1.4	1.71
$A_{conveyor}$, ×1000 USD/year	822.28	704.23	649.91	629.58	617.01	613.65	616.66	626.45	638.84

Table 5.4. MIDACO-based optimal multi-drive belt conveyors with three intermediate stations (N=3) under 5.6% inflation rate

	Belt width (mm)								
Parameter	900	1050	1200	1350	1500	1800	2000	2200	2400
P_i, kW	234.53	194.33	174.14	164.5	157.65	151.09	148.69	146.68	144.95
v, m/s	7.25	5.21	3.97	3.07	2.47	1.69	1.36	1.09	0.9
T_i, kNm	5.82	6.71	7.89	9.63	11.51	16.05	19.61	30.21	36.2
$L_{o,1}$, m	503.1	529.72	545.78	554.6	564.28	572.98	576.96	578.23	585.65
$L_{o,3}$, m	679.03	668.64	662.06	657.98	653.9	649.7	647.71	646.84	643.85
$L_{o,5}$, m	679.03	668.64	662.06	657.98	653.9	649.7	647.71	646.84	643.85
$L_{o,7}$, m	640.16	634.32	631.42	630.76	629.24	628.94	628.94	629.71	628.27
α_i, rad	4.19	4.19	4.19	4.19	4.19	3.8	3.98	4.19	4.1
l_o, m	2	2	1.72	2	1.77	1.42	1.13	1.53	1.21
l_u, m	4.5	4.5	4.5	4.5	4.5	3.9	3.2	2.54	4.5
F_{TU}, kN	25.6	38.62	43.44	69.48	76.28	86.95	82.58	149.86	141.48
k_N, kN/m	387.08	418.36	423.64	510.42	530.16	571.28	579.12	739.63	746.39
B, mm	900	1050	1200	1350	1500	1800	2000	2200	2400
D_o, mm	194	133	102	89	63	63	63	63	63

Table 5.4. MIDACO-based optimal multi-drive belt conveyors with three intermediate stations (N=3) under 5.6% inflation rate (continued)

	Belt width (mm)								
Parameter	900	1050	1200	1350	1500	1800	2000	2200	2400
D_u, mm	194	133	102	89	63	63	63	63	63
d_o, mm	25	25	25	25	25	25	25	25	35
d_u, mm	25	25	25	25	25	25	25	25	35
$D_{tr,i}$, mm	400	400	400	400	400	400	400	500	500
A_{energy}, ×1000 USD/year	831.7	689.12	617.52	583.35	559.05	535.79	527.29	520.18	514.03
A_{belt}, ×1000 USD/year	18.44	21.79	24.96	29.12	32.62	39.83	44.41	52.32	57.24
A_{motor}, ×1000 USD/year	7.81	6.48	5.81	5.49	5.26	5.04	4.96	4.9	4.84
A_{gear}, ×1000 USD/year	7.09	7.85	8.87	10.41	12.09	16.24	19.57	29.73	35.6
$A_{carryidler}$, ×1000 USD/year	9.11	5.24	5.32	5.63	6.5	10.9	15.1	13.47	18.55
$A_{returnidler}$, ×1000 USD/year	2.46	1.41	1.12	1.06	0.95	1.19	1.53	2.01	1.71
$A_{conveyor}$, ×1000 USD/year	876.62	731.89	663.6	635.05	616.47	609.01	612.86	622.61	631.98

Table 5.5. MIDACO-based optimal multi-drive belt conveyors with four intermediate stations (N=4) under 5.6% inflation rate

	Belt width (mm)								
Parameter	900	1050	1200	1350	1500	1800	2000	2200	2400
P_i, kW	194.9	159.02	140.52	133.99	126.04	120.04	117.87	116.21	115.02
v, m/s	7.25	5.21	3.97	3.07	2.47	1.69	1.36	1.09	0.9
T_i, kNm	3.81	4.32	5.01	7.85	9.2	12.75	15.55	19.15	28.72
$L_{o,1}$, m	358.19	396.1	416.82	427.76	439.11	447.79	452.41	456.36	460.12
$L_{o,3}$, m	545.96	535.12	528.94	525.38	521.98	518.82	517.17	515.67	514.55
$L_{o,5}$, m	545.96	535.12	528.94	525.38	521.98	518.82	517.17	515.67	514.55
$L_{o,7}$, m	545.96	535.12	528.94	525.38	521.98	518.82	517.17	515.67	514.55
$L_{o,9}$, m	505.31	499.92	497.74	497.82	496.67	497.47	497.8	498.35	498.35
α_i, rad	3.23	3.59	4.19	4.19	3.57	3.28	3.23	4.15	3.17
l_o, m	2	1.73	1.17	1.33	1	1.06	1.01	1.13	1.06
l_u, m	4.5	4.5	4.5	4.5	4.5	4.5	4.5	4.5	4.5
F_{TU}, kN	25.29	31.95	26.01	41.93	37.73	61.44	73.9	107.76	121.79
k_N, kN/m	340.21	343.72	310.54	370.61	359.42	436.24	476.57	565.24	608.75
B, mm	900	1050	1200	1350	1500	1800	2000	2200	2400
D_o, mm	194	133	102	89	63	63	63	63	63
D_u, mm	194	133	102	89	63	63	63	63	63
d_o, mm	25	25	25	25	25	30	35	35	40
d_u, mm	25	25	25	25	25	30	30	30	35
$D_{tr,i}$, mm	315	315	315	400	400	400	400	400	500
A_{energy}, ×1000 USD/year	886.07	717.42	622.88	593.93	565	537.71	527.45	519.4	513.8
A_{belt}, ×1000 USD/year	18.16	21.42	23.87	27.5	31.39	39.35	43.29	48.65	55.35
A_{motor}, ×1000 USD/year	8.33	6.75	5.87	5.6	5.33	5.07	4.98	4.9	4.85
A_{gear}, ×1000 USD/year	6.85	8.61	8	11.04	12.65	20.37	19.89	24.1	35.62

Table 5.5. MIDACO-based optimal multi-drive belt conveyors with four intermediate stations (N=4) under 5.6% inflation rate (continued)

	Belt width (mm)								
Parameter	900	1050	1200	1350	1500	1800	2000	2200	2400
$A_{carryidler}$, ×1000 USD/year	9.11	5.24	7.83	7.08	7.47	9.29	13.99	16.47	17.38
$A_{returnidler}$, ×1000 USD/year	2.46	1.41	1.12	1.06	1.21	1.18	1.34	1.4	1.71
$A_{conveyor}$, ×1000 USD/year	930.98	760.85	669.56	646.21	623.05	612.97	610.94	614.92	628.71

Table 5.6. MIDACO-based optimal multi-drive belt conveyors with five intermediate stations (N=5) under 5.6% inflation rate

	Belt width (mm)								
Parameter	900	1050	1200	1350	1500	1800	2000	2200	2400
P_i, kW	176.91	140.44	121.83	113.21	107.52	101.5	99.34	97.77	96.64
v, m/s	7.25	5.21	3.97	3.07	2.47	1.69	1.36	1.09	0.9
T_i, kNm	3.46	3.82	4.35	6.63	6.18	10.78	13.1	16.11	19.31
$L_{o,1}$, m	279.6	310.56	326.94	338.42	352.73	357.88	364.73	370.96	374.56
$L_{o,3}$, m	452.29	445.17	441.16	438.36	434.79	433.17	431.41	429.76	428.74
$L_{o,5}$, m	452.29	445.17	441.16	438.36	434.79	433.17	431.41	429.76	428.74
$L_{o,7}$, m	452.29	445.17	441.16	438.36	434.79	433.17	431.41	429.76	428.74
$L_{o,9}$, m	452.29	445.17	441.16	438.36	434.79	433.17	431.41	429.76	428.74
$L_{o,11}$, m	412.94	410.46	410.12	410.26	409.81	411.56	411.75	412.12	412.6
α_i, rad	3.47	4.19	4.05	3.62	3.42	4.19	3.73	4.15	3.43
l_o, m	2	1.85	1.8	1.98	1	1.94	1.46	1.14	1.1
l_u, m	4.5	4.5	4.5	4.5	4.5	4.5	4.5	4.5	4.35
F_{TU}, kN	25.72	35.08	46.34	68.97	37.66	126.44	114.54	108.25	127.23
k_N, kN/m	321.57	330.73	351.6	416.4	321.79	540.82	510.26	508.78	554.7
B, mm	900	1050	1200	1350	1500	1800	2000	2200	2400
D_o, mm	194	133	102	89	63	63	63	63	63
D_u, mm	194	133	102	89	63	63	63	63	63
d_o, mm	25	25	30	30	25	35	35	35	40
d_u, mm	25	25	30	25	25	30	30	30	30
$D_{tr,i}$, mm	315	315	315	400	315	400	400	400	400
A_{energy}, ×1000 USD/year	941.06	747.03	648.08	602.23	571.92	539.9	528.45	520.07	514.08
A_{belt}, ×1000 USD/year	17.99	21.06	24.27	28.03	29.98	39.37	43.18	47.47	52.8
A_{motor}, ×1000 USD/year	8.85	7.04	6.12	5.69	5.41	5.11	5	4.93	4.87
A_{gear}, ×1000 USD/year	7.66	8.11	8.76	11.67	11.09	17.15	20.3	24.44	28.92
$A_{carryidler}$, ×1000 USD/year	9.11	5.66	6.09	5.68	9.62	7.96	11.65	16.47	20.46
$A_{returnidler}$, ×1000 USD/year	2.46	1.41	1.38	1.06	0.95	1.29	1.34	1.4	1.5
$A_{conveyor}$, ×1000 USD/year	987.14	790.31	694.7	654.36	628.97	610.78	609.92	614.78	622.64

5.4 OPTIMAL CONVEYOR DESIGNS AND RELATED COSTS UNDER FLUCTUATING INFLATION RATE AT 5.2% ON AVERAGE

The technical specifications and the attached economic performances of the single drive and multi-drive belt conveyors optimized under fluctuating inflation rate with 5.2% on average are provided in Tables 5.7 to 5.12. All the previous observations reported in the case of fixed inflation rate at 5.6% appears to also be valid for the corresponding belt conveyors obtained under the present inflation rate scenario.

Table 5.7. MIDACO-based optimal single drive belt conveyors (N=0) under 5.2% of average inflation rate

	Belt width (mm)								
Parameter	900	1050	1200	1350	1500	1800	2000	2200	2400
P_i, kW	1556.67	1408.66	1339.39	1297.7	1268.88	1238.13	1225.63	1214.99	1208.6
v, m/s	7.25	5.21	3.97	3.07	2.47	1.69	1.36	1.09	0.9
T_i, kNm	60.87	76.59	121.36	152	185.27	328.82	404.16	500.51	754.52
α_i, rad	4.19	4.19	4.19	4.19	4.19	4.19	4.19	4.19	4.19
l_o, m	2	2	2	2	1.85	1.96	2	1.72	1.33
l_u, m	4.5	4.5	4.5	4.5	3.51	4.4	4.5	4.5	4.5
F_{TU}, kN	61.78	80.15	101.96	129.48	159.57	230.2	284.89	355.39	430.85
k_N, kN/m	1177.51	1279.51	1403.76	1568.3	1725.21	2049.72	2271.46	2562.1	2836.3
B, mm	900	1050	1200	1350	1500	1800	2000	2200	2400
D_o, mm	194	133	102	89	63	63	63	63	63
D_u, mm	194	133	102	89	63	63	63	63	63
d_o, mm	25	25	35	30	30	35	40	40	40
d_u, mm	25	25	25	30	25	30	35	35	40
$D_{tr,i}$, mm	630	630	800	800	800	1000	1000	1000	1250
A_{energy}, ×1000 USD/year	716.45	648.33	616.45	597.26	584	569.84	564.09	559.19	556.25
A_{belt}, ×1000 USD/year	25.66	31.21	37.5	44.99	53.06	71.63	85.89	103.89	123.36
A_{motor}, ×1000 USD/year	6.28	5.68	5.4	5.23	5.11	4.99	4.93	4.89	4.86
A_{gear}, ×1000 USD/year	14.47	18.38	29.85	37.91	46.8	86.51	107.98	135.9	211.46
$A_{carryidler}$, ×1000 USD/year	8.91	5.13	6.28	5.51	6.08	7.73	9.24	11.72	16.55
$A_{returnidler}$, ×1000 USD/year	2.42	1.38	1.1	1.29	1.2	1.3	1.57	1.62	1.93
$A_{conveyor}$, ×1000 USD/year	774.19	710.11	696.56	692.18	696.25	741.99	773.7	817.21	914.41

Table 5.8. MIDACO-based optimal multi-drive belt conveyors with one intermediate station (N=1) under 5.2% of average inflation rate (continued)

	Belt width (mm)								
Parameter	900	1050	1200	1350	1500	1800	2000	2200	2400

Table 5.8. MIDACO-based optimal multi-drive belt conveyors with one intermediate station (N=1) under 5.2% of average inflation rate

	Belt width (mm)								
Parameter	900	1050	1200	1350	1500	1800	2000	2200	2400
P_i, kW	410.21	359.23	334.02	321.08	311.41	302.16	298.1	294.98	292.48
v, m/s	7.25	5.21	3.97	3.07	2.47	1.69	1.36	1.09	0.9
T_i, kNm	10.18	15.5	18.92	23.51	28.42	40.12	61.93	76.56	92.03
$L_{o,1}$, m	1176.3	1192.56	1201.27	1206.37	1212.78	1217.93	1219.33	1220.21	1222.2
$L_{o,3}$, m	1324.22	1308.06	1299.35	1294.25	1287.84	1282.69	1281.42	1280.54	1278.55
α_i, rad	3.35	3.92	4.19	3.6	4.19	4.14	4.19	4.19	3.24
l_o, m	2	2	2	2	1.59	1.15	1.45	1.75	1.35
l_u, m	4.5	4.5	4.5	4.5	4.5	4.5	4.5	3.93	3.28
F_{TU}, kN	25.25	38.16	52.01	68.63	66.32	65.37	110.93	173.24	156.22
k_N, kN/m	586.82	641.82	704.14	790.08	813.54	891.99	1047.49	1245.37	1282.2
B, mm	900	1050	1200	1350	1500	1800	2000	2200	2400
D_o, mm	194	133	102	89	63	63	63	63	63
D_u, mm	194	133	102	89	63	63	63	63	63
d_o, mm	25	25	25	30	25	30	30	30	30
d_u, mm	25	25	25	30	25	30	30	30	30
$D_{tr,i}$, mm	400	500	500	500	500	500	630	630	630
A_{energy}, ×1000 USD/year	755.18	661.34	614.92	591.11	573.29	556.27	548.79	543.05	538.46
A_{belt}, ×1000 USD/year	19.99	23.87	28.02	32.71	36.71	45.55	54.06	64.54	71.47
A_{motor}, ×1000 USD/year	6.55	5.73	5.33	5.12	4.96	4.82	4.75	4.7	4.66
A_{gear}, ×1000 USD/year	5.21	7.52	9.04	11.11	13.37	18.87	29.46	36.74	44.57
$A_{carryidler}$, ×1000 USD/year	8.91	5.13	5.37	5.51	7.05	11.61	11.47	11.57	16.31
$A_{returnidler}$, ×1000 USD/year	2.41	1.38	1.09	1.29	0.93	1.27	1.32	1.57	1.94
$A_{conveyor}$, ×1000 USD/year	798.25	704.97	663.77	646.84	636.32	638.39	649.85	662.17	677.4

Table 5.9. MIDACO-based optimal multi-drive belt conveyors with two intermediate stations (N=2) under 5.2% of average inflation rate

	Belt width (mm)								
Parameter	900	1050	1200	1350	1500	1800	2000	2200	2400
P_i, kW	292.6	248.83	226.95	216.75	208.45	200.95	198.02	195.51	193.81
v, m/s	7.25	5.21	3.97	3.07	2.47	1.69	1.36	1.09	0.9
T_i, kNm	7.26	8.59	10.28	12.69	19.02	26.68	32.65	40.27	48.4
$L_{o,1}$, m	726.98	750.1	762.96	773.89	779.48	787.08	790.42	794.27	797.67

Table 5.9. MIDACO-based optimal multi-drive belt conveyors with two intermediate stations (N=2) under 5.2% of average inflation rate (continued)

	Belt width (mm)								
Parameter	900	1050	1200	1350	1500	1800	2000	2200	2400
$L_{o,3}$, m	906.15	892.33	884.07	876.84	873.03	867.28	864.63	861.71	859.25
$L_{o,5}$, m	867.79	858.49	853.89	850.19	848.61	846.76	846.07	845.14	844.2
α_i, rad	4.01	4.19	3.82	4.19	3.29	4.04	4.19	4.19	4.18
l_o, m	2	2	2	1.33	1.87	1.59	1.62	1.43	1.06
l_u, m	4.5	4.5	4.5	4.5	4.5	4.5	4.5	4.28	3.8
F_{TU}, kN	25.49	38.47	52.4	41.26	81.3	99.23	127.29	139.68	119.12
k_N, kN/m	453.1	492.21	537.54	517.75	646.82	721.91	807.2	872.48	876.64
B, mm	900	1050	1200	1350	1500	1800	2000	2200	2400
D_o, mm	194	133	102	89	63	63	63	63	63
D_u, mm	194	133	102	89	63	63	63	63	63
d_o, mm	25	25	25	25	25	30	30	30	30
d_u, mm	25	25	25	25	25	30	30	30	30
$D_{tr,i}$, mm	400	400	400	400	500	500	500	500	500
A_{energy}, ×1000 USD/year	808	687.12	626.73	598.54	575.64	554.91	546.83	539.89	535.19
A_{belt}, ×1000 USD/year	18.9	22.42	26.12	29.14	34.2	42.38	48.84	55.25	60.38
A_{motor}, ×1000 USD/year	6.99	5.95	5.43	5.18	4.98	4.8	4.74	4.68	4.63
A_{gear}, ×1000 USD/year	5.97	6.8	7.87	9.43	13.62	18.85	23.01	28.42	34.27
$A_{carryidler}$, ×1000 USD/year	8.92	5.13	5.37	6.95	6.01	9.53	11.43	14.07	20.78
$A_{returnidler}$, ×1000 USD/year	2.41	1.38	1.09	1.03	0.93	1.27	1.32	1.44	1.68
$A_{conveyor}$, ×1000 USD/year	851.2	728.8	672.61	650.27	635.39	631.74	636.17	643.74	656.93

Table 5.10. MIDACO-based optimal multi-drive belt conveyors with three intermediate stations (N=3) under 5.2% of average inflation rate

	Belt width (mm)								
Parameter	900	1050	1200	1350	1500	1800	2000	2200	2400
P_i, kW	234.53	194.33	174.16	164.5	157.64	151.05	148.55	146.46	144.94
v, m/s	7.25	5.21	3.97	3.07	2.47	1.69	1.36	1.09	0.9
T_i, kNm	5.82	6.71	7.89	9.63	11.51	16.05	19.59	30.17	36.19
$L_{o,1}$, m	503.1	529.72	543.95	554.62	563.82	574.63	578.84	581.41	585.41
$L_{o,3}$, m	679.03	668.64	662.68	657.98	654.06	649.14	647.09	645.77	643.94
$L_{o,5}$, m	679.03	668.64	662.68	657.98	654.06	649.14	647.09	645.77	643.94
$L_{o,7}$, m	640.16	634.32	632.01	630.74	629.38	628.41	628.3	628.67	628.33
α_i, rad	3.96	3.32	3.24	4.18	3.88	3.32	4.19	4.19	4.19
l_o, m	2	2	2	2	1.88	1.15	1.13	1.51	1.27
l_u, m	4.5	4.5	4.5	4.5	4.5	4.5	4.5	4.5	4.5
F_{TU}, kN	25.6	38.62	52.5	69.29	82.21	67.67	83.45	148.62	150
k_N, kN/m	387.08	418.36	455.04	509.86	546.57	526.68	580.51	736.58	761.06
B, mm	900	1050	1200	1350	1500	1800	2000	2200	2400
D_o, mm	194	133	102	89	63	63	63	63	63

Table 5.10. MIDACO-based optimal multi-drive belt conveyors with three intermediate stations (N=3) under 5.2% of average inflation rate (continued)

	Belt width (mm)								
Parameter	900	1050	1200	1350	1500	1800	2000	2200	2400
D_u, mm	194	133	102	89	63	63	63	63	63
d_o, mm	25	25	30	25	25	30	30	35	35
d_u, mm	25	25	30	25	25	30	30	35	35
$D_{tr,i}$, mm	400	400	400	400	400	400	400	500	500
A_{energy}, ×1000 USD/year	863.54	715.5	641.25	605.69	580.41	556.16	546.96	539.25	533.65
A_{belt}, ×1000 USD/year	18.41	21.75	25.24	29.06	32.79	39.02	44.35	52.16	57.5
A_{motor}, ×1000 USD/year	7.47	6.2	5.56	5.25	5.03	4.82	4.74	4.68	4.63
A_{gear}, ×1000 USD/year	6.77	7.5	8.48	9.95	11.55	15.51	18.68	28.36	34.02
$A_{carryidler}$, ×1000 USD/year	8.92	5.13	5.38	5.53	5.97	11.56	14.78	13.41	17.28
$A_{returnidler}$, ×1000 USD/year	2.41	1.38	1.35	1.03	0.93	1.27	1.32	1.62	1.67
$A_{conveyor}$, ×1000 USD/year	907.53	757.46	687.25	656.5	636.69	628.34	630.83	639.49	648.75

Table 5.11. MIDACO-based optimal multi-drive belt conveyors with four intermediate stations (N=4) under 5.2% of average inflation rate

	Belt width (mm)								
Parameter	900	1050	1200	1350	1500	1800	2000	2200	2400
P_i, kW	199.89	161.85	142.63	133.67	127.37	121.27	118.93	117.19	115.93
v, m/s	7.25	5.21	3.97	3.07	2.47	1.69	1.36	1.09	0.9
T_i, kNm	3.91	5.59	6.46	7.83	9.3	12.88	15.69	19.31	28.95
$L_{o,1}$, m	368.89	397.74	415.13	424.78	434.98	443.79	450.18	455.79	458.54
$L_{o,3}$, m	542.87	534.69	529.42	526.15	522.96	519.78	517.69	515.79	514.92
$L_{o,5}$, m	542.87	534.69	529.42	526.15	522.96	519.78	517.69	515.79	514.92
$L_{o,7}$, m	542.87	534.69	529.42	526.15	522.96	519.78	517.69	515.79	514.92
$L_{o,9}$, m	503.88	499.91	498.33	498.49	497.86	498.59	498.47	498.56	498.82
α_i, rad	4.19	4.19	4.18	4.15	3.71	4.16	3.81	4.19	4.19
l_o, m	2	2	1.72	2	1.84	1.68	1.37	1.11	1.21
l_u, m	4.5	4.5	4.5	4.5	4.5	3.94	4.5	4.49	4.18
F_{TU}, kN	25.67	38.71	43.63	69.63	80.05	106.84	105.55	104.5	142.29
k_N, kN/m	347.7	374.34	374.87	455.31	479.36	544.2	545.27	562.16	647.38
B, mm	900	1050	1200	1350	1500	1800	2000	2200	2400
D_o, mm	194	133	102	89	63	63	63	63	63
D_u, mm	194	133	102	89	63	63	63	63	63
d_o, mm	25	25	25	30	30	35	35	35	40
d_u, mm	25	25	25	25	25	25	30	30	30
$D_{tr,i}$, mm	315	400	400	400	400	400	400	400	500
A_{energy}, ×1000 USD/year	919.98	744.88	656.45	615.23	586.22	558.13	547.39	539.34	533.57
A_{belt}, ×1000 USD/year	18.13	21.38	24.44	28.42	31.89	39.33	43.72	48.44	54.8
A_{motor}, ×1000 USD/year	7.97	6.46	5.7	5.34	5.09	4.85	4.76	4.69	4.64
A_{gear}, ×1000 USD/year	6.54	8.23	9.12	10.53	12.08	15.92	19	23.03	34.04

Table 5.11. MIDACO-based optimal multi-drive belt conveyors with four intermediate stations (N=4) under 5.2% of average inflation rate (continued)

	Belt width (mm)								
Parameter	900	1050	1200	1350	1500	1800	2000	2200	2400
$A_{carryidler}$, ×1000 USD/year	8.92	5.13	5.2	5.52	6.13	9.01	12.21	16.56	18.15
$A_{returnidler}$, ×1000 USD/year	2.41	1.38	1.09	1.03	0.93	1.15	1.32	1.37	1.53
$A_{conveyor}$, ×1000 USD/year	963.96	787.46	702	666.07	642.35	628.4	628.39	633.43	646.73

Table 5.12. MIDACO-based optimal multi-drive belt conveyors with five intermediate stations (N=5) under 5.2% of average inflation rate

	Belt width (mm)								
Parameter	900	1050	1200	1350	1500	1800	2000	2200	2400
P_i, kW	176.91	140.25	121.72	113.23	107.3	101.53	99.36	97.81	96.66
v, m/s	7.25	5.21	3.97	3.07	2.47	1.69	1.36	1.09	0.9
T_i, kNm	3.46	3.81	5.51	6.63	7.83	10.79	13.11	16.12	19.31
$L_{o,1}$, m	279.6	309.73	328.13	338.62	348.76	361.2	365.13	370.45	374.76
$L_{o,3}$, m	452.29	445.35	441.1	438.32	435.78	432.5	431.33	429.86	428.69
$L_{o,5}$, m	452.29	445.35	441.1	438.32	435.78	432.5	431.33	429.86	428.69
$L_{o,7}$, m	452.29	445.35	441.1	438.32	435.78	432.5	431.33	429.86	428.69
$L_{o,9}$, m	452.29	445.35	441.1	438.32	435.78	432.5	431.33	429.86	428.69
$L_{o,11}$, m	412.94	410.57	409.59	410.22	410.24	410.92	411.67	412.23	412.6
α_i, rad	3.82	4.19	4.19	4.12	3.17	3.86	3.9	3.94	4.19
l_o, m	2	2	1.72	1.94	1.8	1.15	1.37	1.26	1.06
l_u, m	4.5	4.5	4.5	4.5	4.5	4.2	4.5	4.5	4.37
F_{TU}, kN	25.72	38.78	43.76	67.2	78.01	68.29	106.3	121.89	121.67
k_N, kN/m	321.57	345.08	342.49	410.96	433.12	406.84	493.19	534.66	545.01
B, mm	900	1050	1200	1350	1500	1800	2000	2200	2400
D_o, mm	194	133	102	89	63	63	63	63	63
D_u, mm	194	133	102	89	63	63	63	63	63
d_o, mm	25	25	25	30	30	30	35	40	40
d_u, mm	25	25	25	25	30	25	30	30	30
$D_{tr,i}$, mm	315	315	400	400	400	400	400	400	400
A_{energy}, ×1000 USD/year	977.08	774.57	672.22	625.34	592.62	560.76	548.75	540.19	533.84
A_{belt}, ×1000 USD/year	17.95	21.14	24.14	27.92	31.3	37.16	42.8	47.91	52.49
A_{motor}, ×1000 USD/year	8.46	6.72	5.84	5.44	5.16	4.89	4.79	4.71	4.66
A_{gear}, ×1000 USD/year	7.32	7.74	9.78	11.15	12.65	16.4	19.4	23.36	27.64
$A_{carryidler}$, ×1000 USD/year	8.92	5.13	5.2	5.69	6.27	11.56	12.16	16.02	20.82
$A_{returnidler}$, ×1000 USD/year	2.41	1.38	1.09	1.03	1.19	1.08	1.32	1.37	1.46
$A_{conveyor}$, ×1000 USD/year	1022.16	816.69	718.28	676.58	649.19	631.85	629.21	633.56	640.91

5.5 OPTIMAL CONVEYOR DESIGNS AND RELATED COSTS UNDER FLUCTUATING INFLATION RATE AT 5.8% ON AVERAGE

The technical specifications and the related economic performances of the single drive and multi-drive belt conveyors optimized under fluctuating inflation rate with 5.8% on average are given in Tables 5.13 to 5.18. Similarly, all the previous observations reported in the case of fixed inflation rate at 5.6% appears to also be valid for the corresponding belt conveyors obtained under the present inflation rate scenario.

Table 5.13. MIDACO-based optimal single drive belt conveyors (N=0) under 5.8% of average inflation rate

	Belt width (mm)								
Parameter	900	1050	1200	1350	1500	1800	2000	2200	2400
P_i, kW	1556.67	1408.66	1337.29	1299.26	1268	1238.13	1225.63	1214.99	1209.06
v, m/s	7.25	5.21	3.97	3.07	2.47	1.69	1.36	1.09	0.9
T_i, kNm	60.87	76.59	121.17	152.18	231.42	328.82	404.16	500.51	754.8
α_i, rad	4.19	4.19	4.19	4.19	4.19	4.19	4.19	4.19	4.19
l_o, m	2	2	2	2	2	1.96	2	1.72	1.33
l_u, m	4.5	4.5	4.5	4.34	4.5	4.4	4.5	4.5	3.72
F_{TU}, kN	61.78	80.15	101.78	129.67	159.83	230.2	284.89	355.39	430.58
k_N, kN/m	1177.51	1279.51	1401.48	1570.29	1725.02	2049.72	2271.46	2562.1	2836.63
B, mm	900	1050	1200	1350	1500	1800	2000	2200	2400
D_o, mm	194	133	102	89	63	63	63	63	63
D_u, mm	194	133	102	89	63	63	63	63	63
d_o, mm	25	25	30	35	35	35	40	40	40
d_u, mm	25	25	25	25	30	30	35	35	35
$D_{tr,i}$, mm	630	630	800	800	1000	1000	1000	1000	1250
A_{energy}, ×1000 USD/year	673.38	609.36	578.48	562.03	548.51	535.59	530.18	525.58	523.01
A_{belt}, ×1000 USD/year	25.49	31	37.21	44.72	52.7	71.14	85.31	103.18	122.53
A_{motor}, ×1000 USD/year	6.8	6.15	5.83	5.66	5.53	5.39	5.34	5.29	5.27
A_{gear}, ×1000 USD/year	15.69	19.93	32.3	41.15	64.36	93.79	117.06	147.33	229.35
$A_{carryidler}$, ×1000 USD/year	9.02	5.19	5.44	6.5	6.61	7.83	9.36	11.87	16.76
$A_{returnidler}$, ×1000 USD/year	2.45	1.4	1.11	1.09	1.21	1.31	1.59	1.65	2.05
$A_{conveyor}$, ×1000 USD/year	732.83	673.03	660.38	661.15	678.91	715.06	748.85	794.9	898.98

Table 5.14. MIDACO-based optimal multi-drive belt conveyors with one intermediate station (N=1) under 5.8% of average inflation rate (continued)

	Belt width (mm)								
Parameter	900	1050	1200	1350	1500	1800	2000	2200	2400

Table 5.14. MIDACO-based optimal multi-drive belt conveyors with one intermediate station (N=1) under 5.8% of average inflation rate

	Belt width (mm)								
Parameter	900	1050	1200	1350	1500	1800	2000	2200	2400
P_i, kW	410.21	359.23	334.1	321.8	311.37	302.4	298.1	294.82	292.42
v, m/s	7.25	5.21	3.97	3.07	2.47	1.69	1.36	1.09	0.9
T_i, kNm	10.18	15.5	18.92	23.56	28.41	40.16	61.93	76.51	92.01
$L_{o,1}$, m	1176.3	1192.56	1202.04	1208.59	1211.79	1216.88	1219.33	1222.12	1223.76
$L_{o,3}$, m	1324.22	1308.06	1298.58	1292.03	1288.83	1283.74	1281.42	1278.63	1276.99
α_i, rad	3.26	3.17	3.53	4.19	3.46	4.19	4.06	4.19	3.47
l_o, m	2	2	1.71	1.32	1.85	1.15	1.45	1.13	1.1
l_u, m	4.5	4.5	4.5	4.5	4.5	3.41	4.5	4.5	4.5
F_{TU}, kN	25.25	38.16	42.47	40.4	79.71	64.86	110.93	103.5	123.22
k_N, kN/m	586.82	641.82	671.25	704.49	850.58	891.38	1047.49	1113.13	1224.83
B, mm	900	1050	1200	1350	1500	1800	2000	2200	2400
D_o, mm	194	133	102	89	63	63	63	63	63
D_u, mm	194	133	102	89	63	63	63	63	63
d_o, mm	25	25	25	25	30	25	30	35	35
d_u, mm	25	25	25	25	30	25	30	35	35
$D_{tr,i}$, mm	400	500	500	500	500	500	630	630	630
A_{energy}, ×1000 USD/year	709.79	621.59	578.1	556.82	538.78	523.25	515.81	510.13	505.97
A_{belt}, ×1000 USD/year	19.85	23.71	27.44	31.32	37.04	45.23	53.69	60.7	69.34
A_{motor}, ×1000 USD/year	7.08	6.2	5.76	5.55	5.37	5.22	5.14	5.08	5.04
A_{gear}, ×1000 USD/year	5.65	8.15	9.8	12.07	14.49	20.48	31.94	39.81	48.31
$A_{carryidler}$, ×1000 USD/year	9.03	5.19	5.3	7.06	6.14	11.76	11.62	16.42	20.19
$A_{returnidler}$, ×1000 USD/year	2.44	1.4	1.11	1.05	1.2	1.35	1.33	1.64	1.69
$A_{conveyor}$, ×1000 USD/year	753.84	666.24	627.51	613.87	603.02	607.28	619.53	633.8	650.55

Table 5.15. MIDACO-based optimal multi-drive belt conveyors with two intermediate stations (N=2) under 5.8% of average inflation rate

	Belt width (mm)								
Parameter	900	1050	1200	1350	1500	1800	2000	2200	2400
P_i, kW	292.6	248.83	227	216.33	208.49	201.01	197.9	195.48	193.79
v, m/s	7.25	5.21	3.97	3.07	2.47	1.69	1.36	1.09	0.9
T_i, kNm	7.26	8.59	10.28	12.67	19.03	26.69	32.63	40.26	48.39
$L_{o,1}$, m	726.98	750.1	763.97	772.02	780.13	787.69	791	794.2	797.59

Table 5.15. MIDACO-based optimal multi-drive belt conveyors with two intermediate stations (N=2) under 5.8% of average inflation rate (continued)

	Belt width (mm)								
Parameter	900	1050	1200	1350	1500	1800	2000	2200	2400
$L_{o,3}$, m	906.15	892.33	883.55	877.82	872.69	866.97	864.34	861.74	859.29
$L_{o,5}$, m	867.79	858.49	853.4	851.08	848.3	846.46	845.78	845.18	844.24
α_i, rad	3.75	3.32	4.19	4.19	4.13	4.16	4.19	4.19	4.19
l_o, m	2	2	1.71	1.83	1.68	1.42	1.44	1.51	1.08
l_u, m	4.5	4.5	4.5	4.5	4.5	4.5	4.5	4.47	3.8
F_{TU}, kN	25.49	38.47	43.12	62.27	71.75	86.54	111.41	148.37	121.9
k_N, kN/m	453.1	492.21	505.47	581.66	620.43	692.79	773.86	888.68	881.4
B, mm	900	1050	1200	1350	1500	1800	2000	2200	2400
D_o, mm	194	133	102	89	63	63	63	63	63
D_u, mm	194	133	102	89	63	63	63	63	63
d_o, mm	25	25	25	25	25	30	30	30	30
d_u, mm	25	25	25	25	25	30	30	30	30
$D_{tr,i}$, mm	400	400	400	400	500	500	500	500	500
A_{energy}, ×1000 USD/year	759.43	645.82	589.17	561.48	541.12	521.72	513.64	507.37	502.98
A_{belt}, ×1000 USD/year	18.78	22.27	25.59	29.73	33.59	41.57	47.82	55.25	60.09
A_{motor}, ×1000 USD/year	7.57	6.44	5.87	5.6	5.39	5.2	5.12	5.06	5.02
A_{gear}, ×1000 USD/year	6.47	7.37	8.54	10.21	14.77	20.45	24.93	30.8	37.15
$A_{carryidler}$, ×1000 USD/year	9.03	5.2	5.28	6.09	6.76	10.82	11.7	13.54	20.64
$A_{returnidler}$, ×1000 USD/year	2.44	1.4	1.11	1.05	0.95	1.28	1.33	1.39	1.7
$A_{conveyor}$, ×1000 USD/year	803.72	688.49	635.56	614.15	602.58	601.04	604.55	613.41	627.59

Table 5.16. MIDACO-based optimal multi-drive belt conveyors with three intermediate stations (N=3) under 5.8% of average inflation rate

	Belt width (mm)								
Parameter	900	1050	1200	1350	1500	1800	2000	2200	2400
P_i, kW	234.53	194.33	174.14	164.5	157.66	151.08	148.51	146.47	145.26
v, m/s	7.25	5.21	3.97	3.07	2.47	1.69	1.36	1.09	0.9
T_i, kNm	5.82	6.71	7.89	9.63	11.51	16.05	19.59	30.17	36.27
$L_{o,1}$, m	503.1	529.72	545.78	554.6	564.58	574.77	578.63	581.16	581.66
$L_{o,3}$, m	679.03	668.64	662.06	657.98	653.8	649.1	647.16	645.86	645.19
$L_{o,5}$, m	679.03	668.64	662.06	657.98	653.8	649.1	647.16	645.86	645.19
$L_{o,7}$, m	640.16	634.32	631.42	630.76	629.14	628.35	628.37	628.74	629.58
α_i, rad	3.79	4.19	4.19	3.32	3.66	4.19	4.19	4.19	4.19
l_o, m	2	2	1.72	2	1.69	1.12	1.18	1.52	1.19
l_u, m	4.5	4.5	4.5	4.5	4.5	4.5	4.5	4.5	2.14
F_{TU}, kN	25.6	38.62	43.44	69.48	72.4	65.26	87.95	150	135.79
k_N, kN/m	387.08	418.36	423.64	510.42	519.44	521.22	589.79	739.23	737.56
B, mm	900	1050	1200	1350	1500	1800	2000	2200	2400
D_o, mm	194	133	102	89	63	63	63	63	63

Table 5.16. MIDACO-based optimal multi-drive belt conveyors with three intermediate stations (N=3) under 5.8% of average inflation rate (continued)

	Belt width (mm)								
Parameter	900	1050	1200	1350	1500	1800	2000	2200	2400
D_u, mm	194	133	102	89	63	63	63	63	63
d_o, mm	25	25	25	25	25	30	30	40	25
d_u, mm	25	25	25	25	25	30	30	40	25
$D_{tr,i}$, mm	400	400	400	400	400	400	400	500	500
A_{energy}, ×1000 USD/year	811.63	672.49	602.62	569.27	545.61	522.84	513.95	506.89	502.68
A_{belt}, ×1000 USD/year	18.28	21.61	24.75	28.87	32.19	38.66	44.23	51.86	56.54
A_{motor}, ×1000 USD/year	8.09	6.71	6.01	5.68	5.45	5.22	5.13	5.06	5.02
A_{gear}, ×1000 USD/year	7.34	8.13	9.19	10.79	12.52	16.82	20.25	30.75	36.96
$A_{carryidler}$, ×1000 USD/year	9.03	5.2	5.27	5.58	6.74	12.05	14.34	13.47	18.77
$A_{returnidler}$, ×1000 USD/year	2.44	1.4	1.11	1.05	0.95	1.28	1.33	1.9	2.48
$A_{conveyor}$, ×1000 USD/year	856.82	715.53	648.95	621.24	603.45	596.88	599.23	609.94	622.45

Table 5.17. MIDACO-based optimal multi-drive belt conveyors with four intermediate stations (N=4) under 5.8% of average inflation rate

	Belt width (mm)								
Parameter	900	1050	1200	1350	1500	1800	2000	2200	2400
P_i, kW	199.89	162.11	142.89	133.71	127.51	121.35	118.94	117.22	115.9
v, m/s	7.25	5.21	3.97	3.07	2.47	1.69	1.36	1.09	0.9
T_i, kNm	3.91	5.6	6.47	7.83	9.31	12.89	15.69	19.31	28.94
$L_{o,1}$, m	368.89	397.92	412.51	424.19	434.77	446.11	450.31	456.04	458.21
$L_{o,3}$, m	542.87	534.63	530.07	526.3	523.01	519.19	517.66	515.72	515.01
$L_{o,5}$, m	542.87	534.63	530.07	526.3	523.01	519.19	517.66	515.72	515.01
$L_{o,7}$, m	542.87	534.63	530.07	526.3	523.01	519.19	517.66	515.72	515.01
$L_{o,9}$, m	503.88	499.91	499	498.63	497.92	498.04	498.43	498.52	498.88
α_i, rad	3.56	4.18	4.19	4.08	4.18	4.19	4.19	4.03	4.19
l_o, m	2	2	2	2	1.89	1.27	1.34	1.05	1.33
l_u, m	4.5	4.5	4.5	4.5	4.49	4.5	4.5	4.5	4.5
F_{TU}, kN	25.67	38.71	63.01	69.52	83.11	76.95	102.71	98.17	158.66
k_N, kN/m	347.7	374.82	449.68	455.04	488.72	475.26	539.44	550.27	675.63
B, mm	900	1050	1200	1350	1500	1800	2000	2200	2400
D_o, mm	194	133	102	89	63	63	63	63	63
D_u, mm	194	133	102	89	63	63	63	63	63
d_o, mm	25	30	30	30	35	35	35	35	40
d_u, mm	25	25	25	30	25	30	30	30	35
$D_{tr,i}$, mm	315	400	400	400	400	400	400	400	500
A_{energy}, ×1000 USD/year	864.68	701.24	618.11	578.39	551.57	524.92	514.53	507.06	501.38
A_{belt}, ×1000 USD/year	18.01	21.24	25.03	28.22	31.8	37.95	43.32	47.87	55.09
A_{motor}, ×1000 USD/year	8.62	7	6.18	5.78	5.52	5.26	5.15	5.08	5.02
A_{gear}, ×1000 USD/year	7.1	8.93	9.9	11.42	13.11	17.27	20.6	24.97	36.9

Table 5.17. MIDACO-based optimal multi-drive belt conveyors with four intermediate stations (N=4) under 5.8% of average inflation rate (continued)

	Belt width (mm)								
Parameter	900	1050	1200	1350	1500	1800	2000	2200	2400
$A_{carryidler}$, ×1000 USD/year	9.03	6.12	5.45	5.59	7	12.04	12.66	17.67	16.74
$A_{returnidler}$, ×1000 USD/year	2.44	1.4	1.11	1.3	0.95	1.28	1.33	1.39	1.69
$A_{conveyor}$, ×1000 USD/year	909.88	745.93	665.78	630.71	609.94	598.72	597.58	604.03	616.82

Table 5.18. MIDACO-based optimal multi-drive belt conveyors with five intermediate stations (N=5) under 5.8% of average inflation rate

	Belt width (mm)								
Parameter	900	1050	1200	1350	1500	1800	2000	2200	2400
P_i, kW	176.91	140.25	121.68	113.21	107.54	101.5	99.35	97.83	96.66
v, m/s	7.25	5.21	3.97	3.07	2.47	1.69	1.36	1.09	0.9
T_i, kNm	3.46	3.81	4.34	6.63	6.18	10.78	13.1	16.12	19.31
$L_{o,1}$, m	279.6	309.73	327.99	338.34	352.24	358.59	364.94	370.78	374.73
$L_{o,3}$, m	452.29	445.35	440.96	438.37	434.89	433.03	431.37	429.79	428.7
$L_{o,5}$, m	452.29	445.35	440.96	438.37	434.89	433.03	431.37	429.79	428.7
$L_{o,7}$, m	452.29	445.35	440.96	438.37	434.89	433.03	431.37	429.79	428.7
$L_{o,9}$, m	452.29	445.35	440.96	438.37	434.89	433.03	431.37	429.79	428.7
$L_{o,11}$, m	412.94	410.57	409.87	410.3	409.9	411.41	411.7	412.18	412.59
α_i, rad	3.91	3.56	3.71	4.16	3.19	3.62	4.19	4.02	3.42
l_o, m	2	2	1.72	2	1	1.7	1.42	1.19	1.06
l_u, m	4.5	4.5	4.5	4.5	4.5	4.5	4.5	4.5	4.36
F_{TU}, kN	25.72	38.78	43.76	69.72	37.56	108.31	110.24	113.57	122.56
k_N, kN/m	321.57	345.08	342.44	418.72	321.56	498.97	501.33	519.04	546.56
B, mm	900	1050	1200	1350	1500	1800	2000	2200	2400
D_o, mm	194	133	102	89	63	63	63	63	63
D_u, mm	194	133	102	89	63	63	63	63	63
d_o, mm	25	25	25	30	25	35	35	40	40
d_u, mm	25	25	25	25	30	35	30	30	30
$D_{tr,i}$, mm	315	315	315	400	315	400	400	400	400
A_{energy}, ×1000 USD/year	918.35	728.01	631.64	587.67	558.24	526.87	515.72	507.84	501.74
A_{belt}, ×1000 USD/year	17.83	21	23.97	27.82	29.72	38.35	42.65	47.27	52.17
A_{motor}, ×1000 USD/year	9.16	7.28	6.32	5.89	5.6	5.29	5.18	5.1	5.04
A_{gear}, ×1000 USD/year	7.94	8.39	9.07	12.09	11.49	17.77	21.03	25.34	29.96
$A_{carryidler}$, ×1000 USD/year	9.04	5.2	5.27	5.59	9.54	9.03	11.94	17.24	20.95
$A_{returnidler}$, ×1000 USD/year	2.44	1.4	1.11	1.05	1.2	1.54	1.33	1.39	1.48
$A_{conveyor}$, ×1000 USD/year	964.76	771.28	677.38	640.1	615.79	598.85	597.86	604.16	611.35

CHAPTER 6 DISCUSSION

6.1 CHAPTER OVERVIEW

This chapter presents a discussion on the simulation results introduced in Chapter 5 with the objective of addressing the economic research questions presented in Section 1.3.

6.2 PROFILE OF THE MINIMUM CONVEYOR COSTS

Figure 6.1 displays the evolution of the equivalent annual cost of conveyors under fixed inflation rate at 5.6% as a function of the conveyor speed and the number of intermediate drive stations fitted. The case with $N = 0$ refers to the single drive technology. This figure indicates that, in general, single drive technology will be regarded as the most economic option at high conveyor speed, while the multi-drive technology will only gain in profitability with the decrease of the conveyor speed. Furthermore, at a high conveyor speed, the greater the number of intermediate drive stations, the poorer the economic performance of the multi-drive conveyor system will be. The variation of the conveyor speed finally appears to have a larger impact on the performance of the multiple drive technology compared to the single drive alternative.

6.3 COST-EFFECTIVE BELT CONVEYOR FRONT

The conveyor costs of the cheapest designs with respect to the number of intermediate drive stations installed are summarized in Figure 6.2 along with the respective operating and capital costs. This figure shows that, subject to the assumptions made, the manufacturers supplied information and the optimizer used, the multi-drive belt conveyor fitted with three intermediate drive stations and operated

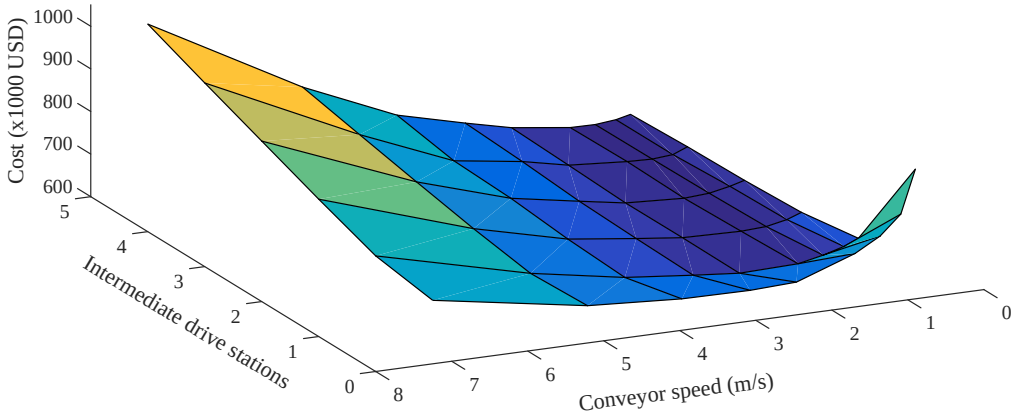

Figure 6.1. Cheapest belt conveyor cost vs belt speed vs intermediate drives

at 1.69 m/s represents the most cost-effective conveyor design with an equivalent annual cost evaluated at $609 010 (USD) per annum. By adopting the cheapest single drive belt conveyor as reference design, the cost saving induced by the most economic conveyor is estimated at $63 131 (USD) per annum over 20 years of the project duration. The focus on the profiles of the capital and operating costs shows that the reduction in costs results primarily from the decrease in energy consumption. With the increase in the number of drive stations, the reduction in power demand becomes less and less significant because of the additional secondary resistance brought in by each intermediate drive station added. Moreover, beyond a single intermediate drive station, the capital cost of belt conveyors also shows an increasing tendency. These two behaviors explain together the shape of the conveyor cost curve. It is finally noted that the optimal speed of conveyors is subject to a progressive decrease as more drive stations are envisaged. This supports the preliminary analysis given in Section 6.2.

Figure 6.3 shows the individual contributions of the bulk material, belt and idler rolls in the overall power consumption of the cost-effective belt conveyors. The variation of their respective percentages suggests that every intermediate drive station added to a conveyor system can assist to achieve higher energy efficiency in transportation. This is because of the steady increase of the proportion of power dedicated to the payload. Taking into account (3.15) and (3.28), higher conveyor cost savings can therefore be expected for systems that operate over longer transport distances.

The breakdown of the capital cost of conveyors by component displayed in Figure 6.4 indicates that the belt will generally form the largest proportion, followed by the group of gear reducers. For these two equipment, beyond a single intermediate drive station, the cost savings achieved through the use

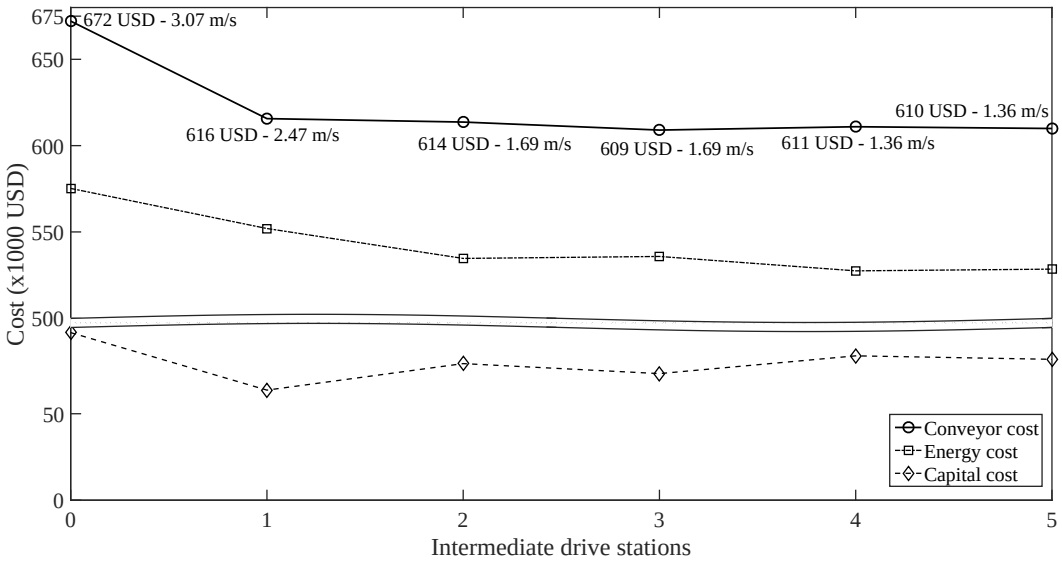

Figure 6.2. Cheapest belt conveyors with respect to the number of intermediate stations

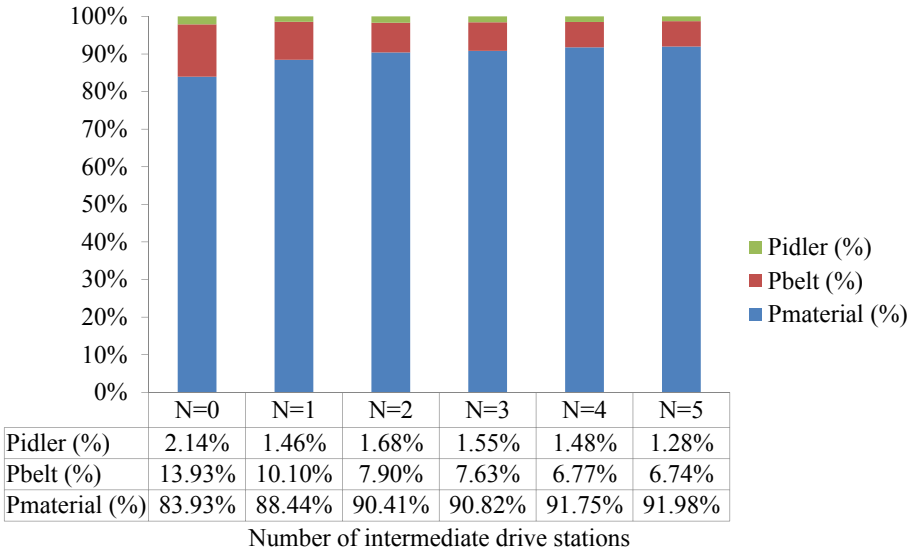

	N=0	N=1	N=2	N=3	N=4	N=5
Pidler (%)	2.14%	1.46%	1.68%	1.55%	1.48%	1.28%
Pbelt (%)	13.93%	10.10%	7.90%	7.63%	6.77%	6.74%
Pmaterial (%)	83.93%	88.44%	90.41%	90.82%	91.75%	91.98%

Figure 6.3. Power consumption per conveyor load component

of lighter belts are annihilated by the need for a wider belt due to the decrease of the optimal conveyor speed. Regarding the motors, the trend in this figure implies that their overall cost is fairly stable, irrespective of the conveyor technology and the number of drive stations fitted. Lastly, the analysis of the costs of idler rolls in Figure 6.4 shows that the cost of carry idler rolls is more sensitive to the variation of belt width in comparison with the return idler rolls.

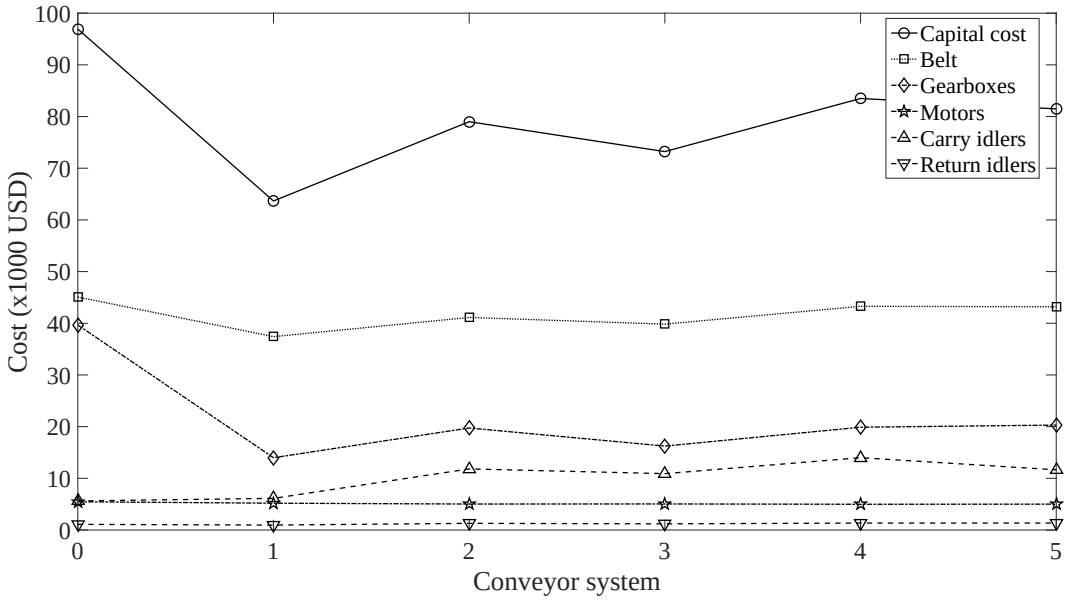

Figure 6.4. Detailed capital cost per belt conveyor component

6.4 INFLATION SENSITIVITY ANALYSIS

The superiority of the multi-drive belt conveyor fitted with three intermediate drive stations and operated at 1.69 m/s as established in Figure 6.2 assumes a general inflation rate fixed at 5.6% per annum over 20 years of the project duration. In practice, however, the inflation is more likely to be slightly different from one year to the next. This sensitivity study aims therefore to verify the robustness of this conveyor design against limited variations of the inflation rate. Besides the above-fixed inflation rate scenario, the following two inflation rate case studies have been presented in Chapter 4:

- stochastic fluctuation of the inflation rate between 4.8% and 5.8 with an average equal to 5.2%
- stochastic fluctuation of the inflation rate between 5.4% and 6.4 with an average equal to 5.8%

The former intends to evaluate the impact of an inflation rate lower than initially expected, the latter aims to investigate the opposite situation. The annual inflation rates and the equivalent annual cost coefficients under these scenarios are detailed in Sections 4.4.2 and 4.4.3.

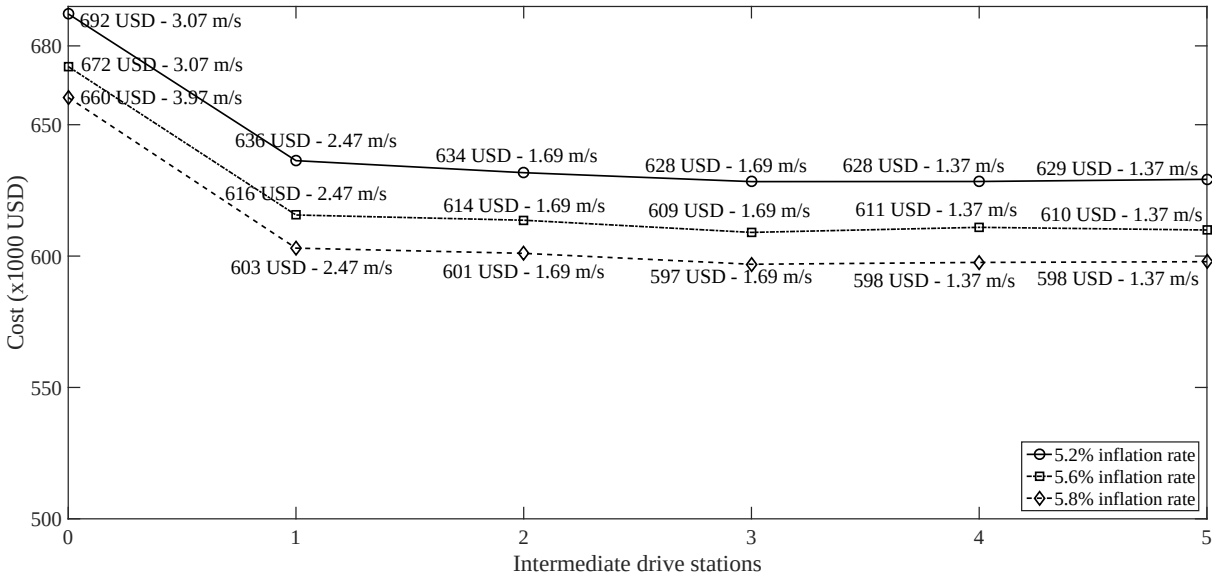

Figure 6.5. Variation of the cost-effective belt conveyors with the inflation rates

Based on the simulation results given in Tables 5.1 to 5.12, Figure 6.5 displays the fronts of the cost-effective belt conveyor designs under the three inflation scenarios envisaged. It is preliminary observed that unlike the single drive conveyor, the optimal conveyor speed of all the multi-drive conveyor designs remains fixed, irrespective of the scenario considered. Moreover, the multi-drive belt conveyor consisted of three intermediate drive stations and operated at 1.69 m/s realizes the lowest conveyor cost under the three inflation scenarios.

The design and cost information of the most cost-effective conveyors under the inflation scenarios are summarized in Table 6.1. It is shown that, except for α_i, k_N, F_{TU} and l_o and l_u, the optimal values of the rest of the design parameters remain fairly constant under the different inflation scenarios.

Further simulation tests focused on α_i showed that no impact on the economic performance is incurred by using wrapping angles superior to those of the best conveyor designs under fixed inflation rate at 5.6% and fluctuating inflation rate at 5.2% of average. Such a modification will only positively affect the design condition (3.47) on the minimum slack side tension to ensure the proper transmission of force between drive pulley and belt. Secondly, the individual comparison of k_N under 5.2% and 5.8% of average inflation rate with the optimal value under fixed inflation rate scenario indicates a reduction of, respectively, 7.81% and 8.76% in this parameter in case the presumed fluctuations are experienced during the project. Still with respect to the best conveyor design under fixed inflation rate,

the inspection of the spacings between idler rolls shows a decline of l_o by 19.01% and 21.13% and an increase of l_u by 15.38% and 15.38% under the 5.2% and 5.8% of average inflation rate scenarios, respectively.

This suggests that the additional costs caused by the use of the initial belt (greater k_N) and the initial return idler spacing (lower l_u) in case the inflation rate fluctuates following the envisaged scenarios will be partially offset by the cost savings due to the lower quantity of carry idler rolls installed (greater l_o). In view of the above, it is concluded that the original most cost-effective belt conveyor obtained under a fixed inflation rate is fairly robust to remain highly competitive in case of limited variations in the inflation rate.

Table 6.1. Cost-effective belt conveyor designs under different inflation trends

Parameter	Average inflation rate		
	5.2%	5.6%	5.8%
N	3	3	3
P_i, kW	151.05	151.09	151.08
v, m/s	1.69	1.69	1.69
T_i, kNm	16.05	16.05	16.05
$L_{o,1}$, m	574.63	572.98	574.77
$L_{o,3}$, m	649.14	649.7	649.1
$L_{o,5}$, m	649.14	649.7	649.1
$L_{o,7}$, m	628.41	628.94	628.35
α_i, rad	3.32	3.8	4.19
l_o, m	1.15	1.42	1.12
l_u, m	4.5	3.9	4.5
F_{TU}, kN	67.67	86.95	65.26
k_N, kN/m	526.68	571.28	521.22
B, mm	1800	1800	1800
D_o, mm	63	63	63
D_u, mm	63	63	63
d_o, mm	30	25	30
d_u, mm	30	25	30
$D_{tr,i}$, mm	400	400	400

Table 6.1. Cost-effective belt conveyor designs under different inflation trends (continued)

Parameter	Average inflation rate		
	5.2%	5.6%	5.8%
A_{energy}, $\times$1000 USD/year	556.16	535.79	522.84
A_{belt}, $\times$1000 USD/year	39.02	39.83	38.66
A_{motor}, $\times$1000 USD/year	4.82	5.04	5.22
A_{gear}, $\times$1000 USD/year	15.51	16.24	16.82
$A_{carryidler}$, $\times$1000 USD/year	11.56	10.9	12.05
$A_{returnidler}$, $\times$1000 USD/year	1.27	1.19	1.28
$A_{conveyor}$, $\times$1000 USD/year	628.34	609.01	596.88

CHAPTER 7 CONCLUSION

7.1 SUMMARY

The present dissertation has reported on a study that aimed at developing a cost-effective design approach for multiple drive belt conveyors. The basic system consisted of a typical uphill multi-drive belt conveyor with trippers distributed along the upper stretch.To search for the lowest cost of transportation over the duration of a project, a nonlinear optimization model combining continuous and discrete design parameters was formulated for a multi-drive belt conveyor including a number of intermediate drive stations specified by the conveyor designer. In this respect, the model intends to optimally set a specified group of design parameters in order to achieve the minimum equivalent annual cost, whilst satisfying the user defined transportation requirements and the various design conditions derived from the DIN 22101 and SANS 1313 standards. To fairly evaluate the effectiveness of the proposed design model, a similar optimization model was constructed for the single drive belt conveyors with the unique drive pulley situated at the head.

Both formulated as MINLPs, the developed optimization problems were solved using the MIDACO solver embedded in the MATLAB platform. Through the simulation results, good capabilities of the proposed design approach in leading to cost-effective conveyor system given a number of drive stations were observed. Following a step-by-step simulation strategy, by manually setting the number of drive stations, the possibility to identify the most cost-effective belt conveyor, also taking into account the single drive technology was also established. The robustness of the cheapest conveyor system against limited fluctuations of the inflation rate during the project was lastly verified through sensitivity analysis.

Although the economic potential of this type of belt conveyor is acknowledged for several decades,

the survey of the literature showed that no previous research work on the methodology to the design cheapest multi-drive belt conveyors was reported. This study is therefore regarded by the author as the very first contribution to this research topic.

7.2 FUTURE WORKS

The study presented in this master's dissertation can be extended as follows:

1. Comprehensive capital costs. The cost of the supporting structure usually represents the largest capital cost item of belt conveyors [35]. Other capital cost items, including the drive, head, tail and other idler pulleys, take-up devices, transfer chutes, transfer stations, walkways and civil works are also significant within the overall costs of a conveyor system. The development of a comprehensive capital cost model will, therefore, lead to the design of cost-effective multi-drive belt conveyors with a larger scope.

2. Advanced frictional resistance models. In practice, the magnitude of primary resistance in a belt section is influenced by several factors, including the belt tension, diameter of idler rolls, belt speed, and ambient temperature. Accordingly, the assumption made of a constant hypothetical frictional resistance involves a certain risk of deviation between the theoretical performances and the actual performances in case of implementation.

3. Dynamic belt tension due to belt vibrations and non-stationary operating conditions. In steady operating condition, the belt is also subject to additional dynamic solicitations due to transverse and longitudinal vibrations. Other dynamic constraints on the belt take place during the acceleration and deceleration of the conveyor system. The introduction of complementary design conditions that account for these dynamic components will allow for the determining of more accurate minimum strength characteristics of the belt in order to ensure the longevity of the system.

REFERENCES

[1] P. Darling, Ed., *SME mining engineering handbook*, 3rd ed. Englewood: Society for Mining Metallurgy & Exploration, 2011.

[2] C. A. Wheeler, A. W. Roberts, and M. G. Jones, "Calculating the flexure resistance of bulk solids transported on belt conveyors," *Particle & Particle Systems Characterization*, vol. 21, no. 4, pp. 340–347, Nov. 2004.

[3] S. Zhang and X. Xia, "Optimal control of operation efficiency of belt conveyor systems," *Applied Energy*, vol. 87, no. 6, pp. 1929–1937, Jun. 2010.

[4] P. Bindzár and D. Malindžák, *Acta Montanistica Slovaca*, vol. 13, no. 4, pp. 524–531, 2008.

[5] M. A. Alspaugh, "The evolution of intermediate driven belt conveyor technology," *Bulk Solids Handling*, vol. 23, no. 3, pp. 168–172, May 2003.

[6] S. Zhang and X. Xia, "A new energy calculation model of belt conveyor," in *IEEE Africon 2009*, Nairobi, 23-25 Sep. 2009, pp. 1–6.

[7] *Continuous mechanical handing equipment - Belt conveyors with carrying idlers - Calculation of operating power and tensile force*, DIN 22101, 2011.

[8] X. Xia and J. Zhang, "Energy efficiency and control systems-from a POET perspective," in *Conf. Control Methodologies and Technology for Energy Efficiency*, Vilamoura, Portugal, 29-31, Mar. 2010, pp. 225–260.

[9] ——, "Modelling and control of heavy-haul trains," *IEEE Control Systems Magazine*, vol. 31, no. 4, pp. 18–31, Aug. 2011.

[10] X. Xia and L. Zhang, "Industrial energy systems in view of energy efficiency and operation control," *Annual Reviews in Control*, vol. 42, pp. 299–308, 2016.

[11] *Conveyor and elevator belt handbook*, Assoc. for Rubber Products Manufacturers Inc., Indianapolis, IN, 2011.

[12] A. T. de Almeida, P. Fonseca, and P. Bertoldi, "Energy-efficient motor systems in the industrial and in the services sectors in the European Union: Characterisation, potentials, barriers and policies," *Energy*, vol. 28, no. 7, pp. 673–690, Jun. 2003.

[13] D. V. Petrović, M. Tanasijević, V. Milić, N. Lilić, S. Stojadinović, and I. Svrkota, "Risk assessment model of mining equipment failure based on fuzzy logic," *Expert Systems with Applications*, vol. 41, no. 18, pp. 8157–8164, Dec. 2014.

[14] D. Mazurkiewicz, "Maintenance of belt conveyors using an expert system based on fuzzy logic," *Archives of Civil and Mechanical Engineering*, vol. 15, no. 2, pp. 412–418, Feb. 2015.

[15] B. Jeftenić, I. Mihailović, M. Bebić, L. Ristić, D. Jevtić, N. Rašić, and S. Štatkić, "Energy efficiency in transportation of bulk material with frequency controlled drives," in *Proc. EPE-PEMC 2010 - 14th Int. Power Electron. and Motion Control Conf.*, Ohrid, Macedonia, 6-8 Sep. 2010, pp. 107–113.

[16] E. Pop, C. Covaciu, A. Avram, and F. Neghina, "Adaptive control strategy for conveyor drive systems," in *Recent Advances in Circuits, Syst., Electron., Control, and Signal Processing*, Puerto De La Cruz, Spain, 14-16, Dec. 2009, pp. 156–161.

[17] S. Zhang and Y. Tang, "Optimal scheduling of belt conveyor systems for energy efficiency with application in a coal-fired power plant," in *Proc. 2011 Chinese Control and Decision Conf.*, Mianyang, China, 23-25, May 2011, pp. 1434–1439.

[18] S. Zhang and X. Xia, "Modeling and energy efficiency optimization of belt conveyors," *Applied Energy*, vol. 88, no. 9, pp. 3061–3071, Sep. 2011.

[19] S. Zhang and Y. Tang, "Optimal control of operation efficiency of belt conveyor," in *Power and Energy Engineering Conf. (APPEEC)*, Wuhan, China, 25-28 Mar. 2011, pp. 1–4.

[20] J. Luo and Y. Shen, "Energy efficiency optimization of belt conveyor for material scheduling problem," in *2015 IEEE Int. Conf. Inform. and Automation*, Lijiang, China, 8-10, Aug. 2015, pp. 122–127.

[21] H. Chen, F. Zeng, J. Du, and S. Zhou, "An Improved Optimal Model for Energy-Saving of Belt Conveyors Based on Genetic Algorithm," in *2015 IEEE Int. Conf. Inform. and Automation*, Yunnan, China, 8-10 Aug. 2015, pp. 2784–2788.

[22] S. Zhang, "Model predictive control of operation efficiency of belt conveyor," in *Proc. 29th Chinese Control Conference*, Beijing, China, 29-31 Jul. 2010, pp. 1854–1858.

[23] J. Luo, W. Huang, and S. Zhang, "Energy cost optimal operation of belt conveyors using model predictive control methodology," *Journal of Cleaner Production*, vol. 105, pp. 196–205, 2015. [Online]. Available: http://www.sciencedirect.com/science/article/pii/S0959652614010130

[24] T. Mathaba, X. Xia, and J. Zhang, "Optimal scheduling of conveyor belt systems under critical peak pricing," in *10th Int. Conf. Power and Energy*, Ho Chi Minh City, Vietnam, 12-13, Dec. 2012, pp. 315–320.

[25] A. Middelberg, J. Zhang, and X. Xia, "An optimal control model for load shifting - With application in the energy management of a colliery," *Applied Energy*, vol. 86, no. 7-8, pp. 1266–1273, 2009. [Online]. Available: http://dx.doi.org/10.1016/j.apenergy.2008.09.011

[26] S. Windmann, O. Niggemann, and H. Stichweh, "Energy efficiency optimization by automatic coordination of motor speeds in conveying systems," in *Proc. IEEE Int. Conf. Ind. Technology*, Seville, Spain, 17-19, Mar. 2015, pp. 731–737.

[27] A. V. Reicks, "Belt conveyor idler roll behaviors," in *Bulk Material Handling by Conveyor Belt 7*, M. A. Alspaugh, Ed. Englewood: Society for Mining Metallurgy & Exploration, Feb. 2008, vol. 7, pp. 35–40.

[28] A. E. Maton, "The effects of idler selection on conveyor belt power consumption," *Bulk Solids Handling*, vol. 22, no. 1, pp. 46–49, Jan. 2003.

[29] A. Tapp, "Conveying technology-energy saving troughing idler technology," *Bulk Solids Handling*, vol. 20, no. 4, pp. 437–449, Oct. 2000.

[30] M. Hager and H. Simonsen, "Calculation and design of belt conveyors for bulk material," *Braunkohle Surface Mining*, vol. 52, no. 3, pp. 245–260, May-Jun. 2000.

[31] G. Lodewijks, "Determination of rolling resistance of belt conveyors using rubber data: Fact or fiction?" *Bulk Solids Handling*, vol. 23, no. 6, pp. 384–391, Nov. 2003.

[32] C. Wheeler, "Indentation rolling resistance of belt conveyors–a finite element solution," *Bulk Solids Handling*, vol. 26, no. 1, pp. 40–43, Jan. 2006.

[33] R. T. J. Reicks, Allen V. and C. A. Wheeler, "A comparison of calculated and measured indentation losses in rubber belt covers," *Bulk Solids Handling*, vol. 32, no. 3, pp. 52–57, 2012.

[34] J. Schützhold, K. Benath, V. Müller, and W. Hofmann, "Design criteria for energy efficient belt conveyor drives," in *2014 Int. Symp. on Power Electron., Elect. Drives, Automation and Motion*, Ischia, Italy, 18-20, Jun. 2014, pp. 1256–1263.

[35] A. Roberts, "Economic analysis in the optimization of belt conveyor systems," in *Proc. Beltcon 1 Conf.*, Johannesburg, South Africa, 16-17, Sep. 1981, pp. 1–33.

[36] C. A. Wheeler, "Evolutionary belt conveyor design: Optimizing costs," in *Bulk Material Handling by Conveyor Belt 7*, M. A. Alspaugh, Ed. Englewood: Society for Mining Metallurgy & Exploration, Feb. 2008, vol. 7, pp. 3–11.

[37] A. J. G. Nuttall, "Design aspects of multiple driven belt conveyors," Ph.D. dissertation, TU Delft, Delft University of Technology, 2007.

[38] A. J. G. Nuttall and G. Lodewijks, "Dynamics of multiple drive belt conveyor systems," *Particle and Particle Systems Characterization*, vol. 24, no. 4-5, pp. 365–369, 2007.

[39] *Belt conveyors for bulk materials*, 5th ed., Conveyor Equipment Manufacturers Assoc., Naples, FL, 1997.

[40] A. Frittella and S. Curry, "Conveyor idlers - SANS 1313 and selection procedures," in *Proc. Beltcon 15 Conf.*, Johannesburg, South Africa, 2-3, Sep. 2009, pp. 1–14.

[41] *Design criteria for product selection - Pulleys, idlers, and materials handling systems*, Handling Sandvik Materials, Sandviken, Sweden, 2013.

[42] N. R. Draper and H. Smith, *Applied regression analysis*, 3rd ed. New York: John Wiley & Sons, 1998.

[43] M. Schlüter, J. A. Egea, and J. R. Banga, "Extended ant colony optimization for non-convex mixed integer nonlinear programming," *Computers & Operations Research*, vol. 36, no. 7, pp. 2217–2229, Jul. 2009.

[44] T. Eschenbach, *Engineering economy: applying theory to practice*, 2nd ed. New York: Oxford University Press, 2003.

ADDENDUM A FORMULATION OF THE EQUIVALENT ANNUAL COST COEFFICIENTS

This section describes the procedure to be followed in order to determine the equivalent annual cost coefficients in case the annual escalation rate of energy and the general inflation rate can vary from year to year. It constitutes an extension and also a summary of the basic calculation approach presented in the literature [35, 44].

A.1 CALCULATION OF THE EQUIVALENT ANNUAL ENERGY COST COEFFICIENT

In case the annual escalation rate of energy r_e and the general inflation rate r can vary from year to year, the equivalent annual energy cost coefficient is calculated by:

$$k_0 = \left(\frac{a}{p}\right)_Z^{i_f^0} \sum_{i=1}^{Z} \left(\frac{p}{f}\right)_i^{i_f} \prod_{j=1}^{i} (1 + r_{e,j}), \tag{A.1}$$

where $\left(\frac{a}{p}\right)_Z^{i_f^0}$ denotes the capital recovery factor of the project, $\left(\frac{p}{f}\right)_i^{i_f}$ denotes the present equivalent cost factor over i-year period of time, $r_{e,j}$ denotes the annual escalation rate of energy during the year j of the project, and Z denotes the project lifetime. The capital recovery factor is obtained by:

$$\left(\frac{a}{p}\right)_Z^{i_f^0} = \frac{i_f^0\left(1+i_f^0\right)^Z}{\left(1+i_f^0\right)^Z - 1}, \tag{A.2}$$

where the time value of money when all cash flows are converted from inflated value to constant year zero value, noted by i_f^0, is given by:

$$i_f^0 = \frac{(1-t)\, r_d i_d - r_d r_{avg}}{1+r_{avg}} + (1-r_d)\, i_e. \tag{A.3}$$

In this relation, t denotes the income tax rate, r_d denotes the proportion of debt capital maintained constant by the company, i_d denotes the interest rate on debt, r_{avg} denotes the average inflation rate over the project duration, and i_e denotes the after-tax return required on equity funds with zero inflation rate. Since the inflation rate is assumed to be variable throughout the project, the present equivalent cost factor over i-year period of time is determined by:

$$\left(\frac{p}{f}\right)_i^{i_f} = \frac{1}{\prod_{j=1}^{i}(1+i_{f,j})}, \tag{A.4}$$

where $i_{f,j}$ denotes inflation modified rate of return of the year j of the project, which is given by:

$$i_{f,j} = (1-t)\, r_d i_d + (1-r_d)\left[(1+r_j)(1+i_e) - 1\right]. \tag{A.5}$$

Here, r_j denotes the general inflation rate during the year j of the project.

The substitution of (A.2) and (A.4) into (A.1), taking into account (A.3) and (A.5), allows to obtain the general expression of k_0.

A.2 CALCULATION OF THE EQUIVALENT ANNUAL COST OF EQUIPMENT

Taking into account the project lifetime and the expected lifetime of an equipment; one or more items of it can be necessary in order to achieve the project duration. In the rest of this section, the concept "equipment" is therefore associated with the set of items purchased and operated throughout the project. As indicated in equation 3.2, the equivalent annual cost of any equipment is expressed by:

$$A_{eq} = k_{eq} C_{eq,0}.$$

This cost is also obtained by multiplying the present equivalent of the capital costs PEC_{eq} of the equipment by the capital recovery factor of the project:

$$A_{eq} = \left(\frac{a}{p}\right)_{Z}^{i_f^0} PEC_{eq}. \tag{A.6}$$

Considering the first item and the replacement items purchased during the project lifetime, the present equivalent of the capital costs of an equipment is expressed by:

$$PEC_{eq} = \frac{PEF_{eq} - PEV_{eq} - tPED_{eq}}{1-t}, \tag{A.7}$$

where PEF_{eq} denotes the overall present equivalent of the first costs of the equipment, PEV_{eq} denotes the overall present equivalent of the salvage values of the equipment, and PED_{eq} denotes the overall present equivalent of depreciations of the equipment.

Denote M the expected lifetime of the given equipment, the total number of items to be purchased over the Z years of the project lifetime, noted by R, is given by:

$$R = \left\lceil \frac{Z}{M} \right\rceil,$$

The year X_i of the purchase of the i-th item ($i = 1,\ldots,R$) should correspond to the end of service life of the previous item:

$$X_i = (i-1)M.$$

In case the inflation-modified rate of return and the annual cost escalation rate r_{eq} of the equipment can vary from year to year, PEF_{eq} is given by:

$$PEF_{eq} = C_{eq,0}\left(1+\sum_{i=2}^{R}\left(\frac{p}{f}\right)_{X_i}^{i_f}\prod_{j=1}^{X_i}(1+r_{eq,j})\right). \tag{A.8}$$

Note that the sum in parenthesis will vanish if a unique item operates over the entire project duration.

On the determination of the salvage of the equipment, denote q_f the estimated percentage remaining value of the first costs of the equipment after it operates over the expected lifetime. Assuming the value of the equipment decreases linearly with time, the remaining value q_i of the i-th item purchased ($i = 1,\ldots,R$) after it operates over its actual lifetime in relation to both the project duration and its expected lifetime is determined by:

$$q_i = 1 - \frac{1-q_f}{M}\min\left(M, Z - M(i-1)\right),$$

The year Y_i of the decommissioning of the i-th item corresponds to the minimum between the year of the purchase of the next item (if any) or the project end:

$$Y_i = \min(iM, Z), \quad \text{with } i = 1,\ldots,R.$$

Considering all the items to be purchased during the project lifetime and the annual increase in the first costs, the present equivalent of the salvage value of the equipment is determined by:

$$PEV_{eq} = C_{eq,0}\left(\left(\frac{p}{f}\right)^{i_f}_{Y_1} q_1 + \sum_{i=2}^{R}\left(\frac{p}{f}\right)^{i_f}_{Y_i} q_i \prod_{j=1}^{X_i}(1+r_{eq,j})\right). \tag{A.9}$$

Note that the sum in parenthesis will vanish if a unique item operates over the entire project duration.

In order to formulate the present equivalent of depreciation under varying inflation-modified rate of return, let $\left(\frac{f}{a}\right)^{i_f}_{M,X_i}$ denote the series compound amount factor, which is given by:

$$\left(\frac{f}{a}\right)^{i_f}_{M,X_i} = 1 + \sum_{i=2}^{M}\prod_{j=i}^{M}(1+i_{f,X_i+j}).$$

This factor intends to convert a uniform series of annual depreciation to a future value for an item purchased at the year X_i of the project and operated over M years. The present equivalent of depreciation of an equipment is therefore obtained by totaling the present equivalents of the future values of the annual depreciation of all the items, taking into account the annual cost escalation rate of the equipment. Adopting the straight-line depreciation method and writing off the depreciations remaining at the end of the project, this results in:

$$\begin{aligned} PED_{eq} = \frac{C_{eq,0}}{M}\Bigg(&\sum_{i=1}^{R-1}\prod_{j=1}^{X_i}(1+r_{eq,j})\left(\frac{p}{f}\right)^{i_f}_{X_i+M}\left(\frac{f}{a}\right)^{i_f}_{M,X_i} + \prod_{j=1}^{S_R}(1+r_{eq,j})\left(\frac{p}{f}\right)^{i_f}_{Z}\left(\frac{f}{a}\right)^{i_f}_{Z-S_R,S_R} \\ &+ (QM-Z)\prod_{j=1}^{S_R}(1+r_{eq,j})\left(\frac{p}{f}\right)^{i_f}_{Z}\Bigg). \end{aligned} \tag{A.10}$$

In case a unique item operates over the entire project duration, that is $R = 1$, PED_{eq} is simplified as follows

$$PED_{eq} = \frac{C_{eq,0}}{M}\left(\left(\frac{p}{f}\right)^{i_f}_{Z}\left(\frac{f}{a}\right)^{i_f}_{Z,0} + (M-Z)\left(\frac{p}{f}\right)^{i_f}_{Z}\right). \tag{A.11}$$

Keeping $C_{eq,0}$ factorized, the substitution of (A.8), (A.9) and (A.10) or (A.11) into (A.7), and of (A.7) into (A.6) allows to obtained k_{eq} as mentioned in (3.2).

ADDENDUM B DERIVATION OF IDLER ROLL MASS MODELS

B.1 CARRY IDLER ROLLS

Table B.1 shows the actual mass of the rotating parts of carry idler rolls, noted by $m_{R,o}$, with respect of D_o, B and d_o. Based on the author's work, the best regression model fitted to the price data indicated in Table B.1 is given by:

$$\hat{m}_{R,o} = 136.39 D_o^{1.722} B^{1.025} + 80.51 d_o, \tag{B.1}$$

where $\hat{m}_{R,o}$ denotes the predicted mass of the rotating part of carry idler rolls. With a R^2 equal to 0.973, this regression model is acceptable to predict $m_{R,o}$ as a function of D_o, B and d_o. The different values of $\hat{m}_{R,o}$ relating to the fitting data are given in Table B.1.

Table B.1. Mass of the rotating parts of carry idlers roll with respect to design parameters[1]

D_o [mm]	$B[mm]$	d_o [mm]	$m_{R,o}$ [kg]	$\hat{m}_{R,o}$ [kg]
89	650	25	2.6	3.4
89	800	25	3.2	3.7
89	1000	25	3.5	4.1
89	1200	25	4.1	4.6
89	1400	25	4.5	5

[1]Transroll: "Catalogue rollers for belt conveyors" (6300 bearing series). Available at: `http://www.transroll.cz/obrazky-soubory/katalog-valecku-57802.pdf`

Table B.1. Mass of the rotating parts of carry idlers roll with respect to design parameters (continued)

D_o [mm]	$B[mm]$	d_o [mm]	$m_{R,o}$ [kg]	$\hat{m}_{R,o}$ [kg]
89	1600	25	4.9	5.4
102	650	25	3.1	3.7
102	800	25	3.9	4.1
102	1000	25	4.2	4.7
102	1200	25	4.9	5.2
102	1400	25	5.3	5.8
102	1600	25	6.1	6.3
108	650	25	3.4	3.9
108	800	25	4	4.4
108	1000	25	4.6	5
108	1200	25	5.4	5.6
108	1400	25	6	6.2
108	1600	25	6.6	6.8
127	800	25	5	5.1
127	1000	25	5.8	5.9
127	1200	25	6.8	6.7
127	1400	25	7.6	7.5
127	1600	25	8.4	8.3
133	800	25	5.3	5.4
133	1000	25	6.1	6.2
133	1200	25	7.2	7.1
133	1400	25	8.1	8
133	1600	25	9	8.9
133	1800	25	9.8	9.7
133	800	30	6.1	5.8
133	1000	30	7	6.6
133	1200	30	8	7.5
133	1400	30	8.8	8.4
133	1600	30	9.7	9.3
133	1800	30	10.6	10.1

Table B.1. Mass of the rotating parts of carry idlers roll with respect to design parameters (continued)

D_o [mm]	$B[mm]$	d_o [mm]	$m_{R,o}$ [kg]	$\hat{m}_{R,o}$ [kg]
152	1000	25	7.3	7.3
152	1200	25	8.6	8.4
152	1400	25	9.7	9.5
152	1600	25	10.8	10.6
152	1800	25	11.8	11.7
152	1000	30	8.5	7.7
152	1200	30	9.9	8.8
152	1400	30	10.9	9.9
152	1600	30	12.1	11
152	1800	30	13.2	12.1
152	1000	40	8	8.5
152	1200	40	9.4	9.6
152	1400	40	10.4	10.7
152	1600	40	11.6	11.8
152	1800	40	12.7	12.9
152	2000	40	14	14
159	1000	25	7.3	7.8
159	1200	25	8.6	8.9
159	1400	25	9.6	10.1
159	1600	25	11	11.3
159	1800	25	11.8	12.5
159	1000	30	7.1	8.2
159	1200	30	8.4	9.3
159	1400	30	9.4	10.5
159	1600	30	10.5	11.7
159	1800	30	11.3	12.9
159	1000	40	10	9
159	1200	40	11.5	10.1
159	1400	40	12.6	11.3
159	1600	40	13.8	12.5

Table B.1. Mass of the rotating parts of carry idlers roll with respect to design parameters (continued)

D_o [mm]	$B[mm]$	d_o [mm]	$m_{R,o}$ [kg]	$\hat{m}_{R,o}$ [kg]
159	1800	40	15	13.7
159	2000	40	16.4	14.9
194	1400	40	14.8	14.6
194	1600	40	16.3	16.3
194	1800	40	17.8	18
194	2000	40	19.4	19.7
194	2200	40	20.3	21.4

B.2 RETURN IDLER ROLLS

Table B.2 shows actual mass $m_{R,u}$ of the rotating parts of return idler rolls with respect of D_u, B and d_u. Based on the author's work, the best regression model fitted to the price data in Table B.2 is given by:

$$\hat{m}_{R,u} = 172 D_u^{1.287} B + 124.99 d_u, \tag{B.2}$$

where $\hat{m}_{R,u}$ denotes the predicted mass of the rotating part of return idler rolls. With a R^2 equal to 0.964, this regression model is acceptable to predict $m_{R,u}$ as a function of D_u, B and d_u. The different values of $\hat{m}_{R,u}$ relating to the fitting data are given in Table B.2.

On the basis of (B.1) and (B.2), the mass m_R of the rotating part of any idler roll is therefore modelled by:

$$m_R = z_1 D^{z_2} B^{z_3} + z_4 d, \tag{B.3}$$

where z_1 to z_4 denote the model coefficients, D denotes the shell diameter of the idler roll and d denotes the shaft diameter of the idler roll.

Table B.2. Mass of the rotating parts of return idler rolls with respect to design parameters[2]

D_u [mm]	$B[mm]$	d_u [mm]	$m_{R,u}$ [kg]	$\hat{m}_{R,u}$ [kg]
89	650	25	5.8	8.1
89	800	25	7.2	9.2
89	1000	25	8.4	10.8
89	1200	25	9.9	12.3
89	1400	25	11.3	13.8
89	1600	25	12.5	15.3
102	650	25	7.4	9
102	800	25	9.1	10.4
102	1000	25	10.8	12.2
102	1200	25	12.1	14.1
102	1400	25	14.6	15.9
102	1600	25	16.3	17.7
108	650	25	7.9	9.5
108	800	25	9.7	11
108	1000	25	11.5	12.9
108	1200	25	13.8	14.9
108	1400	25	15.6	16.8
108	1600	25	17.4	18.8
127	650	25	10.3	11
127	800	25	12.7	12.8
127	1000	25	15.1	15.2
127	1200	25	18.1	17.6
127	1400	25	20.6	20
127	1600	25	23	22.4
133	650	25	10.8	11.5
133	800	25	13.4	13.4
133	1000	25	16	15.9
133	1200	25	19.1	18.5

[2]Transroll: "Catalogue rollers for belt conveyors" (6300 bearing series). Available at: `http://www.transroll.cz/obrazky-soubory/katalog-valecku-57802.pdf`

Table B.2. Mass of the rotating parts of return idler rolls with respect to design parameters (continued)

D_u [mm]	$B[mm]$	d_u [mm]	$m_{R,u}$ [kg]	$\hat{m}_{R,u}$ [kg]
133	1400	25	21.7	21.1
133	1600	25	24.2	23.6
133	800	30	14.2	14
133	1000	30	16.7	16.6
133	1200	30	19.9	19.1
133	1400	30	22.4	21.7
133	1600	30	25	24.3
152	650	25	12.8	13
152	800	25	16	15.3
152	1000	25	19.1	18.3
152	1200	25	23	21.4
152	1400	25	26	24.4
152	1600	25	29	27.5
152	800	30	17.8	15.9
152	1000	30	21.1	19
152	1200	30	25.2	22
152	1400	30	28.4	25.1
152	1600	30	31.7	28.1
152	1000	40	20.6	20.2
152	1200	40	24.7	23.3
152	1400	40	27.9	26.3
152	1600	40	31.2	29.3
159	650	25	13	13.6
159	800	25	16	16
159	1000	25	19	19.2
159	1200	25	23	22.5
159	1400	25	26	25.7
159	1600	25	29.1	28.9
159	650	30	12.8	14.2
159	800	30	16.9	16.6

Table B.2. Mass of the rotating parts of return idler rolls with respect to design parameters (continued)

D_u [mm]	$B[mm]$	d_u [mm]	$m_{R,u}$ [kg]	$\hat{m}_{R,u}$ [kg]
159	1000	30	19.8	19.9
159	1200	30	22.8	23.1
159	1400	30	25.9	26.3
159	1600	30	29	29.5
159	1000	40	23.3	21.1
159	1200	40	27.6	24.3
159	1400	40	31	27.6
159	1600	40	34.5	30.8
194	1000	40	27.8	25.8
194	1200	40	32.9	30
194	1400	40	37.1	34.2
194	1600	40	41.3	38.3
194	1600	45	32.8	39
194	1800	45	35.4	43.1
194	2000	45	39.2	47.3

ADDENDUM C DERIVATION OF BELT PARAMETER MODELS

Table C.1 shows γ_{belt} and d_{Gk} of a series of steelcord conveyor belt in relation to their k_N. Fig. C.1 and Fig. C.2 displays the graphs of these data along with the regression models fitted. The equations of the regression models are given by:

$$\hat{\gamma}_{belt} = 13.823 + 8.174 \cdot 10^{-3} {k_N}^1, \tag{C.1}$$

$$\hat{d}_{G,k} = 1.002 \cdot 10^{-3} + 0.012 \cdot 10^{-3} k_N^{0.7712}, \tag{C.2}$$

where $\hat{\gamma}_{belt}$ and $\hat{d}_{G,k}$ denote, respectively, the predicted specific mass of the belt in kg/m^2 and the predicted diameter of tensile members of the belt in m. With R^2 equal to, respectively, 0.985 and 0.996, the regression models (C.1) and (C.2) proposed to predict, respectively, γ_{belt} and $d_{G,k}$ on the basis of k_N are therefore acceptable.

Table C.1. Specific mass and diameter of tensile members vs rated tensile strength of steelcord belts[3]

k_N [kN/m]	γ_{belt} [kg/m^2]	d_{Gk} [mm]
500	18.7	2.7
630	16.5	2.8
800	17.6	3.1
1000	26.6	3.7

[3]Metso Minerals: "Conveyor solutions. Trellex®classic steelcord conveyor belts". Available at: `http://www.metso.com/miningandconstruction/MaTobox7.nsf/DocsByID/3D167D0421CB6020C225768D004328E6/$File/2343-Trellex Steelcord Belts_PT.pdf`

Table C.1. Specific mass and diameter of tensile members vs rated tensile strength of steelcord belts (continued)

k_N [kN/m]	γ_{belt} [kg/m^2]	d_{Gk} [mm]
1250	23	4.2
1400	25.2	4.4
1600	29	4.7
1800	30.2	5.1
2000	31.5	5.5
2250	32.3	5.7
2500	33.9	6.8
2800	36	7.3
3150	39.8	7.6
3500	41.8	8
4000	45.5	8.6
4500	46.7	9.1
5000	54	10.5
5400	55.7	10.8
5800	62.2	11.5
6300	67.5	12
6700	70.6	12.7

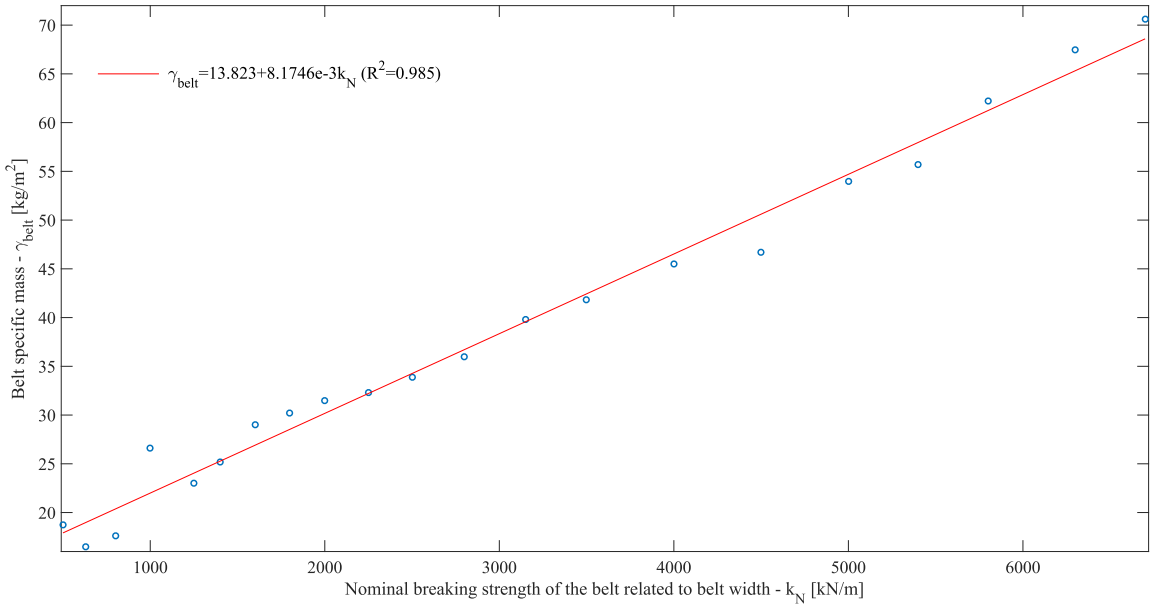

Figure C.1. Belt weight versus nominal breaking strength of the belt related to belt width

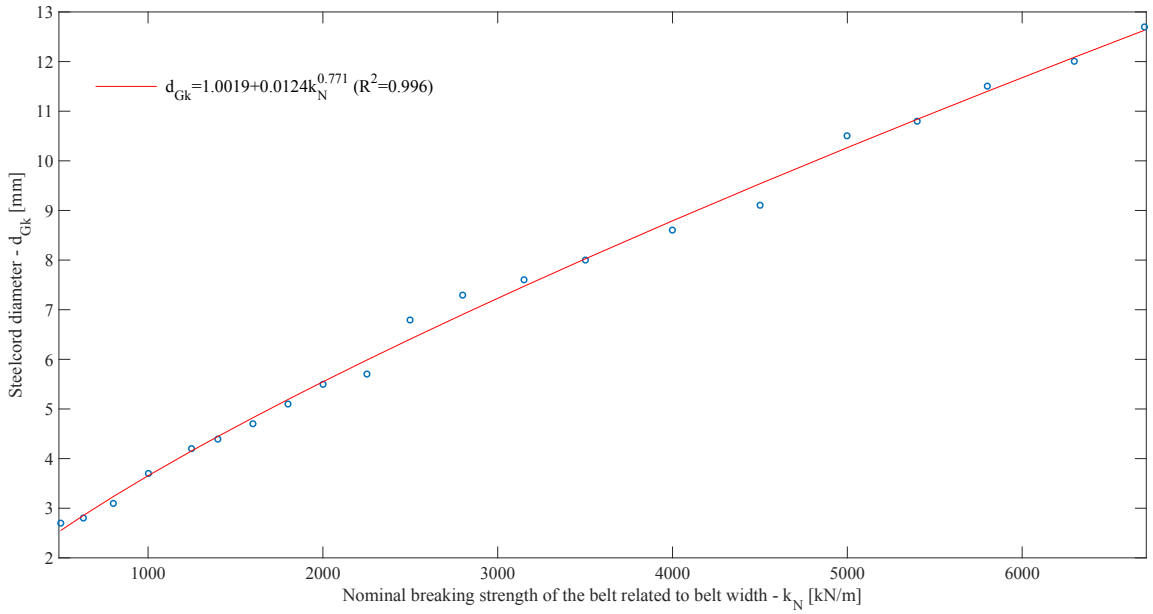

Figure C.2. Longitudinal tension member thickness versus nominal breaking strength of the belt related to belt width

ADDENDUM D DERIVATION OF IDLER ROLL PRICING MODELS

D.1 CARRY IDLER ROLLS

Table D.1 presents the manufacturer supplied price $p_{carryidler}$ of carry idler rolls as a function of parameters B, D_o and d_o. Note that the lengths are expressed in mm for convenience only.

Based on the author's work, the best regression model fitted to the price data in Table D.1 is given by:

$$\hat{p}_{carryidler} = -10.553 + 389.63 d_o^{0.951} + 189.37 D_o^{1.755} + 2.407 B^{1.747}, \tag{D.1}$$

where $\hat{p}_{carryidler}$ the predicted priced of the idler roll.

With a R^2 equal to 0.987, this regression model is acceptable to predict $p_{carryidler}$ as a function of D_o, B and d_o. The prices $\hat{p}_{carryidler}$ as predicted by (D.1) are displayed in Table D.1.

Table D.1. Carry idler roll manufacturer's data

B [mm]	D_o [mm]	d_o [mm]	$p_{carryidler}$ [USD]	$\hat{p}_{carryidler}$ [USD]
500	76	25	4.33	3.89
500	89	25	4.3	4.55
500	108	25	5.98	5.65
500	108	30	7.53	7.85
650	76	25	4.72	4.31

Table D.1. Carry idler roll manufacturer's data (continued)

B [mm]	D_o [mm]	d_o [mm]	$p_{carryidler}$ [USD]	$\hat{p}_{carryidler}$ [USD]
650	89	25	4.69	4.96
650	108	25	6.45	6.06
650	108	30	7.92	8.27
800	89	25	5.2	5.46
800	108	25	7.08	6.56
800	108	30	8.7	8.77
800	133	30	10.45	10.45
800	159	30	11.86	12.47
1000	108	25	7.7	7.33
1000	108	30	9.61	9.54
1000	103	25	6.69	7.03
1000	133	30	11.36	11.23
1000	159	30	12.95	13.25
1200	108	25	8.52	8.24
1200	108	30	10.74	10.45
1200	103	25	7.47	7.93
1200	133	30	12.53	12.13
1200	159	30	14.41	14.15
1400	108	25	9.17	9.26
1400	108	30	11.53	11.47
1400	103	25	8.09	8.96
1400	133	30	13.44	13.15
1400	159	30	15.53	15.17

D.2 RETURN IDLER ROLLS

Table D.2 shows the manufacturer supplied price $p_{returnidler}$ of return idler rolls as function of parameters B, D_u and d_u as gathered from a manufacturer. Note that the lengths are expressed in mm for convenience only.

Based on the author's works, the best regression model fitted to the price data in Table D.2 is given by:

$$\hat{p}_{returnidler} = -23.157 + 757.88 d_o^1 + 153.42 D_o^{1.051} + 2.808 B^1, \tag{D.2}$$

where $\hat{p}_{returnidler}$ the predicted priced of the idler roll.

With a R^2 equal to 0.745, this regression model is acceptable to predict $p_{returnidler}$ as a function of D_u, B and d_u. The prices $\hat{p}_{returnidler}$ as predicted by (D.1) are displayed in Table D.1.

Table D.2. Return idler roll manufacturer's data

B [mm]	D_o [mm]	d_o [mm]	$p_{returnidler}$ [USD]	$\hat{p}_{returnidler}$ [USD]
500	76	25	7.58	7.42
500	89	25	7.69	9.26
500	108	25	9.88	11.99
500	108	30	12.55	15.77
650	76	25	8.73	7.84
650	89	25	8.7	9.68
650	108	25	11.3	12.41
650	108	30	14.5	16.2
800	89	25	10.23	10.11
800	108	25	13.52	12.83
800	108	30	17.06	16.62
800	133	30	19.58	20.24
800	159	30	23.02	24.04
1000	108	25	15.47	13.39
1000	108	30	20.06	17.18
1000	103	25	14.19	12.67
1000	133	30	22.38	20.8
1000	159	30	26.45	24.6
1200	108	25	17.88	13.95
1200	108	30	23.33	17.74
1200	103	25	16.5	13.23

Table D.2. Return idler roll manufacturer's data (continued)

B [mm]	D_u [mm]	d_u [mm]	$p_{returnidler}$ [USD]	$\hat{p}_{returnidler}$ [USD]
1200	133	30	25.81	21.36
1200	159	30	30.67	25.16
1400	108	25	11.3	14.51
1400	108	30	14.5	18.3
1400	103	25	10.14	13.79
1400	133	30	16.48	21.92
1400	159	30	19.28	25.72